The influence of fold and fracture development on reservoir behavior of the Lisburne Group of northern Alaska

First semi-annual report

Reporting period: May to October, 1999

Principal investigator and report editor:
Wesley K. Wallace

Co-principal investigators:
Catherine L. Hanks
Michael T. Whalen
Jerry Jensen[1]

Student contributors:
Paul K. Atkinson
Joseph S. Brinton

Report date: May, 2000

Department of Energy Award DE-AC26-98BC15102--01

Submitting organization:

Geophysical Institute
University of Alaska
Fairbanks, Alaska
99775-5780

[1]Department of Petroleum Engineering and Department of Geology and Geophysics, Texas A&M University, College Station, Texas 77843-3116

Disclaimer

Abstract

The Lisburne Group is a major carbonate reservoir unit in northern Alaska. The Lisburne is detachment folded where it is exposed throughout the northeastern Brooks Range, but is relatively undeformed in areas of current production in the subsurface of the North Slope. The objectives of this study are to develop a better understanding of four major aspects of the Lisburne:

1. The geometry and kinematics of detachment folds and their truncation by thrust faults.
2. The influence of folding and lithostratigraphy on fracture patterns.
3. Lithostratigraphy and its influence on folding, faulting, fracturing, and reservoir characteristics.
4. The influence of lithostratigraphy and deformation on fluid flow.

The results of field work during the summer of 1999 offer some preliminary insights:

The Lisburne Limestone displays a range of symmetrical detachment fold geometries throughout the northeastern Brooks Range. The variation in fold geometry suggests a generalized progression in fold geometry with increasing shortening: Straight-limbed, narrow-crested folds at low shortening, box folds at intermediate shortening, and folds with a large height-to-width ratio and thickened hinges at high shortening. This sequence is interpreted to represent a progressive change in the dominant shortening mechanism from flexural-slip at low shortening to bulk strain at higher shortening. Structural variations in bed thickness occur throughout this progression. Parasitic folding accommodates structural thickening at low shortening and is gradually succeeded by penetrative strain as shortening increases. The amount of structural thickening at low to intermediate shortening may be inversely related to the local amount of structural thickening of the Kayak Shale, the incompetent unit that underlies the Lisburne.

The Lisburne Limestone displays a different structural style in the south, across the boundary between the northeastern Brooks Range and the main axis of the Brooks Range fold-and-thrust belt. The steep forelimbs of angular asymmetrical folds typically have been cut and displaced by thrust faults, resulting in superposition of a fault-bend fold geometry on the truncated folds. Remnant uncut folds within trains of thrust-truncated folds and the predominance of detachment folds to the north suggest that these folds originated as detachment folds. Fold asymmetry and a more uniformly competent Lisburne Limestone may have favored accommodation of a significant proportion of shortening by thrust faulting, in contrast with the dominance of fold shortening to the north.

Two dominant sets of fractures are present in the least deformed Lisburne Limestone: Early extension fractures normal to the regional fold trend and late extension and shear fractures parallel to the regional fold trend. These two major fracture sets remain as deformation increases, but they are more variable in orientation, character, and relative age. Compared to fold limbs, the fold hinges display greater density and extent of fractures, more conjugate and shear fractures, and more evidence of penetrative strain. This suggests that hinges remained fixed during fold growth. Late extension fractures normal to the fold axis are common even where penetrative strain is greatest. Fracture density is greater in fine-grained carbonates than in coarse-grained carbonates over the entire spectrum of deformation.

High-resolution lithostratigraphic data were collected from well-exposed sections in the areas where folds and fractures were studied in detail. The focus was on the Alapah Formation, the lower, less-studied formation of the Lisburne. This work identified four mechanical units within the Alapah that correspond approximately with differences in the weathering profile. These units reflect different patterns of depositional cyclicity, as defined by distinctive characteristics of cycle

thickness, bed thickness, and arrangement of component rock types. Cycles generally grade upward from finer-grained open-shelf deposits to coarser-grained shoal deposits, with an overall increase in proportion of coarser-grained deposits up-section in the formation. Outcrop gamma ray profiles were also collected and will be used to identify poorly exposed shaly or argillaceous intervals and as a tool for correlation between outcrops and between the surface and subsurface.

Table of contents

List of figures

Part B: Baseline stratigraphy of the Lisburne Group

Part C: Detachment folds and their truncation by thrust faults

Part D: A geometric analysis of detachment folds in the Lisburne Limestone, Arctic National Wildlife Refuge, Alaska

Part E: Fracturing in the Lisburne Group as a function of lithology and position in detachment folds

List of tables

Part B: Baseline stratigraphy of the Lisburne Group

Part E: Fracturing in the Lisburne Group as a function of lithology and position in detachment folds

Introduction and project summary

Definition of problem and objectives

Carbonate rocks of the Carboniferous Lisburne Group are found throughout a vast region of northern Alaska, including the subsurface of the North Slope and the northern Brooks Range. The Lisburne is a major hydrocarbon reservoir in the North Slope: It was the original target at Prudhoe Bay and is the currently producing reservoir in the Lisburne oil field. Folded and thrust-faulted Lisburne has been a past exploration target in the foothills of the Brooks Range, and remains an important potential future target there and in the coastal plain of the Arctic National Wildlife Refuge (1002 area). However, relatively little is known about the reservoir characteristics and behavior of the Lisburne and how they change as a result of deformation.

As in many carbonate reservoirs, most of the hydrocarbon production from the Lisburne Group in the subsurface is from naturally occurring fractures. Natural fractures play an essential role in production from the reservoir, but the geologic factors that control the origin, distribution, and character of these fractures are poorly understood. In the Lisburne oil field, less than 10% of the 2 billion barrels in place is recoverable at the present time. A clearer understanding of the nature and origin of these fractures has the potential to aid in the development of secondary and tertiary recovery programs for this large, but difficult to produce, reservoir.

Future targets for exploration in the Lisburne likely will be along the northern edge of the Brooks Range orogen, where the Lisburne has been modified by fold-and-thrust deformation. Such deformation has long been recognized both to enhance porosity and permeability, largely through the formation of fractures, and to reduce them by compression, as reflected by the formation of cleavage and stylolites. However, the ability to predict patterns of porosity/permeability enhancement or reduction and how they vary within a particular fold trap remain quite limited. Recent rapid advances in the understanding of the geometry and kinematics of different types of folds that form in fold-and-thrust settings offer great potential to improve the systematic understanding of porosity/permeability enhancement or reduction in fold traps, but these advances have only begun to be applied.

The Lisburne Group is a structurally competent unit that overlies an incompetent unit. Hence, the Lisburne undergoes a progressive evolution as shortening increases, from its undeformed state, to tightening detachment folds, to detachment folds that are truncated by thrust faults. How trap geometry and reservoir characteristics vary as this evolution progresses is not systematically understood, particularly with respect to differences in lithology and position within a fold. The basic objective of this study is to document and develop predictive models for structurally induced changes in reservoir geometry and characteristics at different stages in the evolution of detachment folds in the Lisburne Group.

Extensive exposures of the Lisburne Group in the northeastern Brooks Range fold-and-thrust belt offer the opportunity to develop a clearer understanding of the origin, distribution, and character of structurally induced enhancement and reduction of porosity and permeability in the Lisburne Group. The Lisburne Group has deformed into detachment folds evolved to different degrees, and thus provides a series of natural experiments in which to observe those structures and to develop models for their formation and for the resulting patterns of enhancement and reduction of porosity and permeability. The results of these field-based observations and models can then be used to develop quantitative models for characterization of Lisburne reservoirs and the fluid flow within them for a spectrum of traps from relatively undeformed to highly folded and thrust faulted.

This study of the Lisburne Group has the following major objectives:

•Establish 'baseline' reservoir characteristics in a relatively undeformed section and develop fracture and fluid flow models and a wellbore placement strategy in such reservoir.

•Document the evolution of trap-scale fold geometry with increasing shortening, with emphasis on changes in thickness across the fold and with respect to mechanical stratigraphy.

•Determine patterns in reservoir enhancement and destruction within a fold trap as a function of mechanical stratigraphy and of position within folds at different stages of evolution.

•Use observations of natural folds to constrain predictive models for the evolution of trap-scale fold geometry with increasing shortening and for the resulting modifications of reservoir characteristics.

•Use observations of natural folds and predictive fold models as a basis for fracture models for fluid flow and wellbore placement strategies in fold traps.

The results of this study will apply to current production in relatively undeformed Lisburne and to future exploration in deformed Lisburne. At least as important, the results will apply generally to carbonate reservoirs and to folded reservoirs, both of which are major producers and exploration targets worldwide.

Scope of this report

This report summarizes the results of the first season of field work for this project, which was conducted during the summer of 1999. The report presents initial examples of compiled data and preliminary interpretations based on field observations, and reflects progress through the fall of 1999. Results of further data compilation, analysis, and interpretation will be presented in future reports. Participants include two Master's students (Paul Atkinson and Joseph Brinton), three University of Alaska faculty (Wesley Wallace, Catherine Hanks, and Michael Whalen), and a visiting scientist from Sandia National Laboratory (John Lorenz). Two projects participants, Jerry Jensen, from Texas A & M University, and his Master's student, are not included in this report. Their models for fluid flow in the Lisburne require input from the field data and so will be addressed in future reports.

The report consists of four parts that each summarize a different aspect of the study and are written by different authors. These include:

•Detachment folds and their truncation by thrust faults, by Wesley K. Wallace

•A geometric analysis of detachment folds in the Lisburne Limestone, Arctic National Wildlife Refuge, by Paul Atkinson

•Fracturing in the Lisburne Group as a function of lithology and position in detachment folds, by Catherine L. Hanks, Joseph Brinton, and John Lorenz

•Baseline Lisburne stratigraphy, by Michael T. Whalen

Results of field work

Field work during the summer of 1999 yielded the following major results, as summarized in this report:

•Mapping and reconnaissance structural observations along a transect containing folds that represent a wide range in amount of shortening

•Reconnaissance investigation of an area with good exposures of thrust-truncated folds planned as a site for future study of fold and thrust geometry and kinematics, associated fractures, and lithostratigraphy

•Mapping, surveying, and detailed structural observations of seven folds that reflect different amounts of shortening
•Detailed observations of fractures in folds that reflect different amounts of shortening, at three different locations
•Detailed lithostratigraphic observations and measurement of partial stratigraphic sections at four locations to calibrate and fill gaps in previous work
•Outcrop gamma ray measurements in two previously measured sections

Significant preliminary conclusions

Preliminary conclusions that can be drawn from the field work include:
•Symmetrical detachment folds in the Lisburne Limestone display significant departure from parallel fold geometry, with thickness changes by some combination of parasitic folding and penetrative strain.
•Variations in fold geometry throughout the northeastern Brooks Range at different amounts of shortening suggest a possible progression in fold geometry from gentle to open angular folds at low shortening, to open to isoclinal folds with flat to gently curved crests at intermediate shortening, to tight to isoclinal folds with significantly thickened hinges and thinned limbs at high shortening.
•This progression in fold geometry with increasing shortening suggests a change in the dominant mechanism of fold shortening from flexural-slip to bulk strain as limb dips increase.
•An inverse relationship may exist between the local amount of structural thickening of the incompetent Kayak Shale and the amount of structural thickening of the overlying Lisburne at low to intermediate shortening.

Analysis of field results

Analysis of the compiled field results will serve as the basis for the following:
•Development and evaluation of geometric-kinematic models for evolution of detachment folds with increasing shortening
•Description of the fracture patterns associated with typical Lisburne detachment folds, and assessment of their relationship to the geometric-kinematic models
•Description of the lithostratigraphy of the Lisburne in the study area, and interpretation of its depositional significance
•Interpretation of the Lisburne lithostratigraphy in terms of mechanical stratigraphy, and interpretation of its relation to patterns of folding and fracturing
•Incorporation of the fold, fracture, and stratigraphic data and interpretations into models of fluid flow in Lisburne

This work will form the basis for two Master's projects in structural geology, one Master's project in petroleum engineering, and several projects by faculty participants.

Plans for the summer of 2000

Field work during the summer of 2000 will focus on the geometry and kinematics of thrust-truncated detachment folds. The geographic focus of the work will be on the Porcupine Lake valley area, where asymmetrical and thrust-truncated detachment folds are well-exposed south of the symmetrical detachment folds of the northeastern Brooks Range. Two new Master's projects will focus on the geometry, kinematics, and fracture patterns of thrust-truncated detachment folds. A new Ph.D. project will address the lithostratigraphy of the Lisburne Group both in the Porcupine Lake valley area and to the north. Faculty participants will both supervise students and conduct

studies of their own in the Porcupine Lake area and in areas to the north to fill gaps or address key problems identified by work during the summer of 1999.

Baseline stratigraphy of the Lisburne Group

by Michael T. Whalen, Geophysical Institute and Department of Geology and Geophysics, University of Alaska, Fairbanks, Alaska 99775-5780

ABSTRACT

Significant progress has been made on establishing the baseline stratigraphy for the Lisburne Group in the Brooks Range, northern Alaska and the subsurface of Prudhoe Bay. This part of the project employs a multi-phase approach including: collection of high-resolution lithostratigraphic, petrographic, mineralogic, X-ray diffraction, and outcrop spectral gamma ray data along with comparable subsurface geophysical logs. Most of our fieldwork during 1999 concentrated on the Alapah Formation, but some data were collected in the lower Wahoo Formation as well. Several partial stratigraphic sections were measured in the eastern Sadlerochit Mountains and the Fourth Range. Broad-scale weathering patterns and lithostratigraphy in the Fourth Range was used to subdivide the Alapah Formation into four major mechanical units. Lithostratigraphy combined with large-scale outcrop photos aided in overall mechanical subdivision. Finer-scale cyclicity (parasequences) was also noted in the Alapah Formation, but more detailed work will be necessary to further document meter-scale cycles. Lithostratigraphic data were also collected from one subsurface core from Prudhoe Bay. Core analysis revealed meter-scale cyclicity that was not readily observable in outcrop. Outcrop gamma ray data were collected in eastern Sadlerochit Mountains and central Shublik Mountains. These data have assisted in identification of shaly or argillaceous units that are poorly exposed in outcrop and should serve as a useful correlation tool between well-exposed outcrops and between the surface and subsurface.

Data will eventually be used to construct high-resolution lithostratigraphic sections that document mechanical and cyclic stratigraphy at a variety of scales and seismic-scale stratigraphic cross sections to document both large- and small-scale reservoir properties. Petrographic and x-ray diffraction data will augment outcrop, core, and gamma ray data in the evaluation of reservoir properties.

OBJECTIVE

The goals of this phase of the research project are to establish a “baseline” for Lisburne reservoir characteristics in relatively undeformed rocks using surface and subsurface data. The goals of this portion of the project are being met through a multi-phase approach to stratigraphic data collection to insure the development of a comprehensive database for establishing the stratigraphic baseline. The multi-phase approach includes collection of high-resolution lithostratigraphic data, petrographic, mineralogic, and X-ray diffraction data, and outcrop spectral gamma ray profiles and comparable subsurface geophysical logs. Progress on the baseline stratigraphic study of the Lisburne Group includes acquisition of: outcrop lithologic and gamma-ray data, lithologic data from subsurface core, and contribution, by ARCO Alaska, Inc., of an entire suite of subsurface geophysical logs from Prudhoe Bay wells that penetrate the Lisburne Group.

METHODS

High-resolution lithostratigraphic data were collected from six partial sections of the Lisburne Group in the northeastern Brooks Range (Table 1) and from one subsurface core from the Prudhoe Bay area. Data collection was mainly in the previously less-studied Alapah Formation, although part of the lower Wahoo Formation was also examined in outcrop. High-resolution stratigraphic data collected included: general mineralogic composition (limestone/dolostone), grain size, macroscopic porosity and fracturing, lithologic contrasts, bed thickness, and other post-depositional fabrics that will help define mechanically important horizons and other Lisburne reservoir characteristics. Petrographic analysis will also be undertaken to identify microscopic variations in lithofacies, porosity, and diagenesis that might influence reservoir properties. These

lithostratigraphic data will help identify lithologic heterogeneities, on the scale of meters to tens of meters, related to original depositional or diagenetic processes and mechanical stratigraphy. All of these lithologic characteristics can influence reservoir properties. Collection of stratigraphic data concentrated on identification of cyclic packages or parasequences (Van Wagoner and others, 1988) that will permit the classification of units that are genetically related and may have similar reservoir properties. Recognition of lithologic variations such as those recorded in shale-based cycles or parasequences (Jameson, 1994; Watts et al., 1995) or those controlled by post-depositional diagenetic processes (cementation, dolomitization) will be significant in identifying genetic packages that act both as reservoir partitions and reservoir and mechanical units.

Outcrop spectral gamma ray profiles were acquired through seven measured stratigraphic sections in the northeastern Brooks Range (Table 1) and comparable data are available from 88 well borings from the Lisburne field in Prudhoe Bay. Gamma ray profiles will aid in the identification of stratal surfaces such as parasequence and sequence boundaries and will assist in the accurate correlation from outcrop to the subsurface. Identification of argillaceous or shaly intervals in outcrop is important not only in defining the bases of parasequences but also in identifying relatively impermeable zones or incompetent horizons that separate more mechanically competent lithologic units. Shaly intervals at the bases of genetic packages are commonly poorly exposed in outcrop, but outcrop gamma ray data have successfully identified some of these horizons.

Other portions of the multiphase stratigraphic approach will be completed during the next several months and will contribute to the baseline data for undeformed Lisburne reservoir characterization. High-resolution stratigraphy will also provide the necessary data to document important mechanical stratigraphic packages that influenced later deformation and subsequent changes in reservoir characteristics.

OBSERVATIONS AND PRELIMINARY INTERPRETATIONS

Outcrop Data

Lithostratigraphy

During the summer of 1999, outcrop data were collected in the northeastern Brooks Range mainly by Michael Whalen and Andrea Krumhardt, with some assistance from Paul Atkinson. Outcrop sections were examined in the eastern Sadlerochit (ES) Mountains, Straight Creek (SC) and "Mosquito Bee Creek" (MB) in the Fourth Range, and "Flintstone Creek" (FC) in the central Shublik Mountains (Table 1). Data were collected from new stratigraphic sections as well as in sections previously measured by Gruzlovic (1991). A preliminary measured section from Straight Creek (SC-1, Fig. 1) provides an example of the lithostratigraphic data collected during this study. Other measured sections from the summer of 1999 have yet to be drafted and previously measured sections by Gruzlovic (1991) are being reevaluated in light of new observations.

The bulk of the stratigraphic data collected were from the Alapah Formation although portions of the lower Wahoo Formation were measured and sections of Wahoo measured by Gruzlovic (1991) were reexamined. The Alapah Formation displays depositional cyclicity at the scale of meters to tens of meters but because of the poor exposure, the number of parasequences and their lithologic character throughout all but the uppermost part of the section remain obscured (Fig. 1). Similar problems with exposure prevented collection of high-resolution stratigraphic data at several of the Alapah sections visited. At the best-exposed Alapah section, (MB-1, Table 1), high water prevented collection of detailed stratigraphic data. This site will be a target for future field work.

The general lithologic character of the Alapah changes upsection, with the lower part of the unit containing a higher proportion of mudstone and wackestone than the upper (Fig. 1). Depositional cycles usually record the change from sparsely fossiliferous calcareous shales or argillaceous mudstones or wackestones, representing relatively deep open-shelf environments, to cross-bedded, crinoid-dominated packstones, grainstones, or rudstones representing shoal deposits (Fig. 1). Laminated dolomud/wackestones with replaced evaporite nodules, representing tidal flat or supratidal environments, cap several cycles in the Alapah (Fig. 1).

Outcrop Gamma Ray Data

Gamma ray data were collected in the eastern Sadlerochit Mountains and the central Shublik Mountains (Table 1). Data from the eastern Sadlerochit Mountains (Fig. 2) proved to be the most useful due to more continuous outcrop exposure and detailed gamma ray data wer collected through five partial stratigraphic sections at this locality. Four of these sections (ES –1 through 4) represent a relatively continuous succession from the lower Alapah through the lower upper Wahoo Formations (Fig. 2). The fifth section (ES-5) was in the lower Alapah Formation and provides preliminary correlations between ES-1 and ES-5 based on gamma ray curves (Fig. 2). In the central Shublik Mountains, poor exposure produced multiple gaps of several tens of meters in gamma ray data from the Alapah Formation (Fig. 3). In general, the Alapah Formation appears to exhibit a higher degree of variation in gamma ray signature than the Wahoo (Figs. 2 and 3). Peaks in gamma ray signature are most commonly associated with the bases of stratigraphic cycles where argillaceous facies or thin covered intervals, that probably represent non-resistant shaly facies, are present (Figs. 2 and 3). Local gamma ray peaks in the upper portions of some stratigraphic cycles appear to coincide with cherty or stylolitized horizons and might be related to diagenesis.

Mechanical Stratigraphy

Large-scale outcrop weathering patterns provide a first-order approximation of mechanical stratigraphic properties. Based on field observations and our measured stratigraphic sections, the Alapah Formation appears to contain four major mechanical units each of which displays internal mechanical heterogeneities (Fig. 4). As observed in section SC-1, Unit 1 is dominantly recessive weathering and extends from the gradational contact with the underlying Kayak Formation up to a thick resistant package of packstones and grainstones ending at approximately 120 m (Figs. 1 and 4). Unit 2 is almost entirely recessive weathering except for resistant beds that appear to be the tops of decameter-scale parasequences (Figs. 1 and 4). Unit 3 is relatively resistant and begins with a thick package of cherty wackstones, fine-grained packstones, and minor grainstones that form the most resistant unit in the entire Alapah (Figs. 1 and 4). Unit 4 represents the remainder of the Alapah Formation and displays weathering characteristics gradational between the overall less resistant Alapah and the more resistant Wahoo Formation.

The mechanical units identified here may not correlate directly with genetic lithostratistratigraphic units (cycles or parasequences). The thick covered intervals in much of the Alapah have, so far, precluded detailed observation of cycle stacking patterns. In general, cycles tend to coarsen upward and beds within cycles tend to thicken upward, reflecting a change from finer-grained, open marine, argillaceous facies to coarser-grained shoal deposits. Mechanical competence generally increases upsection in such cyclic units. Locally, however, cycles are capped by fine-grained, thin-bedded peritidal facies. The peritidal facies might be relatively incompetent so a mechanical boundary would exist within the cycle. A direct correlation between increasing grain-size and bed thickness and mechanical competence is also not entirely borne out by field observations. Several thick-bedded, coarse-grained grainstones (especially in unit 4, SC-1) were highly fractured and recessive weathering, and are mechanically less competent than some finer-grained units. Portions of the Alapah Formation also appear to be relatively non-cyclic. Most of unit 3 (SC-1) is a thick package of relatively fine-grained, non-cyclic facies with abundant chert nodules. This package appears to be the most mechanically competent unit at this locality. Thick non-cyclic packages were probably deposited at depths below the influence of short-term relative sea-level changes, and facies do not record trends in grain size and bed thickness that would yield mechanical heterogeneties.

Where cycles are well defined by changes in grain size and bed thickness, they should permit some level of predictability of mechanical competence/incompetence. The highly cyclic nature and the ledge- and cliff-forming topography of the Wahoo Formation (Gruzlovic, 1991; Watts et al, 1995) imply a cyclic mechanical stratigraphy as well. More detailed field work and evaluation of previous research (Gruzlovic, 1991; Watts et al, 1995) on the Wahoo Formation will be necessary to assess its mechanical stratigraphy.

In the subsurface, the Alapah Formation is subdivided into four major units overlain by a green shale that thins to the south, and pinches out to the north of all outcrop exposures (Schafer, pers. comm., 1999). The four major units of the subsurface Alapah Formation appear to roughly correlate with the four mechanical stratigraphic units we have observed in the field. More detailed subsurface observations and comparison with outcrop data, however, will be necessary to evaluate the relationship between the units.

Subsurface Data

ARCO Alaska has granted permission for access, viewing, and some sampling of all subsurface drill core from Prudhoe Bay that penetrates the Lisburne Group (Table 2), and has donated digital public domain geophysical log data for 88 wells.

During spring and fall 1999, a portion of one subsurface core (L4-15) was examined and logged on a foot-by-foot basis at ARCO Alaska's core facility in Anchorage. Logging revealed meter-scale cyclicity in the Alapah Formation that was not readily observable in relatively poor outcrop exposures. A generalized cycle within the lower Alapah consists of laminated or low-angle cross-bedded argillaceous dolo-wackestone that is commonly oil stained, overlain by laminated or burrowed packstone and burrow-mottled packstone with calcite-replaced evaporites (Fig. 5). These cycles record shallowing upward from below fairweather wave base to intertidal or supratidal environments. The pay zone in these cycles is at the base of the cycles where dolomitization appears to have enhanced porosity and permeability.

ARCO Alaska has also temporarily loaned core L2-06 to us for research related to this project as well as for teaching purposes. This core was recently transported to the UAF campus and examination of the core will begin in the near future.

CONCLUSIONS

Through our field observations, collection of outcrop gamma ray data, and examination of subsurface core we have made significant progress toward establishing a stratigraphic baseline for the project. Detailed lithostratigraphic data collected from outcrop and subsurface core have helped identify parasequences with shallowing-upward trends that define mechanical units on the scale of meters. Four large-scale packages in the Alapah Formation appear to represent major mechanical units, on the scale of tens of meters, comparable in scale and number to units identified in the subsurface. Facies variations between cyclic and non-cyclic intervals are important in defining some major mechanical units (unit 3, SC-1). Variations within cycles also have mechanical significance. Thin-bedded, fine-grained, argillaceous-rich units are commonly mechanically incompetent, while thick-bedded, coarser-grained facies are usually more competent. Exceptions to these generalizations were observed, implying that caution is recommended when interpreting mechanical properties based on rock-type and vice versa. Further field observation, reevaluation of previous measured sections (Gruzlovic, 1991), and logging of subsurface core will be needed to verify the large- scale mechanical packages identified in the Alapah Formation (Figs. 2 and 3), to identify smaller-scale mechanical packages and parasequences, and to extend this analysis to the overlying Wahoo Formation. Outcrop gamma ray data have helped identify several "kicks" in poorly exposed portions of the Alapah that might indicate shaly or argillaceous horizons or diagenetic patterns. Gamma ray data have also provided preliminary correlations between sections in the lower Alapah. Further evaluation of subsurface geophysical logs will enhance surface to subsurface correlations.

RESEARCH PLAN FOR PROJECT COMPLETION

Fieldwork during 1999 has permitted identification of priorities for research during the next two summers. The ultimate goal of this portion of the project is to develop a stratigraphic baseline along a proximal-to-distal transect. This necessitates visiting the best-exposed outcrop sections to refine the stratigraphic data base. One priority is to revisit the well-exposed section at "Mosquito

Bee Creek" in the Fourth Range to help document small-scale stratigraphic cycles and to collect gamma ray data. This section is exposed in the creek drainage and will provide some of the most continuous exposure of the Alapah in the distal end of the stratigraphic transect. Other well-exposed sections along strike or to the south of the Fourth Range will also be examined to provide detailed stratigraphic data from the distal portion of the field area. Revisiting the eastern Sadlerochit Mountains is also important as it will permit us to collect gamma ray data at some of the best-exposed proximal sections of the Wahoo Formation. Well-exposed sections in the northern and southern portions of the field area have thus been identified. Sections examined in the central Shublik Mountains were both poorly exposed and more structurally deformed. Identification of more suitable sections in the Shublik Mountains is therefore a priority. Analysis of subsurface core and log data is also an integral part of this study. At least two entire cores of the Lisburne Group from Prudhoe Bay will be logged in detail. Cores targeted for analysis include: L2-06, L4-15, and possibly L5-13. The arrival of a new Ph.D. student in January 2000, who has begun working on both subsurface and outcrop stratigraphic data, will help achieve the ultimate goals of the project.

Field and subsurface stratigraphic data will ultimately be drafted as stratigraphic sections and important mechanical and sequence stratigraphic subdivisions will be identified. High-resolution lithostratigraphy will identify lithologic heterogeneities, on the scale of meters to tens of meters, that influence reservoir properties. Identification of sedimentary cycles or parasequences (Van Wagoner and others, 1988) will permit the classification of units that are genetically related and may have similar reservoir properties due either to depositional or post-depositional processes. Identification of different phases of diagenesis will also lend insight into variations in reservoir characteristics. Petrographic analysis will be used to identify microscopic variations in lithofacies important to determining reservoir properties. X-ray diffraction will be employed to quantify the percentage of calcite and dolomite in lithologic samples collected from outcrop and core. These data, along with quantitative porosity and fracture-related data, will allow us to gauge the importance of differing patterns of dolomitization on reservoir development.

Seismic-scale outcrop and subsurface analysis will permit the identification of large-scale (tens to hundreds of meters) lithologic variations that might influence reservoir characteristics. Because the Lisburne represents a broad carbonate ramp (Gruzlovic, 1991; Watts and others, 1995), lateral facies variations may not be apparent in single outcrops or cores. Analysis of facies variations along a transect from paleogeographically proximal cores in the subsurface at Prudhoe Bay to more distal outcrop localities in the northeastern Brooks Range will help identify lithologic trends that produce lateral reservoir heterogeneities. Seismic-scale analyses in conjunction with high-resolution lithostratigraphy will also aid in the identification of larger-scale depositional sequences, the boundaries of which may be related to subaerial exposure surfaces or other stratal discontinuities with reservoir or mechanical significance.

RECOMMENDED APPROACH FOR FUTURE SIMILAR RESEARCH

The Lisburne Group presents significant challenges to obtaining high-resolution stratigraphic data in outcrop. Large-scale weathering patterns that define outcrop exposure are related to the overall mechanical stratigraphy. A fruitful approach to determining overall mechanical stratigraphy involves relating sections measured in the field to outcrop photos or photomosaics (Fig. 3). Relating the weathering patterns to lithology will permit further evaluation of the lithologic controls on mechanical stratigraphy. Outcrop gamma ray profiles of well-exposed sections also appear to be a useful correlation tool although nearly continuous exposure is necessary for this tool to be used effectively. Application of these methods to future studies in the Brooks Range and correlation of outcrop exposures with the subsurface will enhance our understanding of the geologic history of Arctic Alaska and improve our ability to predict the reservoir potential of folded and fractured carbonates.

REFERENCES

Gruzlovic, P. D., 1991, Stratigraphic evolution and lateral facies changes across a carbonate ramp

and their effect on parasequences of the Carboniferous Lisburne Group, Arctic National Wildlife Refuge, northeastern Alaska, M.S. Thesis, University of Alaska Fairbanks, 201 p.

Jameson, J., 1994, Models of porosity formation and their impact on reservoir description, Lisburne field, Prudhoe Bay, Alaska: American Association of Petroleum Geologists Bulletin, v. 78, p. 1651-1678.

Van Wagoner, J.C., Posamentier, H.W., Mitchum, R.M., Vail, P.R., Sarg, J.F., Loutit, T.S., and Hardenbol, J., 1988, An overview of the fundamentals of sequence stratigraphy, in Wilgus, C.K., and others, eds., Sea-level change: an integrated approach: SEPM Special Publication 42, p. 39-45.

Watts, K.F., Harris, A.G., Carlson, R.C., Eckstein, M.K., Gruzlovic, P.D., Imm, T.A., Krumhardt, A.P., Lasota, D.K., Morgan, S.K., Dumoulin, J.A., Enos, P., Goldstein, R.H., and Mamet, B.L., 1995, Analysis of reservoir heterogeneities due to shallowing-upward cycles in carbonate rocks of the Pennsylvanian Wahoo Limestone of northeastern Alaska: U. S. Department of Energy, Final Report for 1989-1992 (DOE/BC/14471-19), Bartlesville Project Office, 433 p.

Table 1

Section	Section Measured	Thickness/ Strat. Interval	# Gamma Ray Measurements	# Lithologic Samples
ES1	Summer 1999	88 m, Lower Alapah	89	N/A
ES 2	Gruzlovic, 1991	70 m, Lower Wahoo	73	N/A
ES 3	Summer 1999	12 m, Upper Alapah	14	N/A
ES 4	Summer 1999	33 m, Upper Wahoo	36	N/A
ES 5	Summer 1999	61 m, Lower? Alapah	58	18
SC 1	Summer 1999	422 m, uppermost Kayak, Alapah, Lower Wahoo	N/A	66
SC 2	Summer 1999	182 m, Upper Alapah, Lower Wahoo	N/A	41
SC 3	Summer 1999	119 m, Upper Kayak, lowermost Alapah	N/A	18
MB 1	Summer 1999	16 m, upper Kayak	N/A	2
FC 1	Gruzlovic, 1991	391 m, Alapah, lowermost Wahoo	246	7
FC 2	Gruzlovic, 1991	114 m, Lower Wahoo, lowermost Upper Wahoo	111	N/A

Table 1. Summary of outcrop data collected in the northeastern Brooks Range during summer 1999.

Table 2

Well	Cored Ft.	Alapah	Wahoo	API
E. Bay St	399	√	√	500292013300
L1-09	580		√	500292126500
L1-10	606		√	500292134000
L1-21	514	√	√	500292030400
L2-06	1324	√	√	500292093000
L2-13	540		√	500292144000
L2-14	127		√	500292175800
L2-20	467		√	500292137600
L2-24	510		√	500292134600
L2-26	540		√	500292135900
L2-28	559		√	500292129800
L2-29	179		√	500292150500
L2-30	492		√	500292127200
L3-08	759		√	500292101900
L3-12	497		√	500292165100
L3-23	460		√	500292151300
L4-03	491		√	500292183100
L4-15	1514	√	√	500292095200
L5-12	426		√	500292169400
L5-13	1194	√	√	500292105900
L5-21	508		√	500292173200
L5-24	205	√		500292132700
LGI-12	267		√	500292156000
Prudhoe Bay St. 1	201	√	√	500292000100
Sag Delta 01	476	√		500292017600
Sag Delta 2	551	√		500292023400
Sag Delta 5	503	√	√	500292052700
Term Well A	44		√	500292040600
West Beech St. #2	116	√		500292016100

Table 2. List of cored subsurface wells with total feet of core, whether core interval contains Alapah and/or Wahoo Formations, and API number.

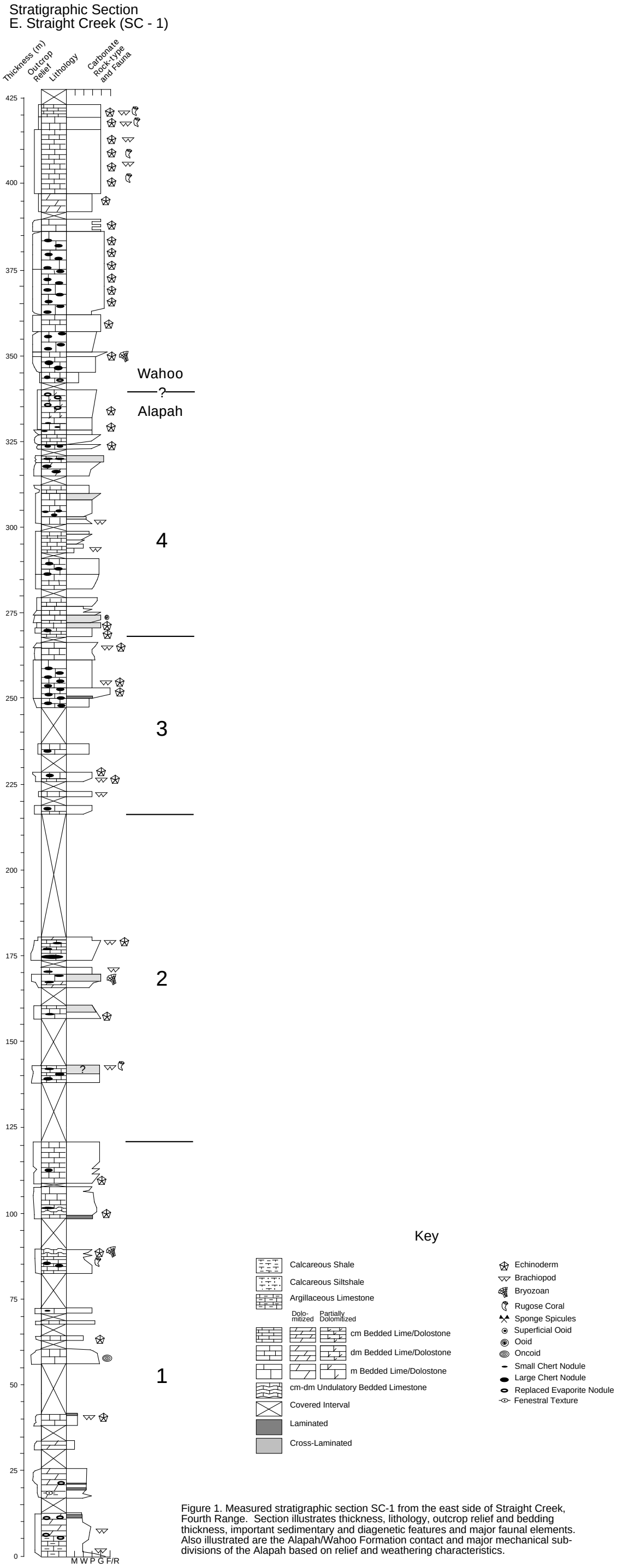

Figure 1. Measured stratigraphic section SC-1 from the east side of Straight Creek, Fourth Range. Section illustrates thickness, lithology, outcrop relief and bedding thickness, important sedimentary and diagenetic features and major faunal elements. Also illustrated are the Alapah/Wahoo Formation contact and major mechanical sub-divisions of the Alapah based on relief and weathering characteristics.

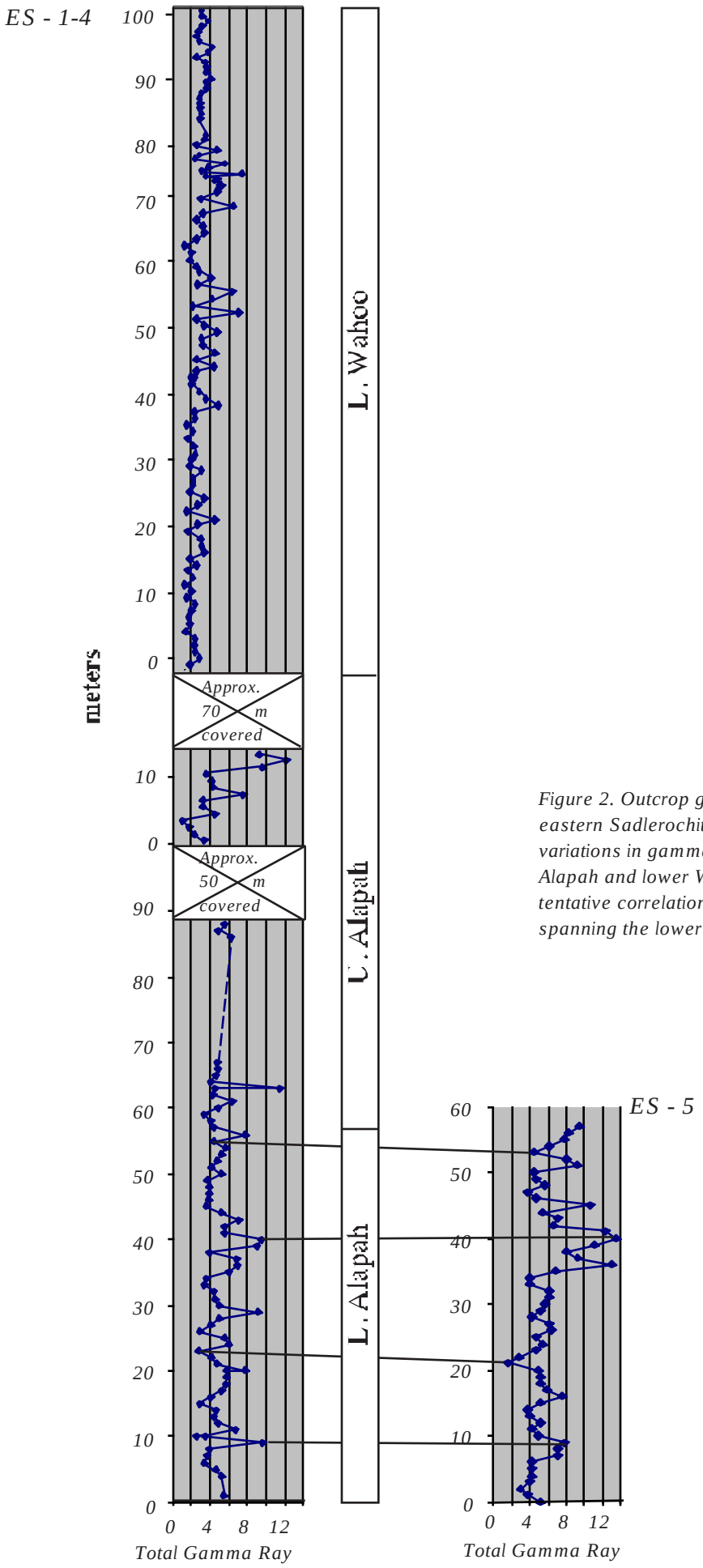

Figure 2. Outcrop gamma ray logs from the eastern Sadlerochit Mountains illustrating variations in gamma ray signature in the Alapah and lower Wahoo Formations and tentative correlations between two sections spanning the lower Alapah.

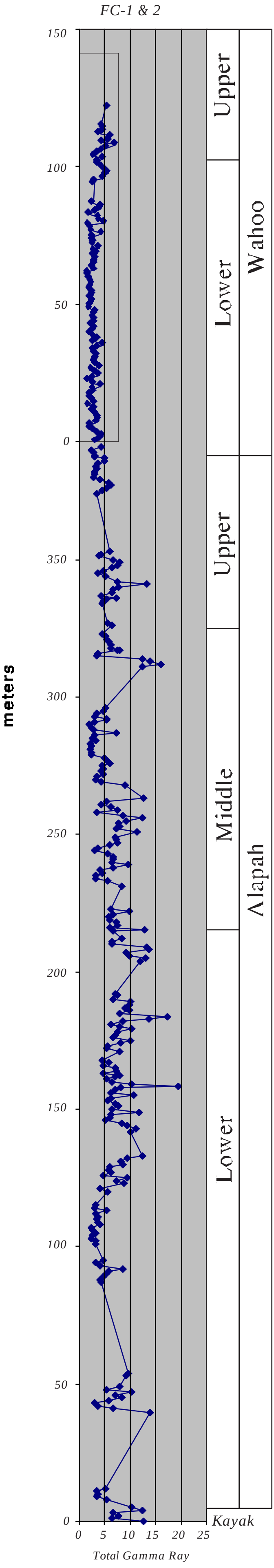

Figure 3. Outcrop gamma ray log fromthe central Shublik Mountains illustratingthe gamma ray signature of the Alapah amd lower Wahoo Formations. Note the gaps in gamma ray data between abou 10 and 100 m and 290 to 320 m.

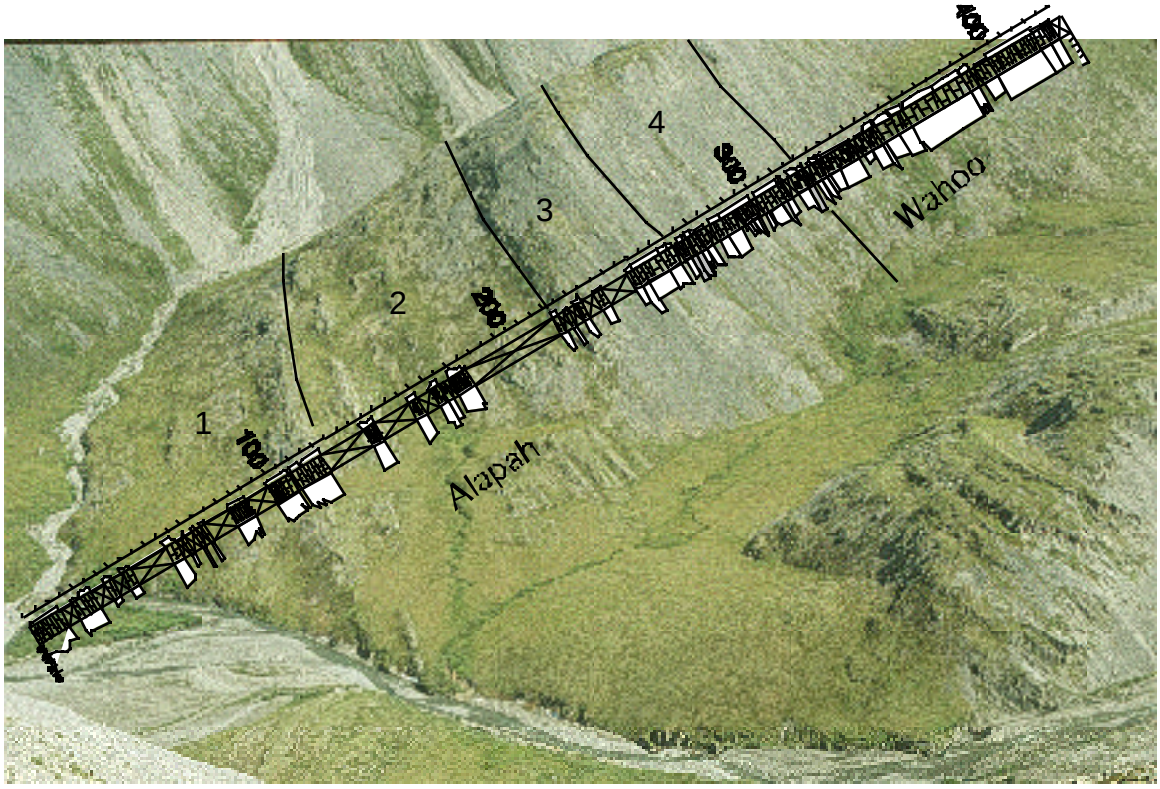

Figure 4. Outcrop photo of stratigraphic section SC-1 at Straight Creek in the Fourth Range. Superimposed on the photo is the measured stratigraphic section indicating four major mechanical subdivisions of the Alapah Formation. Note that toward the top of the stratigraphic section the correlation between the measured section and the outcrop photo becomes more tenuous due to the perspective of the photo.

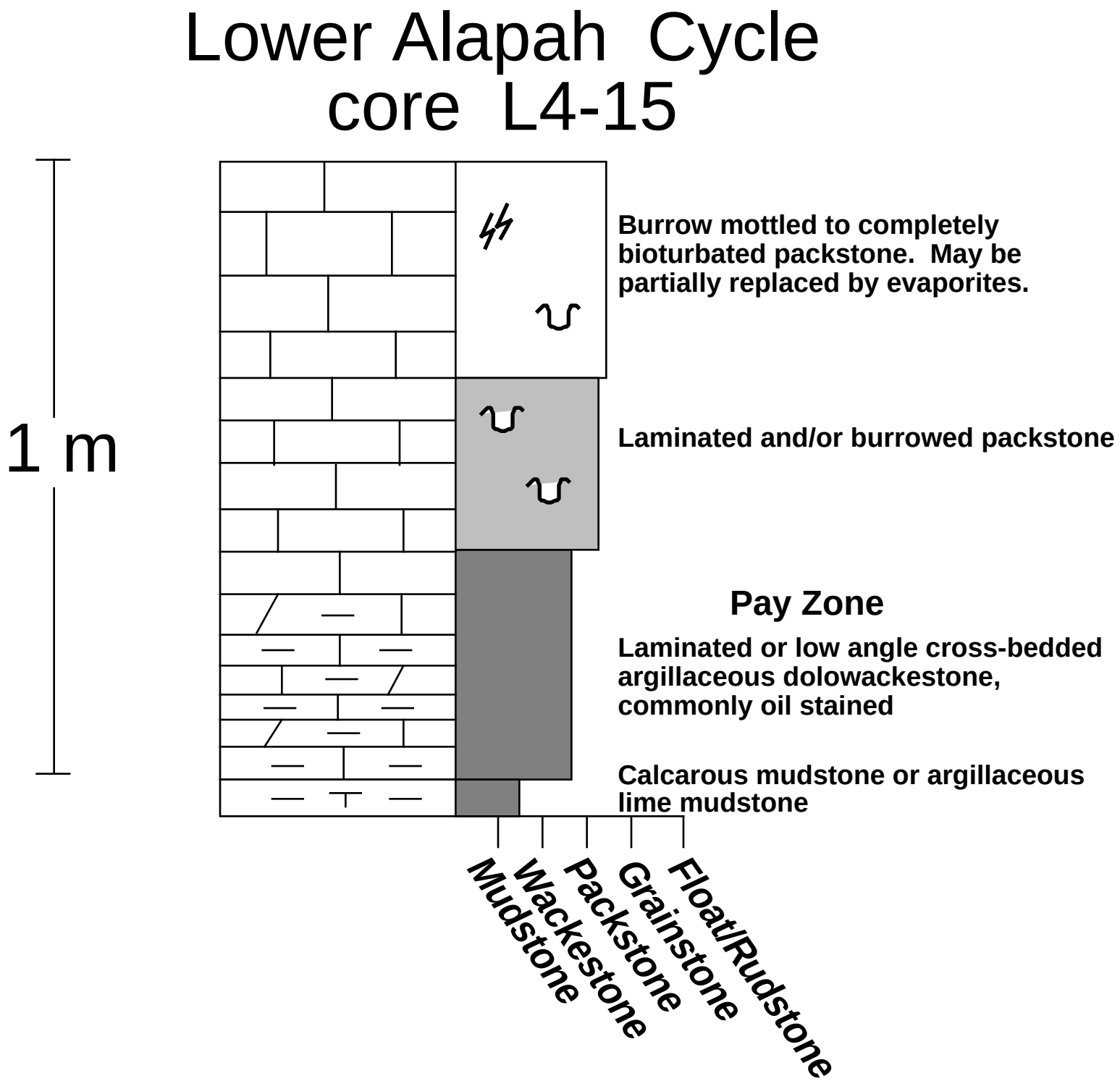

Figure 5. Schematic diagram illustrating the architecture of cycles observed in the lower Alapah Formation in subsurface core L4-15 from Prudhoe Bay. Note that the "pay zone" with high porosity and permeability is confined to dolomitized facies near the base of the cycle.

Detachment folds and their truncation by thrust faults

by Wesley K. Wallace, Geophysical Institute and Department of Geology and Geophysics, University of Alaska, Fairbanks, Alaska 99775-5780. wallace@gi.alaska.edu

Abstract

The Lisburne Limestone displays a range of symmetrical detachment fold geometries throughout the northeastern Brooks Range. The variation in geometry suggests a generalized progression with increasing shortening. At low shortening, folds with interlimb angles of ~180-90° are characterized by long straight limbs and angular hinges that broaden upward into gently curved hinge zones or relatively narrow flat crests. Parasitic folds commonly reflect structural thickening, especially in the lower part of the Lisburne. At intermediate shortening, folds with interlimb angles of ~90-0° and roughly equal width and height commonly display a box-fold geometry, with a flat to gently curved crest separated from straight limbs by inclined hinges. Thickening in the flat central panel is accommodated by parasitic folds and penetrative strain, including solution cleavage. At high shortening, folds with interlimb angles of ~45-0° and a fold height significantly greater than width display angular hinges separated from planar limbs by a zone of gentle curvature. Bedding is thickened in hinges and thinned in limbs by penetrative strain, including solution cleavage. This sequence is interpreted to represent progressive replacement of flexural-slip by bulk strain as the dominant shortening mechanism. A mechanical transition in the lower Lisburne from the underlying incompetent Kayak Shale to the competent upper Lisburne facilitates this style of folding.

The Lisburne Limestone displays a different structural style south of the northeastern Brooks Range. The steep forelimbs of angular asymmetrical folds typically have been cut and displaced by thrust faults, resulting in superposition of a fault-bend geometry. Remnant uncut folds and the transition from detachment folds to the north suggest that these folds originated as detachment folds. Asymmetry and a more uniformly competent Lisburne Limestone may have favored accommodation of a significant proportion of shortening by thrust faulting, in contrast with the dominance of fold shortening to the north.

Introduction

The objective of this part of the study is to document the geometry of a variety of natural detachment folds, both unbroken and thrust-faulted, to serve as a basis for models of their geometry and evolution. The northeastern Brooks Range provides an excellent natural laboratory for the study of detachment folds. Detachment folds are preserved over a huge area characterized by rugged topography and little cover. The difficult access and steep topography make detailed, hands-on study of individual folds difficult, but the area provides an excellent opportunity to view a wide range of geometries of many map-scale folds. The variation in geometry represents a wide range in shortening, and different areas are dominated either by symmetrical, unbroken folds or asymmetrical, thrust-faulted folds.

The folds are formed in the competent Mississippian to Pennsylvanian Lisburne Limestone (~500 m) above the incompetent Mississippian Kayak Shale (~200 m) (see the section of the report on stratigraphy, by Mike Whalen). The Lisburne is overlain by another incompetent unit that consists dominantly of shale and sandstone, the Permian to Triassic Sadlerochit Group. Throughout the northeastern Brooks Range, the Kayak forms the roof thrust for a duplex of horses formed in the underlying basement rocks (Wallace and Hanks, 1990; Wallace, 1993, Hanks, 1993). In the

western part of the northeastern Brooks Range, thrust spacing is sufficiently greater than displacement so that individual fault-bend anticlines are separated by synclines. These folds are an order of magnitude larger than the detachment folds within the cover and are superimposed on the overlying cover to form anticlinoria and synclinoria (Figure 1). The detachment folds generally reflect the greatest shortening in the synclinoria, although significant shortening has also occurred over some anticlinoria. A general decrease in detachment fold shortening is evident to the north, approaching the range front, but shortening still displays considerable local variation.

A profound change in structural style is present along the southern margin of the northeastern Brooks Range, across a boundary that has been referred to as the Continental Divide thrust front (Figure 1) (Wallace and Hanks, 1990). This boundary separates an area to the north dominated by symmetrical, unbroken detachment folds from an area to the south dominated by asymmetrical, thrust-faulted folds. This boundary also coincides with the dramatic southward thickening of a clastic succession beneath the Kayak Shale and the disappearance of basement-cored anticlinoria as a major influence on the structure of the cover. The folds south of the Continental Divide thrust front are interpreted to be thrust-truncated detachment folds (Wallace, 1993; Wallace et al., 1997; Wallace and Homza, in review) based on an apparent transition from the detachment folds of the northeastern Brooks Range and the local preservation of unbroken detachment folds south of the boundary.

Field studies on detachment folds during the summer of 1999 centered on three different areas (Figure 1). Detailed studies of the geometry of folds in the Straight Creek and Shublik Mountains area were conducted mainly by Paul Atkinson, who has summarized his results in a separate section of this report. As part of a mapping project for the Alaska Division of Geological and Geophysical Surveys, Wes Wallace documented the geometry of detachment folds across the Echooka anticlinorium, the northernmost exposed basement-cored anticlinorium in the western part of the northeastern Brooks Range. Wes Wallace and Cathy Hanks reconnoitered an area south of the Continental Divide thrust front near Porcupine Lake to lay the groundwork for a more detailed study during the summer of 2000. This section of the report summarizes observations of folds in the Echooka anticlinorium, Straight Creek, and Porcupine Lake areas, as well as some more general observations and interpretations based on work throughout the Brooks Range since 1983. This section is divided into two parts, one on the detachment folds of the northeastern Brooks Range and another on the thrust-truncated folds south of the Continental Divide thrust front.

Detachment-folds of the northeastern Brooks Range

Mechanical stratigraphy

The Lisburne Limestone is known to display significant changes in thickness and facies from the Shublik Mountains to the north, to the north Franklin Mountains anticlinorium and south limb of the Echooka anticlinorium to the south (Figure 1) (Watts et al., 1995). Preliminary stratigraphic descriptions of Lisburne in the Fourth Range and Shublik Mountains are presented in the section of this report on stratigraphy, by Mike Whalen. The Lisburne is divided for structural mapping purposes into lower and upper units that can be identified from a distance based on color, resistance to erosion, and bedding characteristics. These mapping units correspond roughly with the stratigraphic subdivisions of the Lisburne into Alapah (lower) and Wahoo (upper), but placement of the Alapah-Wahoo contact varies depending on microfossil zonation and facies and does not everywhere correspond with the mappable boundary between the darker-colored, less-resistant lower Lisburne and the lighter-colored, more-resistant upper Lisburne.

The Lisburne appears to display a relatively consistent pattern of mechanical stratigraphic behavior from the Shublik Mountains south to the Continental Divide thrust front. Within this area, well-defined mechanical layering is evident throughout the section, with a strong competency contrast between Kayak (very incompetent) and upper Lisburne (very competent) being separated by a zone of mechanical transition in the lower Lisburne. Kayak Shale consists mostly of uniform shale that deforms incompetently by a combination of small-scale folds, thrust faults, and penetrative fabrics, including solution cleavage. Folds parasitic to map-scale detachment folds are locally displayed by ~1-10 m thick competent interbeds of limestone near the top of Kayak and of sandstone lower in the section. In the lower Lisburne, well-defined and fairly evenly spaced bedding forms mechanical layering throughout, but is divided at a larger scale into alternating competent and incompetent intervals that vary in relative thickness throughout the section. The percentage and thickness of competent intervals generally increases upward, but the pattern is sufficiently uneven to facilitate the development of parasitic folds that commonly vary in wavelength and are disharmonic throughout the section. The upper Lisburne also has well-defined, evenly spaced mechanical layering throughout, but these layers are thicker, more competent, and more uniform in competency than in lower Lisburne. The Lisburne is sharply overlain by a significantly less competent unit, the Sadlerochit Group, which consists dominantly of thin-bedded shale to fine-grained sandstone in the northeastern Brooks Range.

Echooka anticlinorium

The Echooka anticlinorium is the westernmost anticlinorium in the northeastern Brooks Range that exposes basement rocks (Figure 1). It also has lower structural relief than most of the other anticlinoria in the northeastern Brooks Range. The cover rocks in the anticlinorium display a range of detachment fold geometries (Figure 2), including some of the lowest-shortening detachment folds in the northeastern Brooks Range. The folds display interlimb angles of ~170-30° and wavelengths of ~0.5-3 km. Most have narrow curved hinges that separate planar to gently curved limbs and they commonly have multiple hinges that define a box-fold geometry. The folds typically are symmetrical, although hinges are commonly inclined because of dip toward the center of a box fold or inferred tilt of the underlying detachment surface. The folds appear to adjoin each other throughout the area, leaving few if any panels that have not been folded. Shortening is at a minimum over the flat crest of the anticlinorium, with the narrow angular hinge zones of anticlines becoming wider and more curved up section. Shortening increases toward the limbs of the anticlinorium. Local thrust breakthrough of a few folds has occurred through steep limbs of inclined folds in the limbs of the anticlinorium, including a minor backthrust on the south limb of the anticlinorium. Parasitic folds are common, with increasing abundance down section and toward the cores of folds. Smaller parasitic folds commonly are disharmonic in the lower Lisburne, which contains alternating intervals with significant competency contrast. Visible thickening in fold cores is accommodated by parasitic folding and internal thickening of less competent intervals, with parasitic folding generally decreasing and internal thickening generally increasing with increasing shortening.

Straight Creek

Straight Creek provides a natural cross section from Fourth Range anticlinorium across an intervening synclinorium to the north Franklin Mountains anticlinorium (Figures 1, 3). Fold shortening displayed on this transect ranges from relatively small over the crest of the Fourth Range anticlinorium to some of the tightest folds in the northeastern Brooks Range in the synclinorium to the south. The general characteristics of folds on the transect are summarized here, with more detailed descriptions of individual folds being presented in the part of the report by Paul

Atkinson. Folds on the transect display interlimb angles of ~130-10° and wavelengths of ~0.6-2.2 km. Folds across the Fourth Range anticlinorium display characteristics similar to those described for the Echooka anticlinorium except that many fewer folds are present across the narrower Fourth Range anticlinorium. This description will focus on the higher-shortening folds in the synclinorium and won't repeat the description of lower-shortening folds over the anticlinorium.

Folds in the synclinorium display progressive changes from interlimb angles of about 90° to 0°. They are upright and symmetrical except for an asymmetrical syncline (interlimb angle ~60°) on the backlimb of the Fourth Range anticlinorium. Folds at the higher end of the interlimb angle range still display angular box-fold geometry, but have well-developed solution cleavage in hinges. At ~45° interlimb angles, folds are straight-limbed and angular. Parasitic folds are confined mainly to narrow hinge zones and some layers are thickened in hinges. Changes in bed thickness across the fold become more evident approaching interlimb angles of 0°. Beds display significant thickening relative to limbs in narrow hinge zones, with the amount of thickening varying from interval to interval. Thick, resistant, light-colored beds commonly display such thickening although they are the most competent beds where shortening is less. Beds in both limbs and hinges display penetrative solution cleavage and internal strain, most obviously displayed by rotated and distorted crinoid columnals. The high strain in limbs suggests that beds there have been thinned and extended, while they were thickened and shortened in hinges. The tightest folds are all upright and symmetrical and have high ratios of amplitude to wavelength. Fold shape varies from the core to the outer arc. Cores are essentially isoclinal with very narrow hinge zones. Outer arcs display sharp angular hinges that curve gently to subisoclinal limbs, yielding an ogive shape that reflects relative hinge thickening. Kayak Shale is not exposed in the tightest folds, but limitations on space in exposed lower Lisburne suggest that Kayak has been largely to totally squeezed out of fold cores. One near-isoclinal anticline has been displaced on a steeply dipping (~65°) thrust fault where a near-vertical limb places Lisburne against Sadlerochit in a deep syncline.

Generalized characteristics of northeastern Brooks Range detachment folds

The observations above, combined with previous observations from throughout the northeastern Brooks Range, suggest that the folds can be roughly categorized into three groups representing increasing shortening (Figure 4). Throughout the spectrum of shortening, the folds are characterized by planar to gently curved dip panels that are separated by narrow, curved to angular hinges.

1. Low shortening (Figure 4a)

Folds representing low shortening are not common in the northeastern Brooks Range, but where present are characterized by long straight limbs. Folds with interlimb angles in the range ~180-90° are included in this group. Anticlines are sharp and angular at the base of the Lisburne, but broaden upward into gently curved hinge zones or relatively narrow flat crests. Parasitic folds are common in the lower Lisburne. Both first-order detachment folds and parasitic folds are mostly symmetrical, but locally asymmetrical parasitic folds are present on the limbs of larger folds.

2. Intermediate shortening (Figure 4b)

Most folds in the northeastern Brooks Range probably belong to this group of folds. This includes folds with interlimb angles in the range ~90-0°, but interlimb angle alone is not sufficient basis to categorize these folds. For lower interlimb angles (~45-0°), folds are included in this group if their wavelength (distance between synclinal hinges measured parallel to detachment) roughly equals fold height (distance between crest and trough measured normal to detachment).

This shortening range includes a complete spectrum of fold geometries from angular box folds, through folds with curved outer arcs, to chevron folds. These folds commonly display a box-fold geometry, with a flat to gently curved crest separated from straight limbs by inclined hinges. Parasitic folds are most common between these hinges, especially lower in the Lisburne. Angular parasitic folds are common in the more chevron-like folds and do not appear to form preferentially in any particular part of the fold or the stratigraphic section. Relative thickening of some incompetent intervals is evident in hinge zones of first-order and parasitic folds, as is spaced solution cleavage and other indicators of penetrative strain.

3. High shortening (Figure 4c)

This group of folds is restricted mainly to synclinoria between basement-cored anticlinoria. This group includes folds with interlimb angles of ~45-0° and a fold height significantly greater than wavelength. Hinges are angular but separated from planar limbs by a zone of gentle curvature. Bedding is thickened in hinges and thinned in limbs, and solution cleavage and other indicators of penetrative strain are present throughout the folds. Parasitic folds are rare, but locally present in a narrow zone near the hinge.

Geometric-kinematic models for detachment folds

A variety of models have been proposed for the geometry and kinematics of detachment folds (e.g., Jamison, 1987; Mitra and Namson, 1989; Dahlstrom, 1990; Epard and Groshong, 1995; Homza and Wallace, 1995; Poblet and McClay, 1996). Most assume a sharp contact between an underlying weak layer and an overlying competent layer, and that the competent layer shortens by parallel folding (no change in bed length or thickness). A very important kinematic distinction between different models is whether fold hinges remain fixed or migrate with respect to the rock. Limbs must rotate if all hinges are fixed during fold evolution, whereas limbs may or may not rotate depending on how hinges migrate (e.g., Homza and Wallace, 1995; Poblet and McClay, 1996). Observations of small-scale structures in folds in the northeastern Brook Range suggest that hinges remain fixed (Homza and Wallace, 1997), an interpretation that is supported elsewhere by similar studies (e.g., Fischer et al., 1992; Rowan and Kligfield, 1992) and, at least for anticlinal hinges, by observations of the geometry of syntectonic strata in folds (e.g., Poblet and Hardy, 1995; Poblet et al., 1997).

The conclusion that at least anticlinal hinges are fixed will be taken as a working assumption here. Several models have been proposed for the evolution of detachment folds with fixed anticlinal hinges. Detachment depth, or thickness of the incompetent unit beneath the bounding synclines, is commonly assumed to remain constant during fold evolution. However, if both anticlinal and synclinal hinges remain fixed, changes in the area of the core of the fold as shortening progresses require a change in thickness of the incompetent unit beneath the bounding synclines (Homza and Wallace, 1995, 1997; Wallace and Homza, 1998). This can easily be accommodated if adjacent anticlines meet at a common synclinal hinge (Figure 5). However, if adjacent anticlines are separated by a horizontal panel that has not been folded, area change must be accommodated by some mechanism such as addition of a synclinal hinge, either outside or inside of the fixed synclinal hinge (Figure 6). Constant detachment depth can be maintained if only the anticlinal hinge is fixed. In this case, constant detachment depth and competent bed length are maintained as bed length and area within the fold increase as material enters the fold through the synclinal hinges (Figure 7) (e.g., Dahlstrom, 1990; Poblet and McClay, 1996). In this case, a definite relationship exists between fold size and interlimb angle. Constant detachment depth can be maintained while both anticlinal and synclinal hinges remain fixed if beds do not remain constant in thickness and bed length during fold evolution (Figure 8) (Epard and Groshong, 1995). This model does not

take into account differences in competency between different units, although the required changes in bed thickness and length may be accommodated by different mechanisms (faulting, folding, or penetrative strain) depending on unit competency.

Preliminary model for northeastern Brooks Range detachment folds

What model best fits the natural detachment folds of the northeastern Brooks Range? No obvious and systematic increase in fold size with decreasing interlimb angle was noted in field observation, as would be expected if folds evolved with fixed anticlinal hinges and migrating synclinal hinges. This interpretation can be more rigorously tested when cross sections have been constructed to scale and can be used to compare interlimb angle against limb length. Adjacent anticlines meet at a common synclinal hinge in most places throughout the northeastern Brooks Range, although intervening flat panels may be present in a few places where shortening is least. This provides a geometrically and kinematically simple mechanism to vary incompetent unit thickness beneath synclines while maintaining constant bed thickness and length in the competent unit. Observed variation in incompetent unit thickness (Homza and Wallace, 1997), particularly thickening at higher shortening, is consistent with this possibility. However, the incompetent unit is not sufficiently well exposed to determine whether its actual thickness is consistent with parallel folding of the competent unit. Changes in bed thickness and length clearly are present in the competent unit, especially with increasing shortening. However, these changes are significantly less than in the incompetent unit and do not appear sufficient to allow fixed-hinge, constant-depth folding according to the ideal, uniform-competency model of Epard and Groshong (1995). Construction of detailed, quantitively constrained cross sections of individual folds will allow this interpretation to be tested better.

The observed characteristics of the northeastern Brooks Range detachment folds suggest a fixed-hinge model that is a hybrid between two idealized end-member models: A variable detachment-depth model in which bed thickness and length are constant within a distinct competent unit (Homza and Wallace, 1997; Wallace and Homza, 1998) and a constant detachment-depth model in which bed thickness and length vary smoothly throughout the fold, with no internal differences in competency (Epard and Groshong, 1995). A competency contrast clearly exists in the northeastern Brooks Range, although a zone of transition exists between the least competent and most competent intervals. However, the competent unit displays some structural thickness changes over the full range of shortening observed, especially in its lower part where competency is transitional. These thickness changes in the competent unit could reduce the changes in incompetent unit thickness required by the idealized variable detachment-depth model. The observations suggest that the northeastern Brooks Range detachment folds evolve by a process in which bulk strain gradually replaces flexural-slip folding as the dominant shortening mechanism in the competent unit as shortening progresses:

Low shortening: Shortening is primarily fixed-hinge buckling by flexural slip. The area of the fold core tends to increase as the fold grows, favoring a decrease in detachment depth as incompetent material moves into the fold core. The increase in area is partially compensated by parasitic folding in the competent unit, thereby reducing the required decrease in detachment depth.

Intermediate shortening: Fixed-hinge buckling by flexural slip continues. The area of the fold core increases to a maximum at interlimb angles of ~90°, then begins to decrease. The flat fold crest progressively widens in the competent unit with decreasing interlimb angle, favoring development of a box-fold geometry. This geometry allows the shortening accommodated by non-parallel folding in the incompetent unit to be accommodated in the competent unit with minimum

departure from parallel folding. Parasitic folding and increasing strain in the fold core in the competent unit, especially between the hinges bounding the crest, continue to compensate for the area change and reduce the change in detachment depth. The ratio of fold height to wavelength increases, and eventually detachment depth increases as incompetent material is expelled from the fold core.

High shortening: As area in the fold core decreases and mechanical resistance to flexural-slip folding increases, bulk strain replaces flexural slip as the dominant mechanism of shortening in the competent unit. The existing fold decreases in width and increases in amplitude by strain in both the fold core and limbs. Thus, the final evolution of the fold is primarily by passive amplification, thereby approaching similar geometry.

This interpretation has been derived independently from observations of map-scale detachment folds in the northeastern Brooks Range over a range of shortening. A similar evolution has been widely hypothesized for outcrop-scale buckle folds on the basis of theory, models, and observation (e.g., De Sitter, 1956; Ramsay, 1967; Behzadi and Dubey, 1980; Ramsay and Huber, 1987; Gray and Wilman, 1991; Bhattacharya, 1992; Yang and Gray, 1994; Fowler and Winsor, 1997). However, the concept has not been widely recognized to apply to map-scale folds, where geometry and strain are difficult to quantify precisely at the scale of an entire fold, and where a very complex multi-layered mechanical stratigraphy is typical.

The interpretatation presented here is preliminary and highly generalized. It does not address other important factors that may influence fold geometry and kinematics, and does not account for the entire range of fold geometries observed. Departures from plane strain are likely, both by flow of incompetent material along strike and by loss of volume due to dissolution. The geometry and evolution of structure in the underlying basement has had a significant effect on detachment dip and local shortening in the detachment-folded cover. Resulting local differences in structural thickness of the incompetent Kayak Shale likely resulted in differences in detachment fold evolution. Specifically, the amount of structural thickening of Lisburne by parasitic folding at low to intermediate shortening may be inversely related to the local amount of structural thickening of the Kayak Shale.

Thrust-truncated detachment folds of the Porcupine Lake area

Mechanical stratigraphy

Previous work did not identify any significant change in mechanical stratigraphy across the Continental Divide thrust front in the Porcupine Lake area (Figure 1). In particular, the thickness of the incompetent Kayak Shale relative to the competent Lisburne Limestone doesn't appear to change significantly. Decrease in incompetent unit thickness has been suggested as one major factor that may control transition from folding to thrust faulting (e.g., Stewart, 1996, 1999), but that does not appear to be a factor in this area. Work during the summer of 1999 did, however, identify an apparent difference in the mechanical stratigraphy of the Lisburne Limestone: The unit appears to be more structurally competent and uniform south of the thrust front, with mechanical layering that is poorly defined through most of the section. The section displays two cycles that consist of a lower relatively thin and well-bedded interval under a thick massive interval. Carbonate mudstones dominate the well-bedded intervals and grainstones dominate the massive intervals. The section will be described and measured in detail in work planned for the summer of 2000.

Structural characteristics in western Porcupine Lake valley

The Porcupine Lake valley synclinorium marks the transition between unbroken symmetrical detachment folds to the north and thrust-truncated asymmetrical folds to the south (Figures 1, 9) (Wallace and Hanks, 1990; Wallace, 1993). The south limb of the synclinorium is defined by an anticlinal stack of thrust-truncated folds that probably is a remnant of the eastward continuation of the range front of the central Brooks Range that was preserved during younger formation of the northeastern Brooks Range. Observations during the summer of 1999 were based on a transect from the core of this synclinorium toward its south limb (Figure 10). The dominant structural elements on this transect are inclined asymmetrical folds commonly separated by non-folded panels. The short, steep limbs of most folds have been cut by thrust faults to produce hangingwall anticlines and footwall synclines, although one anticline-syncline pair has not been cut. Displacement on these thrusts is commonly sufficiently large to have resulted in long flat-on-flat panels. These panels indicate not only that thrust displacement was significant but that most individual folds formed in isolation, rather than being immediately adjacent to other folds as is typical throughout the northeastern Brooks Range. The folds have planar limbs with angular to narrow curved hinges and few parasitic folds. Interlimb angles typically are 70-50°, but locally are as small as 10°. Folds with larger interlimb angles may have a box-fold geometry in the outer arc, with a flat crest or trough bounded by two hinges that converge toward the fold core. Detailed work during the summer of 2000 will aim not only to document the fold and thrust geometry, but also to reconstruct the distance between folds prior to thrust displacement.

Evolution of thrust-truncated folds

Similar structures have also been observed south of the Continental Divide thrust front at the east end of Porcupine Lake valley on a transect along the Marsh Fork of the Canning River (Figure 9) (Wallace, 1993; Wallace and Homza, in review). The observations on these transects suggest that the folds originated prior to faulting, probably as detachment folds, and were later cut through their steep limbs by thrust faults (Figure 11). The presence of local syncline-anticline pairs that have not been cut by thrust faults, the presence of footwall synclines, and cutoff angles that typically are large indicate that the folds formed prior to their being cut and displaced by thrust faults. Kayak Shale is present in thrust sheets and fold cores farther to the south. This, the presence of unbroken folds, the fold-before-thrust timing, and the transition from the detachment folds of the northeastern Brooks Range suggest that the folds probably originated as detachment folds rather than fault-bend or fault-propagation folds (Wallace, 1993; Wallace and Homza, in review).

Why folds south of the Continental Divide thrust front typically are cut by thrusts and those to the north are not remains an unanswered question. Other differences to the south are the asymmetry of the folds, the lack of parasitic folds, the presence of non-folded panels between folds, and the apparently more competent mechanical stratigraphy. The more uniformly competent character of the Lisburne south of the Continental Divide thrust front probably accounts for the lack of parasitic folds and could have some influence on the distance between folds and the tendency of folds to fail by thrust faulting. Fold asymmetry clearly has a strong relationship to thrust breakthrough since thrusts preferentially cut short limbs. However, the factors that cause fold asymmetry remain unknown, as does the importance of asymmetry relative to other factors that could favor thrust breakthrough of folds.

Plans for future research

Study of detachment folds and their truncation by thrust faults in the Lisburne Limestone of the northeastern Brooks Range will continue in this project at several different levels. Paul Atkinson will construct detailed profiles of the detachment folds he studied in detail in the Fourth Range and Shublik Mountains. Wes Wallace will construct cross sections to scale to show variations in detachment fold geometry across the Echooka anticlinorium. Wallace and Atkinson will explore geometric-kinematic models designed to take into account the observations and interpretations to date, including the progression of fold geometry, changes in bed thickness with increasing shortening, and changes in detachment depth.

Two student thesis projects during the second summer of the study (2000) will focus on thrust-truncated detachment folds south of the Continental Divide thrust front near Porcupine Lake valley. One project will document detailed profiles of well-exposed thrust-truncated and unbroken asymmetrical detachment folds at the eastern end of Porcupine Lake valley. This project will also include mapping of several stacked thrust-truncated detachment folds to document their geometry in three dimensions. The other project will include mapping across several thrust-truncated and unbroken examples of asymmetrical detachment folds at the western end of Porcupine Lake valley. This project will also document the fracture patterns in these folds.
Wes Wallace will continue to document the characteristics of selected folds throughout the region, such as newly identified well-exposed examples of folds that represent low shortening. This is part of an effort to use maps, cross sections, and photographs to document the relationships among fold height, wavelength, arc wavelength, and interlimb angle throughout region.

References

Bhattacharya, A.R., 1992, A quantitative study of hinge thickness of natural folds; Some implications for fold development: Tectonophysics, v. 212, p. 371-377.

Behzadi, H., and Dubey, A.K., 1980, Variation of interlayer slip in space and time during flexural folding: Journal of Structural Geology, v. 2, p. 453-457.

Dahlstrom, C. D. A., 1990, Geometric constraints derived from the law of conservation of volume and applied to evolutionary models for detachment folding: American Association of Petroleum Geologists Bulletin, v. 74, p. 336-344.

De Sitter, L.U., 1956, Structural geology: McGraw-Hill, New York, 552 p.

Epard, J. -L., and Groshong, R. H., Jr., 1995, Kinematic model of detachment folding including limb rotation, fixed hinges and layer-parallel strain: Tectonophysics, v. 247, p. 85-103.

Fischer, M.P., Woodward, N.B., and Mitchell, M.M., 1992, The kinematics of break-thrust folds: Journal of Structural Geology, v. 14, p. 451-460.

Fowler, T.J., and Winsor, C.N., 1997, Characteristics and occurrence of bedding-parallel slip surfaces and laminated veins in chevron folds from the Bendigo-Castlemaine goldfields: Implications for flexural-slip folding: Journal of Structural Geology, v. 19, no. 6, p. 799-815.

Gray, D.R., and Wilman, C.E., 1991, Thrust-related strain gradients and thrusting mechanisms in a chevron-folded sequence, southeastern Australia: Journal of Structural Geology, v. 13, no. 6, p. 691-710.

Hanks, C.L., 1993, The Cenozoic structural evolution of a fold-and-thrust belt, northeastern Brooks Range, Alaska: Geological Society of America Bulletin, v. 105, no. 3, p. 287-305.

Homza, T.X., and Wallace, W.K., 1995, Geometric and kinematic models for detachment folds with fixed and variable detachment depths: Journal of Structural Geology, v. 17, no. 4, p. 475-588.

Homza, T.X., and Wallace, W.K., 1997, Detachment folds with fixed hinges and variable detachment depth, northeastern Brooks Range, Alaska: Journal of Structural Geology, v. 19,

nos. 3-4 (special issue on fault-related folding), p. 337-354.
Imm, T.A., Dillon, J.T., and Bakke, A.A., 1993, Generalized geologic map of the Arctic National Wildlife Refuge, northeastern Brooks Range, Alaska: Alaska Division of Geological and Geophysical Surveys Special Report 42, scale 1:500,000.
Jamison, W. R., 1987, Geometric analysis of fold development in overthrust terranes: Journal of Structural Geology, v. 9, p. 207-219.
Mitra, S., and Namson, J. S., 1989, Equal-area balancing: American Journal of Science, v. 289, p. 563-599.
Poblet, J., and Hardy, S., 1995, Reverse modelling of detachment folds; application to the Pico del Aguila anticline in the South Central Pyrenees (Spain): Journal of Structural Geology, v. 17, p. 1707-1724.
Poblet, J., and McClay, K., 1996, Geometry and kinematics of single-layer detachment folds: American Association of Petroleum Geologists Bulletin, v. 80, p. 1085-1109.
Poblet, J. , McClay, K., Storti, F., and Munoz, J.A., 1997, Geometries of syntectonic sediments associated with single-layer detachment folds: Journal of Structural Geology, v. 19, nos. 3-4, p. 369-381.
Ramsay, J. G., 1967, Folding and fracturing of rocks: McGraw Hill, New York, 568 p.
Ramsay, J.G., and Huber, M.I., 1987, The Techniques of Modern Structural Geology, Volume2: Folds and Fractures: Academic Press, New York, 392 p. (p. 309-700)
Rowan, M. G., and Kligfield, R., 1992, Kinematics of large-scale asymmetric buckle folds in overthrust shear: an example from the Helvetic nappes, in McClay, K. R., ed., Thrust tectonics: Chapman and Hall, London, p. 165-174.
Stewart, S.A., 1996, Influence of detachment layer thickness on style of thin-skinned shortening: Journal of Structural Geology, v. 18, no. 10, p. 1271-1274.
Stewart, S.A., 1999, Geometry of thin-skinned tectonic systems in relation to detachment layer thickness in sedimentary basins: Tectonics, v. 18, no. 4, p. 719-732.
Wallace, W.K., 1993, Detachment folds and a passive-roof duplex: Examples from the northeastern Brooks Range, Alaska, in Solie, D.N., and Tannian, F., eds., Short Notes on Alaskan Geology 1993: Alaska Division of Geological and Geophysical Surveys Geologic Report 113, p. 81-99.
Wallace, W.K., and Hanks, C.L., 1990, Structural provinces of the northeastern Brooks Range, Arctic National Wildlife Refuge, Alaska: American Association of Petroleum Geologists Bulletin, v. 74, no. 7, p. 1100-1118.
Wallace, W.K., and Homza, T.X., 1998, Detachment folds with fixed hinges and variable detachment depth, northeastern Brooks Range, Alaska: Reply: Journal of Structural Geology, v. 20, no. 11, p. 1591-1595.
Wallace, W.K., and Homza, T.X., in review (1999), Detachment folds, their truncation by thrust faults, and their distinction from fault-propagation folds, in McClay, K.R., editor, Thrust tectonics and petroleum systems: American Association of Petroleum Geologists Memoir.
Wallace, W.K., Moore, T.E., and Plafker, G., 1997, Multistory duplexes with forward dipping roofs, north central Brooks Range, Alaska: Journal of Geophysical Research, v. 102, no. B9 (special section on the USGS Trans-Alaska Crustal Transect), p. 20,773-20,796.
Watts, K.F., Harris, A.G., Carlson, R.C., Eckstein, M.K., Gruzlovic, P.D., Imm, T.A., Krumhardt, A.P., Lasota, D.K., Morgan, S.K., Dumoulin, J.A., Enos, P., Goldstein, R.H., and Mamet, B.L., 1995, Analysis of reservoir heterogeneities due to shallowing-upward cycles in carbonate rocks of the Pennsylvanian Wahoo Limestone of northeastern Alaska: United States Department of Energy, Final Report for 1989-1992 (DOE/BC/14471-19), Bartlesville Project Office, 433 p.
Yang, X., and Gray, D.R., 1994, Strain, cleavage and microstructure variations in sandstone: Implications for stiff layer behaviour in chevron folding: Journal of Structural Geology, v. 16,

no. 10, p. 1353-1365.

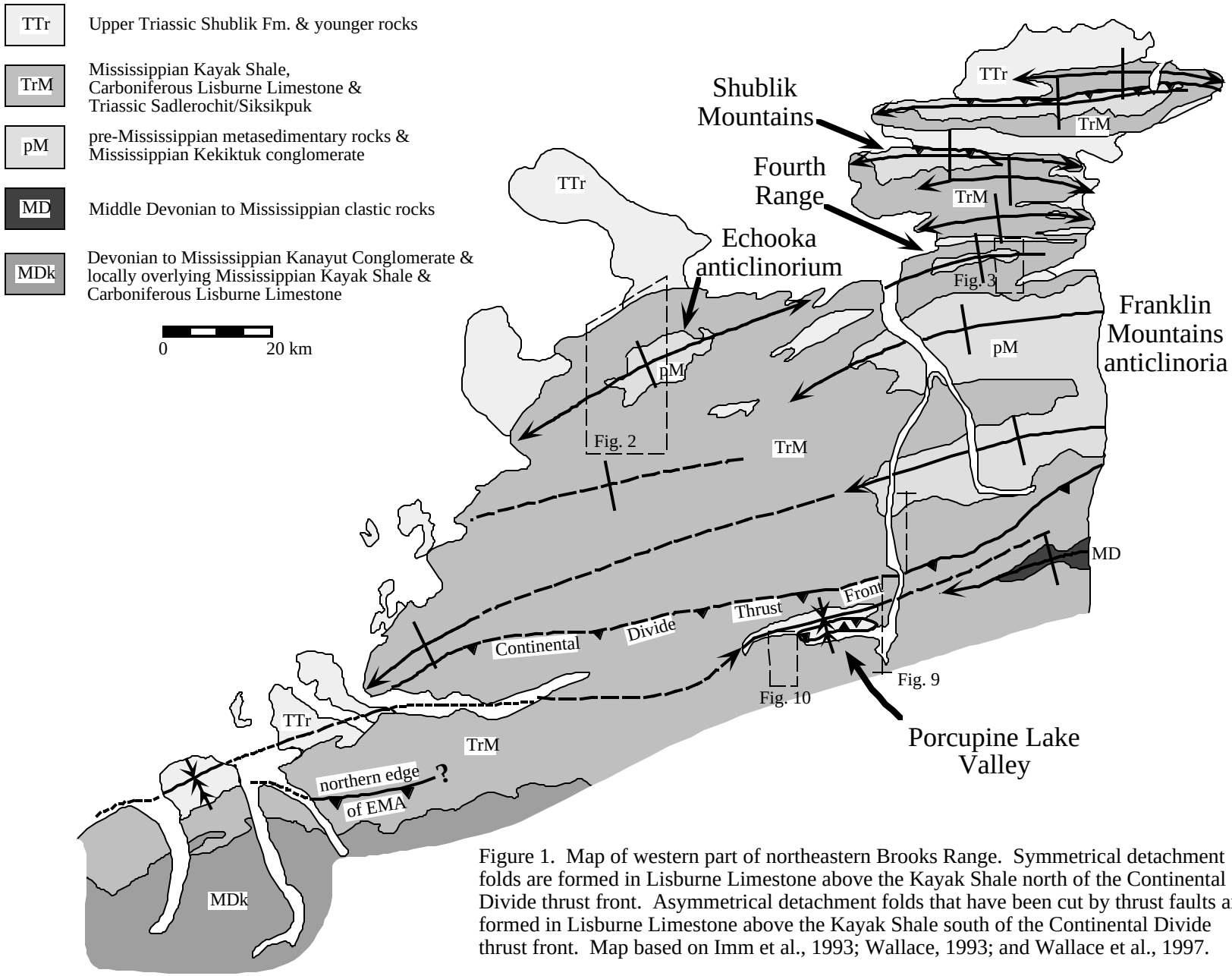

Figure 1. Map of western part of northeastern Brooks Range. Symmetrical detachment folds are formed in Lisburne Limestone above the Kayak Shale north of the Continental Divide thrust front. Asymmetrical detachment folds that have been cut by thrust faults are formed in Lisburne Limestone above the Kayak Shale south of the Continental Divide thrust front. Map based on Imm et al., 1993; Wallace, 1993; and Wallace et al., 1997.

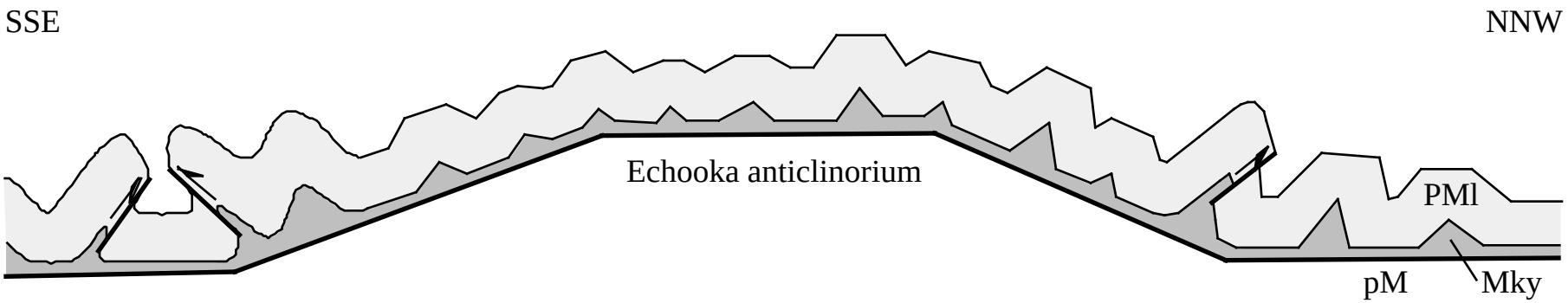

Figure 2. Schematic cross section across the Echooka anticlinorium. This illustrates the approximate location and geometry of structures across the area outlined in figure 1, but is not to scale. pM: Pre-Mississippian rocks and Kekiktuk Conglomerate; Mky: Kayak Shale; PMl: Lisburne Limestone.

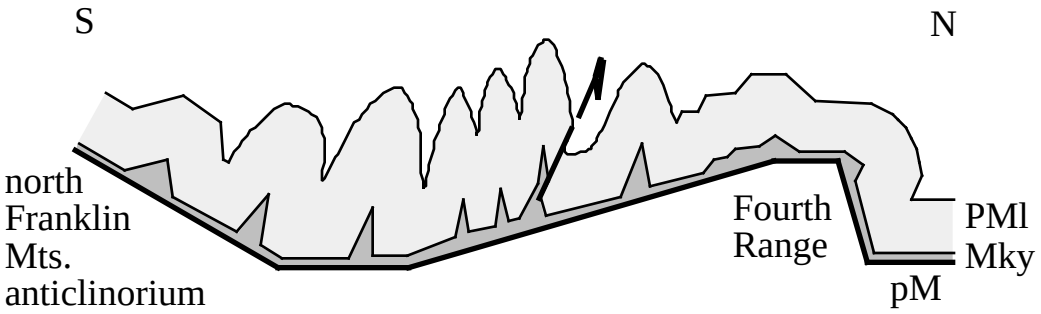

Figure 3. Schematic cross section from the Fourth Range to the northern edge of the northern Franklin Mountains anticlinorium. This illustrates the approximate location and geometry of structures across the area outlined in figure 1, but is not to scale. pM: Pre-Mississippian rocks and Kekiktuk Conglomerate; Mky: Kayak Shale; PMl: Lisburne Limestone.

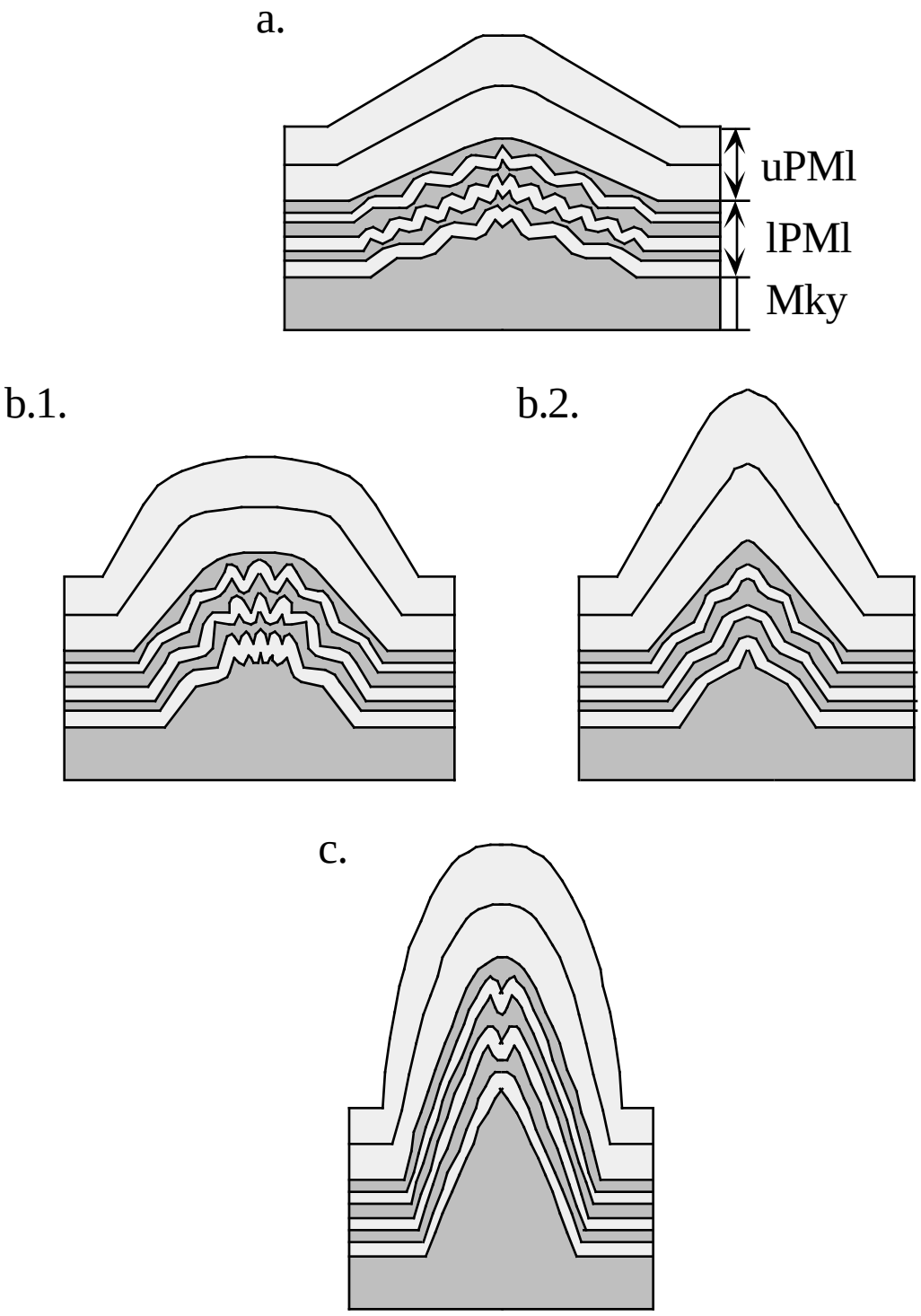

Figure 4. Evolution of detachment folds in the northeastern Brooks Range. Schematic and not balanced. A single isolated fold with constant detachment depth is shown for simplicity. However, most anticlines in the northeastern Brooks Range are separated from adjacent anticlines by synclines, and detachment depth varies. a. Low shortening; b.1. Intermediate shortening, box-fold geometry; b.2. Intermediate shortening, chevron fold geometry; c. High shortening. Note that the flat crest of the box-fold geometry allows these folds to become isoclinal (interlimb angle of 0°) yet still represent only intermediate shortening. Mky: Kayak Shale (incompetent); lPMl: lower Lisburne Limestone (transitional competency); uPMl: upper Lisburne Limestone (competent).

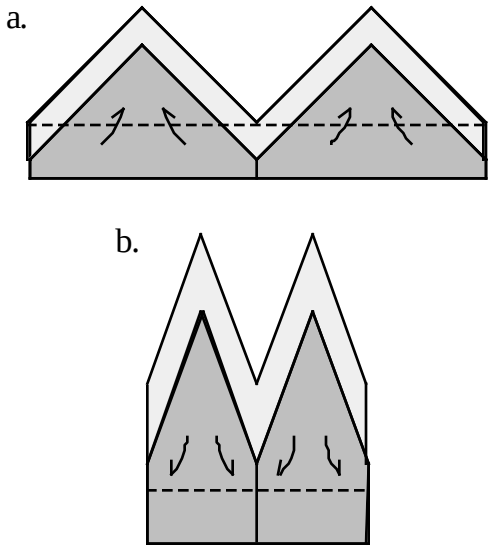

Figure 5. Evolution of neighboring fixed-hinge detachment folds joined at hinges, without an intervening non-folded panel. Light shading: competent unit. Dark shading: incompetent unit. Dashed horizontal line indicates original thickness of incompetent unit. Detachment depth, i.e. thickness of incompetent unit at synclinal hinges (vertical dashed lines), must vary to accommodate changes in cross-sectional area of anticline as interlimb angle decreases. (a) Interlimb angle of 90°. Maximum cross-sectional area of anticline, minimum detachment depth. (b) Interlimb angle of 40°. Cross-sectional area of anticline has decreased significantly, resulting in increase in thickness of incompetent unit to greater than its original thickness.

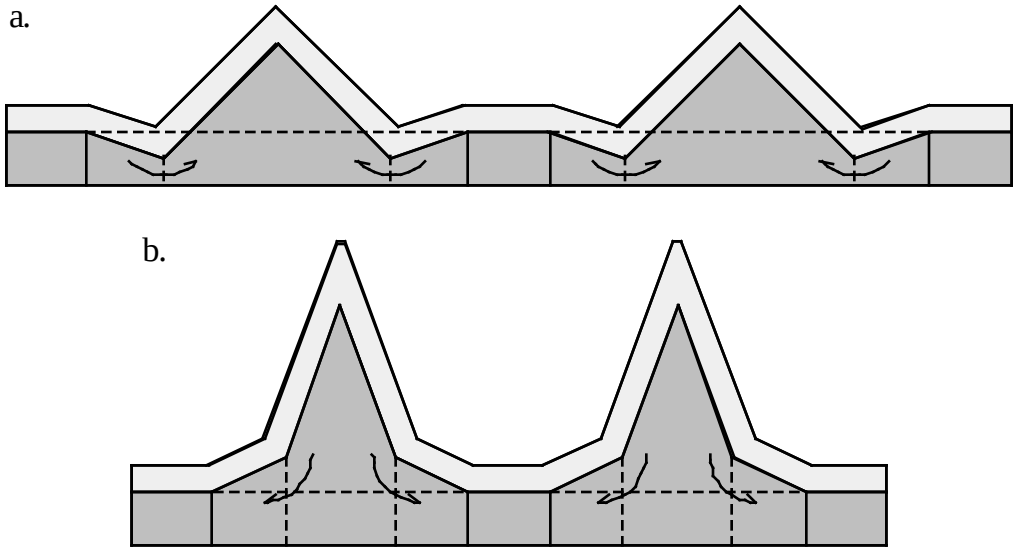

Figure 6. Evolution of neighboring fixed-hinge detachment folds separated by an intervening non-folded panel. Light shading: competent unit. Dark shading: incompetent unit. Dashed horizontal line indicates original thickness of incompetent unit. As interlimb angle decreases, changes in cross-sectional area of anticline are accommodated by movement of incompetent material through the inner synclinal hinges (vertical dashed lines). Resulting changes in cross-sectional area outside of the inner synclinal hinges are distributed evenly beneath outer fold limbs. The outer hinges have a constant detachment depth equal to the original thickness of the incompetent unit and define outer boundaries of the fold (vertical solid lines) through which no net movement of incompetent material has occurred. (a) Interlimb angle of 90°. Maximum cross-sectional area of anticline, minimum detachment depth as measured at inner synclinal hinges. Increase in anticline area has been accommodated by movement of incompetent material inward through inner synclinal hinges. (b) Interlimb angle of 40°. Cross-sectional area of anticline has decreased significantly, resulting in movement of incompetent material outward through inner synclinal hinges. Thickness of incompetent unit is greater than its original thickness everywhere between outer hinges.

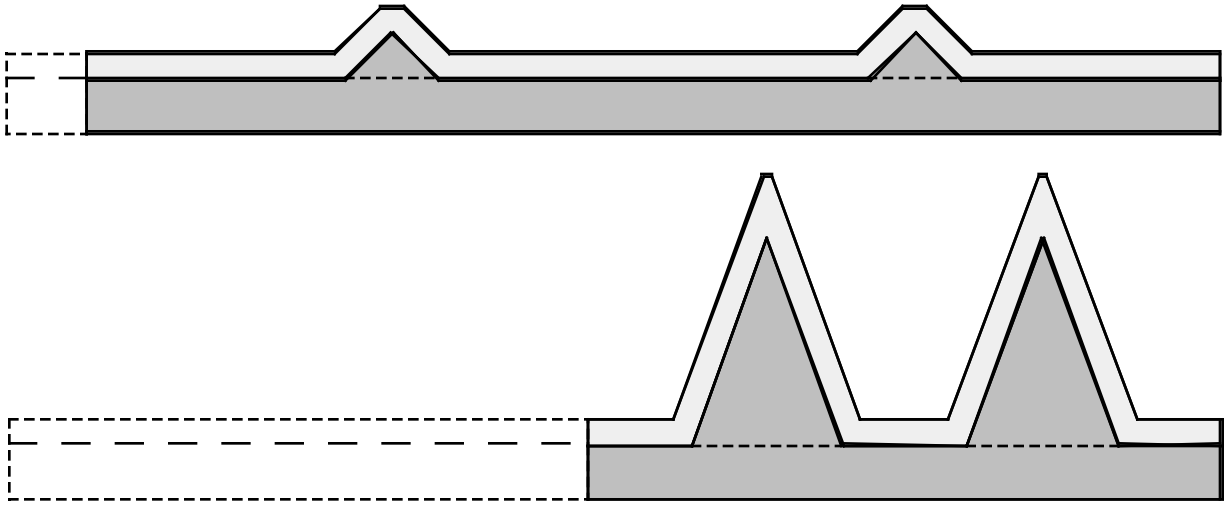

Figure 7. Evolution of detachment folds with fixed anticlinal hinges and migrating synclinal hinges. Light shading: competent unit. Dark shading: incompetent unit. Dashed horizontal line indicates original thickness of incompetent unit. As interlimb angle decreases with increasing shortening, synclinal hinges migrate so that the area of the incompetent unit in the fold core allows detachment depth to remain constant (e.g. Dahlstrom, 1990; Poblet and McClay, 1996). This results in a significant increase in arc length as shortening increases. a. Interlimb angle of 90°. b. Interlimb angle of 40°.

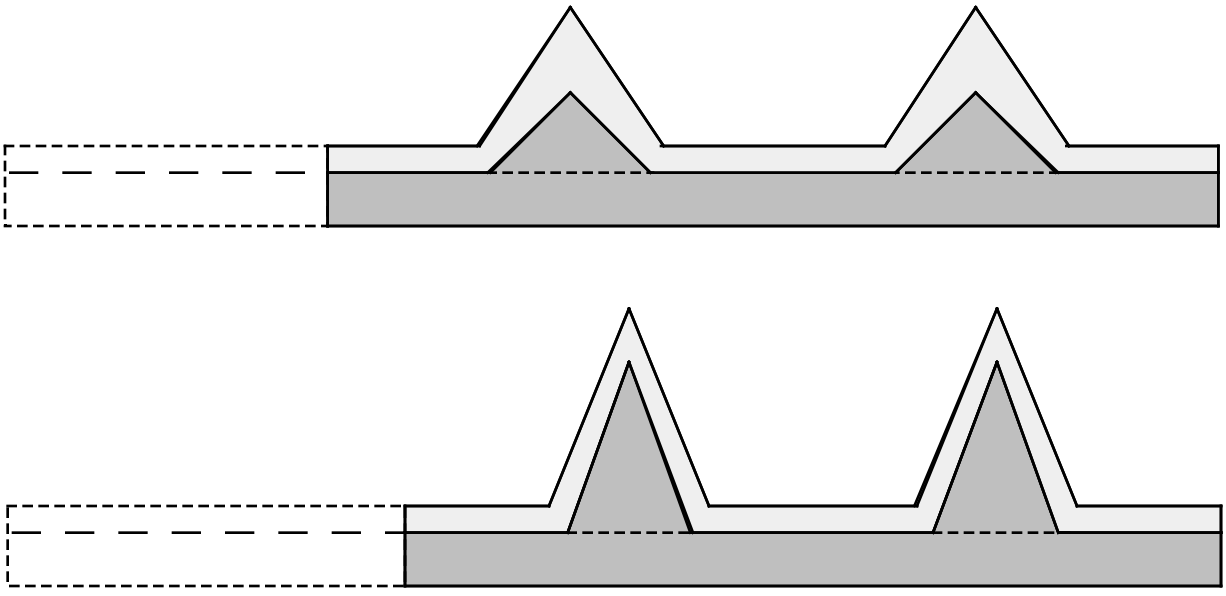

Figure 8. Evolution of detachment folds with fixed hinges and constant detachment depth. Light shading: competent unit. Dark shading: incompetent unit. Dashed horizontal line indicates original thickness of incompetent unit. Maintaining constant detachment depth with fixed hinges requires that the fold maintain constant cross sectional area as shortening increases. This is accomplished by varying bed thickness and length within the fold according to the model of Epard and Groshong (1995). a. Interlimb angle of 90°, displaying thickening of the competent unit in the anticlinal hinge. b. Interlimb angle of 40°, displaying thinning of the competent unit in the anticlinal hinge. Resulting fold geometries will vary according to spacing of hinges and stratigraphic height above the detachment.

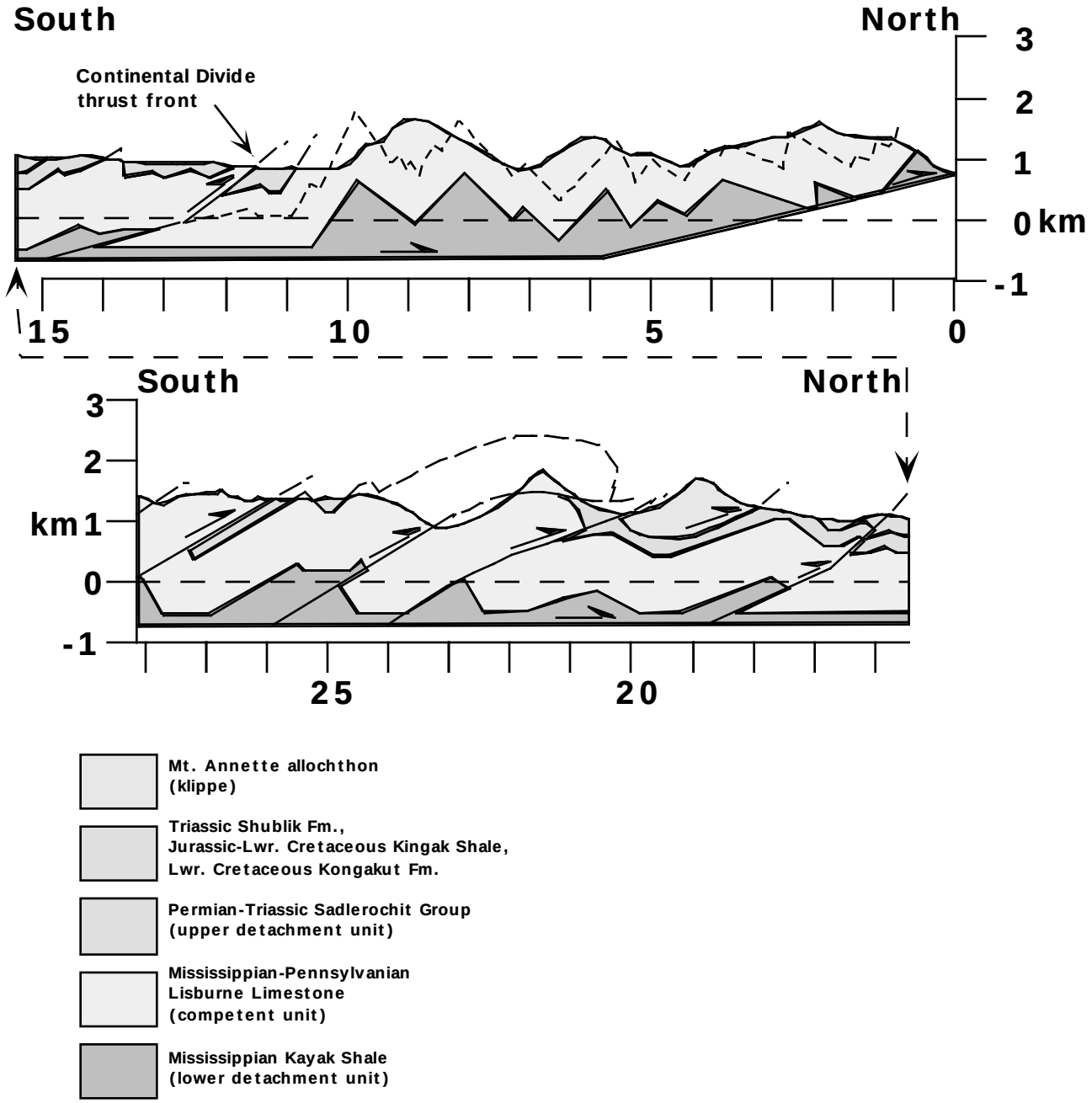

Figure 9. Cross section across eastern Porcupine Lake valley. Line of section is shown in figure 1. The upper (northern) part shows unbroken upright and symmetrical detachment folds typical of the northeastern Brooks Range, north of the Continental Divide thrust front. The lower (southern) part shows thrust-truncated detachment folds typical of the main axis of the Brooks Range, south of the Continental Divide thrust front.

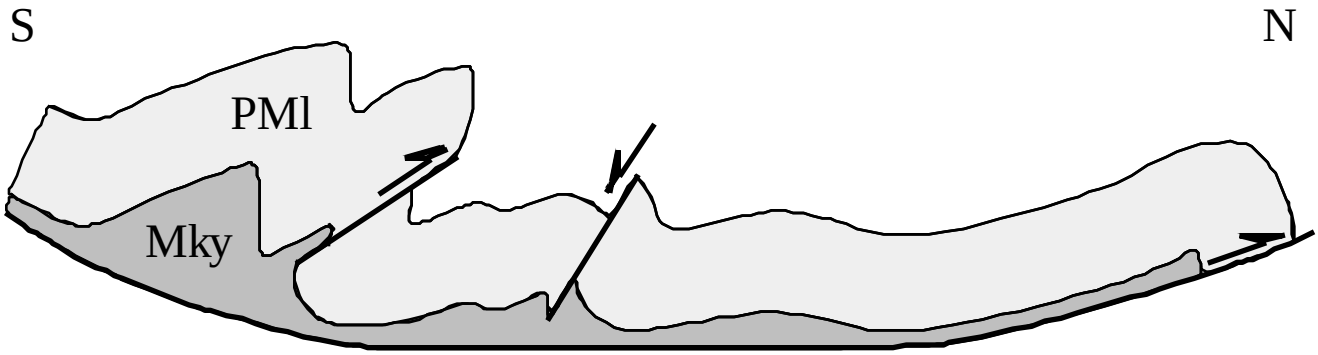

Figure 10. Schematic cross section across the south limb of the Porcupine Lake valley synclinorium at its west end. This illustrates the approximate location and geometry of structures across the area outlined in figure 1, but is not to scale. pM: pre-Mississippian rocks and Kekiktuk Conglomerate; Mky: Kayak Shale; PMl: Lisburne Limestone.

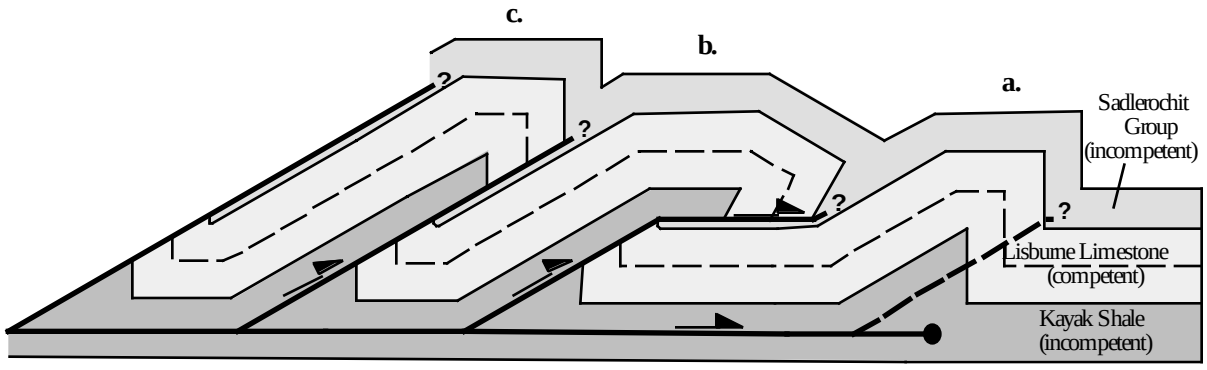

Figure 11. Thrust-truncation of detachment folds. a. Truncated anticlines b. and c. originated from a detachment fold of this geometry by displacement on thrust faults with trajectories as shown by the dashed line. b. Breakthrough and displacement of the anticline onto an upper flat that is not coplanar with the ramp has resulted in formation of a fault-bend fold with an anomalously steep forelimb. c. Breakthrough and displacement of the anticline onto an upper flat that is coplanar with the ramp has resulted in truncation but no other modification of fold geometry. Tilting of the upper flat may have occurred either before or after breakthrough as a normal consequence of thrust imbrication.

A geometric analysis of detachment folds in the Lisburne Limestone

by P.K. Atkinson, Geophysical Institute and Department of Geology and Geophysics, University of Alaska, Fairbanks, Alaska 99775-5780. fspka@aurora.uaf.edu

Abstract

Last summer I studied several well-exposed map-scale detachment folds in the Shublik Mountains and Fourth Range of Arctic National Wildlife Refuge, Alaska. These folds consist of relatively competent Lisburne Limestone overlying relatively incompetent Kayak Shale. I mapped and measured the geometry of these folds in detail, with special emphasis on documenting changes in the thickness and lithology of different layers within the Lisburne.

Preliminary results of my study show that, as a whole, the Lisburne does vary in thickness throughout a fold, with some layers thickening or thinning more than others due to differences in mechanical stratigraphy. Internal strain and higher-order folding and faulting all contribute to these differences in structural thickness. Interlimb angles and orientation of axial surfaces of map-scale folds vary according to their position over the underlying fault-bend anticlinoria. Fold shapes also vary substantially along strike over short distances.

These observations provide evidence that detachment folds form in a manner different from that predicted by existing models. In a modified, hybrid model, both the competent and incompetent layers thicken to varying degrees, and material from the underlying incompetent layer moves into or out of the anticline core (depending on interlimb angle), thus thickening or thinning the incompetent layer in the adjoining synclines.

Introduction

I spent five weeks last summer conducting fieldwork in the Shublik Mountains and Fourth Range of Arctic National Wildlife Refuge, Alaska (Figure 1). My main objective was to document how the Lisburne Limestone in these mountains has responded to shortening by folding above a regional detachment surface (décollement) in the underlying incompetent Kayak Shale (Figures 2 and 3). In particular, I wanted to know how the Lisburne varies in structural thickness across these folds, and how variations in structural competency within the Lisburne have affected folding. A better understanding of these variables could lead to a more realistic model of the kinematic evolution of detachment folds.

Over the past decade, a number of models have been proposed for the evolution of detachment folds. Two of the most recent models have focused on changes in bed length and changes in the thickness of a ductile layer underlying a more competent layer. The Homza and Wallace (1995,

1997) model assumes that detachment folding involves a single, homogeneous, competent layer above a single, homogeneous, less-competent layer, and that the competent layer maintains constant length throughout the folding process. The Epard and Groshong (1994, 1995) model, on the other hand, does not differentiate between mechanical layers in the fold; rather, it implies that all layers are more-or-less equally competent with no mechanical differences. Many natural detachment folds, however, exhibit complicated interbedding patterns with varying mechanical stratigraphy, suggesting that both of these models are greatly oversimplified.

Methods

Excellent exposures of several map-scale detachment folds in the Shublik Mountains and Fourth Range allowed me to document and characterise their geometry in detail using a combination of mapping, surveying, and photographic methods. I mapped and measured marker horizons, attitudes of beds, axial surfaces and hinges, and variation in thickness of beds. Measurements were taken directly, and also remotely using Rockwell Viper laser rangefinder binoculars. In addition, I collected numerous rock samples which I can analyse to better determine rock composition and relative competency, strain directions, ages and burial depths. Figures 4 and 5 show preliminary geological mapping done in the study area; Figures 7 through 9 illustrate some of the types of deformation observed, and Figures 10 through 16 illustrate the general geometry of the major map-scale folds I photographed and measured.

From the data collected, I am now recreating the exact geometry of each of these folds. This will allow me to construct accurate, balanced cross-sections, emphasizing changes in bedding orientation and unit thickness, as well as to reconstruct the evolution of each fold.

Observations

Once in the field, I immediately discovered that the thickness of the Lisburne Limestone can and does vary significantly across a fold. These differences in thickness manifest themselves in a variety of complicated ways, including combinations of higher-order and disharmonic folds (Figure 7), small-scale contractional faults (Figure 8), and internal strain (Figure 9). Beds of differing structural competency within the Lisburne react to shortening very differently, with the thicker-bedded and more massive lower Wahoo Formation generally exhibiting more internal strain, and the underlying Alapah Formation showing a greater tendency to form higher-order and disharmonic folds. Internal strain is obvious both in bed thinning/thickening and in strained crinoid columns.

Fold shapes in the Lisburne vary considerably along a transect across the Shublik Mountains and Fourth Range, some being open and rounded (e.g., Folds 3 and 4; Figures 12 and 13) and others tight to nearly isoclinal (e.g., Fold 1; Figures 9 and 10). Fold shapes change radically along

strike, as well. These folds are, in a three-dimensional, geographical sense, extremely variable and discontinuous. This is especially evident on the Shublik Mountains geologic map (Figure 5), where folds form and fade along strike, constantly changing shape and character. When viewed on a smaller scale, the fractal dimension of some folds in the lower Lisburne becomes apparent, with folds within folds within folds.

Preliminary Interpretations

The obvious variation in structural thickness and structural competency within the Lisburne has broad implications in modelling detachment fold formation. The Homza and Wallace (1995, 1997) model requires that the Lisburne maintain constant bed length with no layer-parallel shortening; thus, to maintain area balance, a large amount of the underlying, ductile Kayak Shale must migrate into the fold as it increases in area in its early development. In fact, if the Kayak is thin relative to limb length, insufficient material can be supplied from under the synclines — either material must be transported from elsewhere or the detachment will lock.

However, if the overlying Lisburne deforms and shortens (due to internal strain, higher-order folding and faulting, solution cleavage, fracturing or a combination of these), less additional ductile material is required to maintain constant area. How much extra incompetent material is required depends not only on limb length and interlimb angle, but also on the stratigraphic thickness of the overlying Lisburne and the degree to which structural thickening occurs in both the Lisburne and the Kayak.

Figures 12a and 12c show how a symmetric, angular fold would form according to the Homza and Wallace, and Epard and Groshong models if we assume realistic initial thicknesses of 500 m and 150 m for the Lisburne and Kayak, respectively, and a limb length of 750 m. Using the Homza and Wallace model, no layer-parallel shortening occurs in the overlying Lisburne, and the detachment locks after 150 m of horizontal displacement (assuming no additional incompetent material is introduced into the fold from outside the plane of section). Under the Epard and Groshong model, constant area is maintained strictly through layer-parallel shortening in both units — an unlikely scenario in light of the obvious contrast in structural competency between the Lisburne Limestone and Kayak Shale. Figure 12b shows one possibility for how a fold might deform using the same fold geometry as described above, together with a moderate amount (281 m) of shortening in the Lisburne. Depending on the amount of shortening, a whole continuum of folds which vary in amplitude and width is possible. We can think of this continuum as simply a hybrid between the Homza and Wallace, and Epard and Groshong end-member models.

The fractal dimension of some of the folds I observed emphasises the importance of scale when modelling fold evolution and geometry. Although relatively competent compared to the underlying Kayak Shale, the Lisburne Limestone itself consists of many beds of varying

competencies, and thus is far from a single homogeneous unit. Especially within the Alapah Formation, thinner, more-competent beds often fold above décollements in underlying less-competent beds, resulting in higher order folds. This can be difficult to quantify at larger, map scales.

The variation in fold shape along a north-south transect across these folds probably reflects a fold's position over the underlying structure in pre-Mississippian rocks. The décollement over which the Kayak and Lisburne detached is not flat, but rather a series of anticlinoria, each formed over a fault-bend folded horse (Wallace, 1993; Figure 3). The more open folds with rounded hinges would likely be found over the horses' heads (e.g., Folds 3 and 4) and tighter folds with small interlimb angles (e.g., Fold 1) in the synclinoria between horses. Folds with steeply inclined axial surfaces (e.g., Folds 2, 5, 6 and 7) have formed over the horses' necks and foreheads.

Finally, the fact that the character of these folds is so variable along strike emphasizes that their evolution is far more complex than we can ever hope to explain with simple two-dimensional models. The development of a fold must certainly depend on everything that is happening to it in *all* directions, not just in a vertical plane in the direction of maximum compression.

Continuing Work

Continuing work on this project includes (1) refining my geologic maps from photographs and new interpretations; (2) tracing the geometry of individual beds within folds in more detail on photographs; (3) processing rangefinder and bedding orientation data to reconstruct the geometry of these folds using a computer three-dimensional surfacing program; (4) processing rock samples for conodont identification and making oriented thin sections to determine age, depth of burial, strain and rock composition; and (5) creating balanced cross-sections of each fold.

I plan to publish preliminary results in a public data file with the Alaska Division of Geological and Geophysical Surveys, as well as present a poster at the Tectonics and Sedimentation Research Group sponsors meeting in Spring, 2000.

Comments

The Rockwell Viper laser rangefinder binoculars were, in my opinion, worth every penny of their (huge) cost, if only because their superb optics allowed me to pick out many details that would otherwise have been completely invisible. Any rangefinder with capabilities less than the Viper (such as the Leica Vector) would have been inadequate for the task since in many instances the only suitable vantage points for looking at entire folds were on ridges more than one km distant.

The binoculars were also valuable for mapping, since I could determine the relative elevations of distant contacts and structures.

Unfortunately, the Viper binoculars were not accurate enough for me to measure thicknesses of individual beds at a distance. I have not yet plotted the rangefinder data I gathered, so am still uncertain if the accuracy is good enough to recreate surface geometries using a computer surfacing program. (Also, while the fold exposures were generally very good, I was rarely able to trace individual beds across an entire fold, thus further complicating computer generation of surfaces.) We probably could improve the accuracy of our data somewhat by taking azimuth and elevation measurements using a small theodolite. This would be difficult and time-consuming since we would have to train two separate instruments on the same point for each measurement, but the improved data obtained might make it worth the effort.

References

Epard, J.-L. and Groshong, R.H., Jr., 1995, Kinematic model of detachment folding including limb rotation, fixed hinges and layer-parallel strain: Tectonophysics, v. 247, p. 85-103.

Groshong, R.H., Jr. and Epard, J.-L., 1994, The role of strain in area-constant detachment folding: Journal of Structural Geology, v. 16, p. 613-618.

Homza, T.X. and Wallace, W.K., 1995, Geometric and kinematic models for detachment folds with fixed and variable detachment depths: Journal of Structural Geology, v. 17, p. 575-588.

Homza, T.X. and Wallace, W.K., 1997, Detachment folds with fixed hinges and variable detachment depth, northeastern Brooks Range, Alaska: Journal of Structural Geology, v. 19, p. 337-354.

Wallace, W.K. 1993, Detachment folds and a passive-roof duplex: examples from the northeastern Brooks Range, Alaska: *in* Solie, D.N. and Tannian, F., eds., Short notes on Alaskan Geology, Alaska Division of Geological and Geophysical Surveys Professional Report 113, p. 81-99.

Wallace, W.K. and Hanks, C.L., 1990, Structural provinces of the northeastern Brooks Range, Arctic National Wildlife Refuge, Alaska: American Association of Petroleum Geologists Bulletin, v. 74, p. 1100-1118.

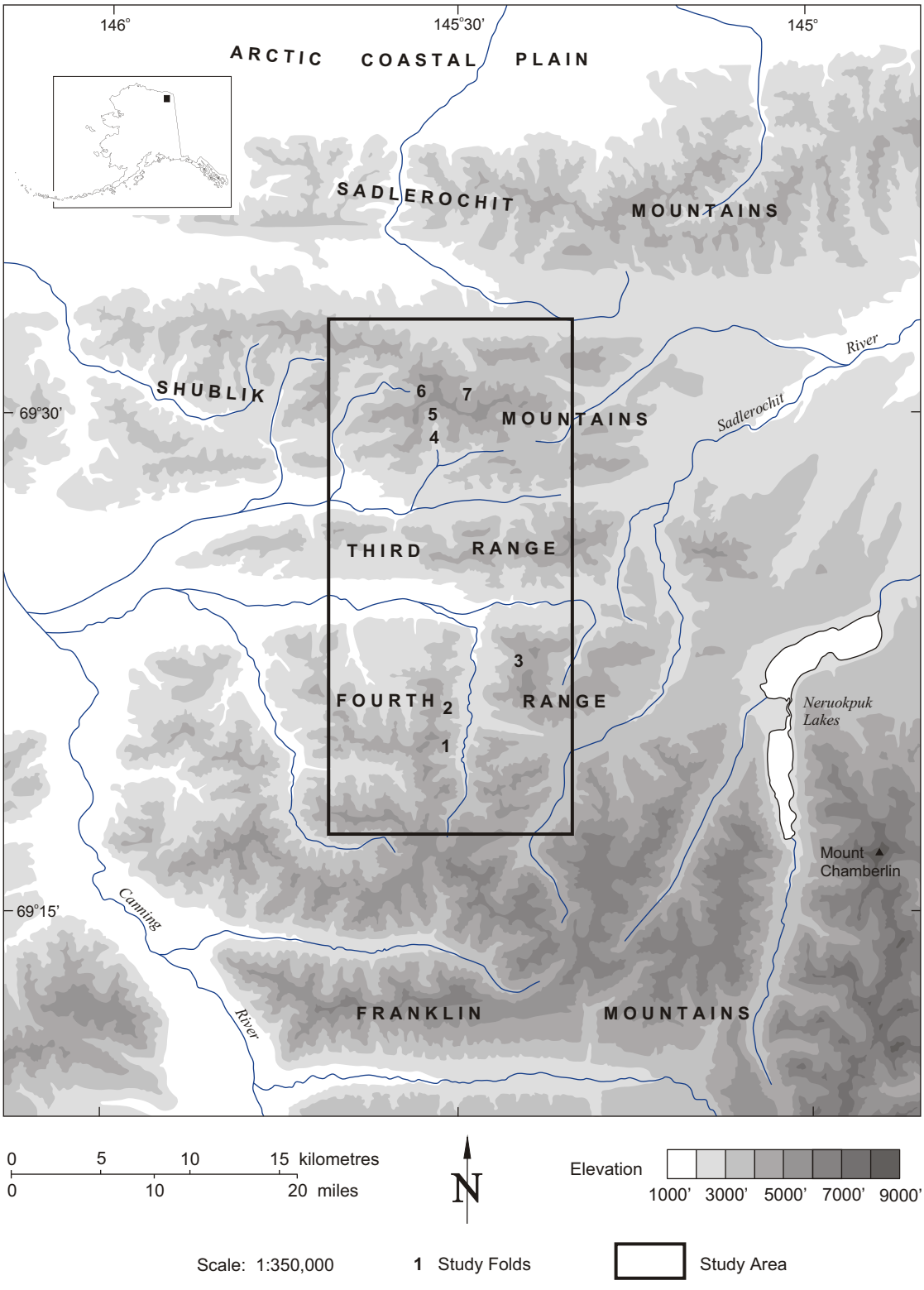

Figure 1: Location and physiography of study area, northeastern Brooks Range, Alaska.

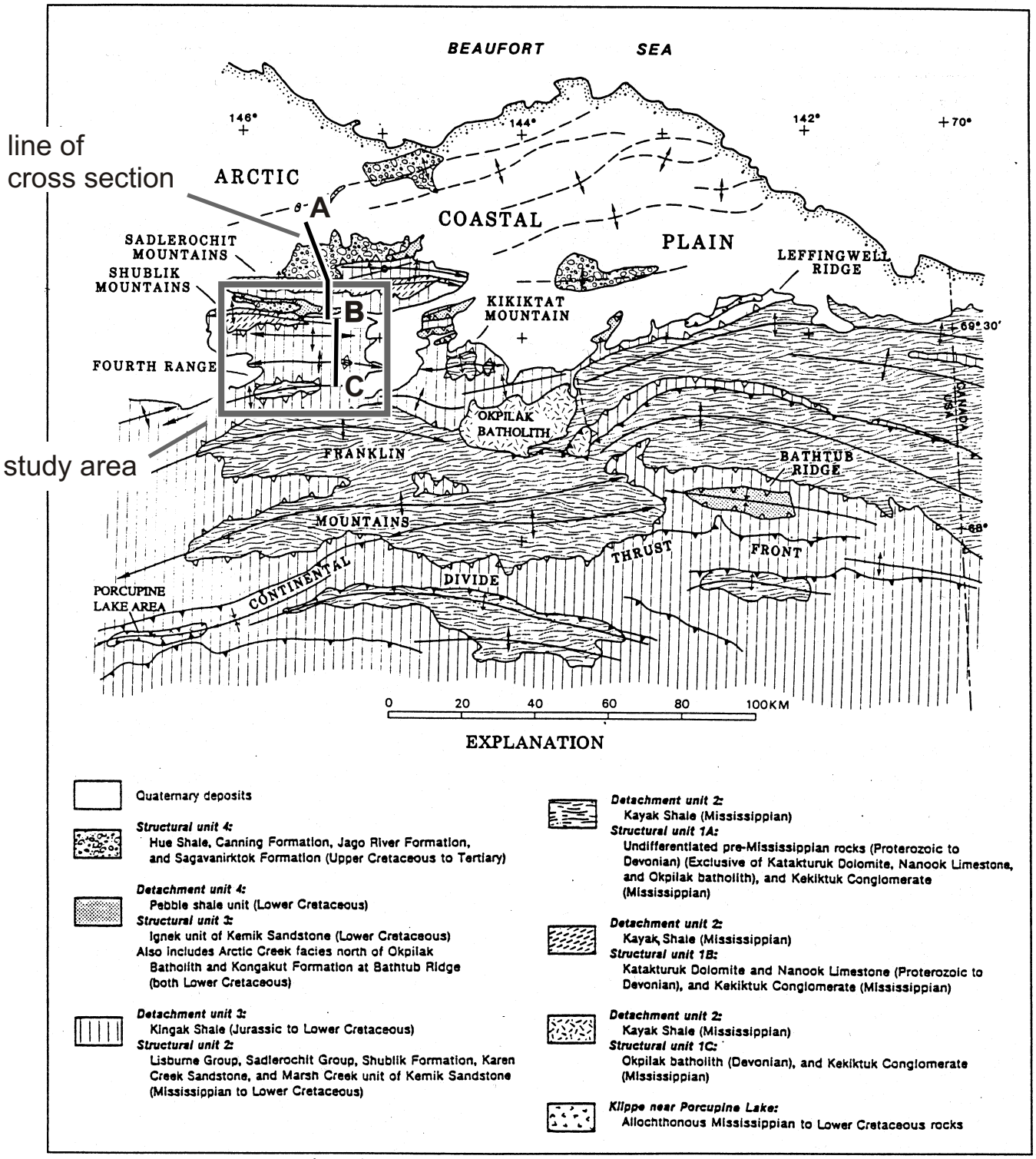

Figure 2: Generalized tectonic map of northeastern Brooks Range, Alaska, showing study area and line of cross-section in Figure 3. Modified from Wallace and Hanks, 1990.

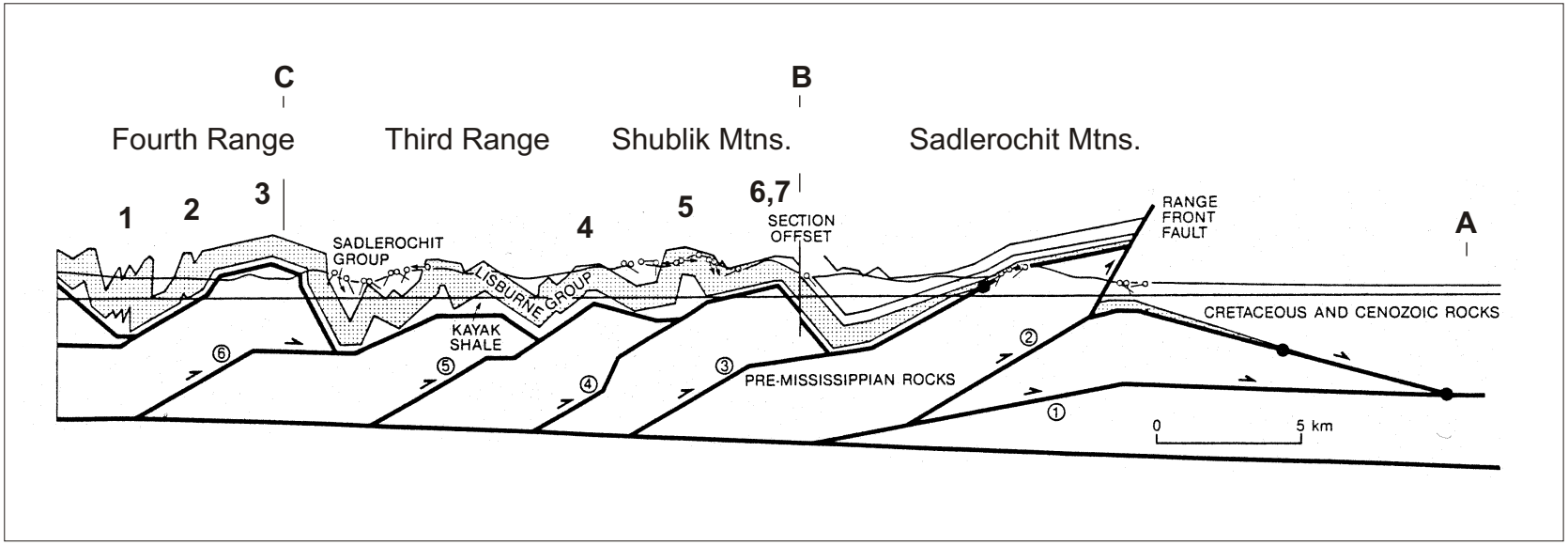

Figure 3: Balanced cross section through study area shown in Figures 1 and 2. Numbers mark approximate locations of detachment folds in Lisburne Limestone which are shown on Figure 1. Open folds with rounded hinges occur over anticlinoria of underlying pre-Mississippian duplexes, while tighter folds occur over synclinoria. Modified from Wallace, 1993.

DE-AC26-98BC15102

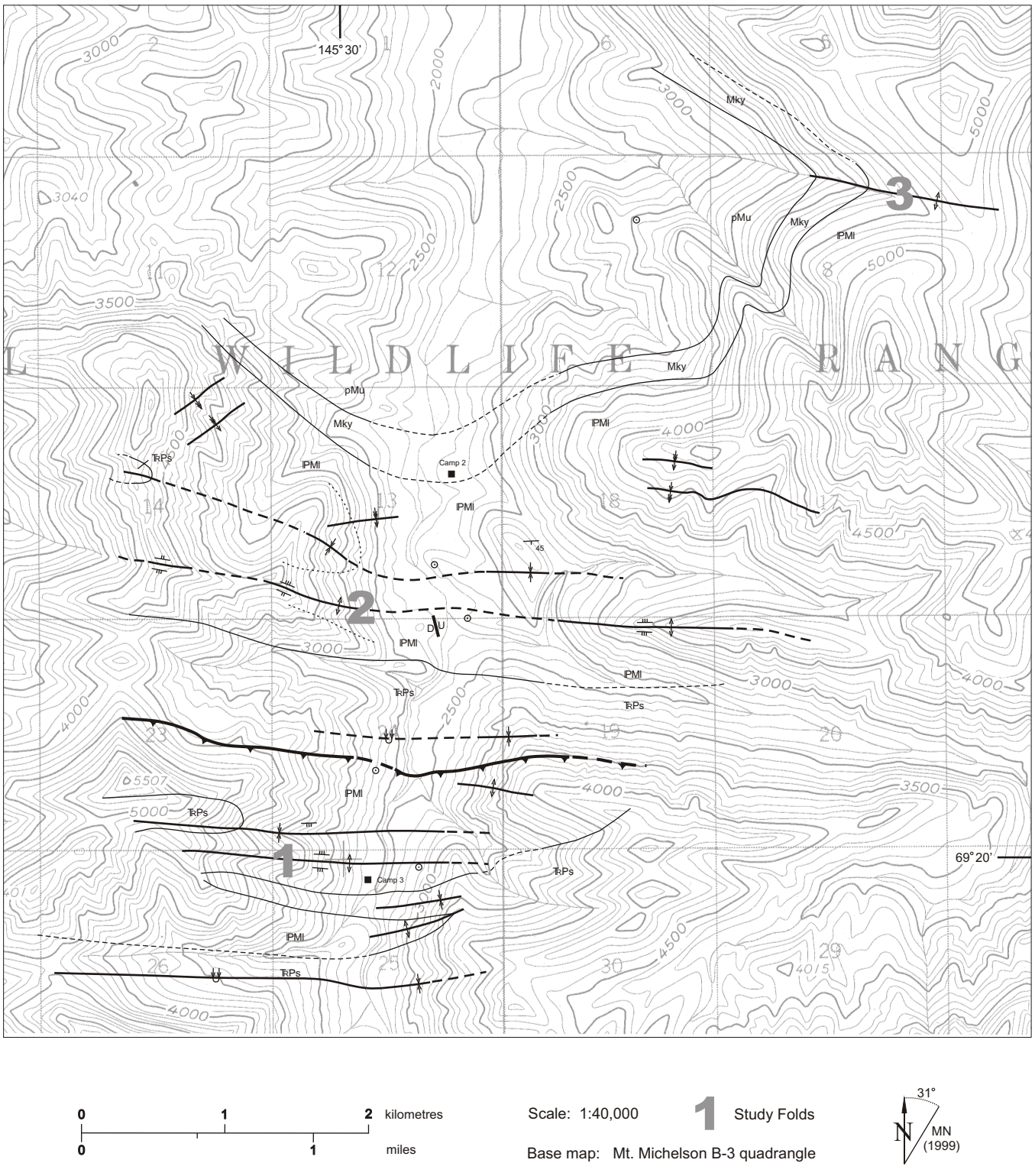

Figure 4: Preliminary bedrock geologic map of the Straight Creek area, Fourth Range, Arctic National Wildlife Refuge, Alaska. See Figure 6 for explanation of symbols.

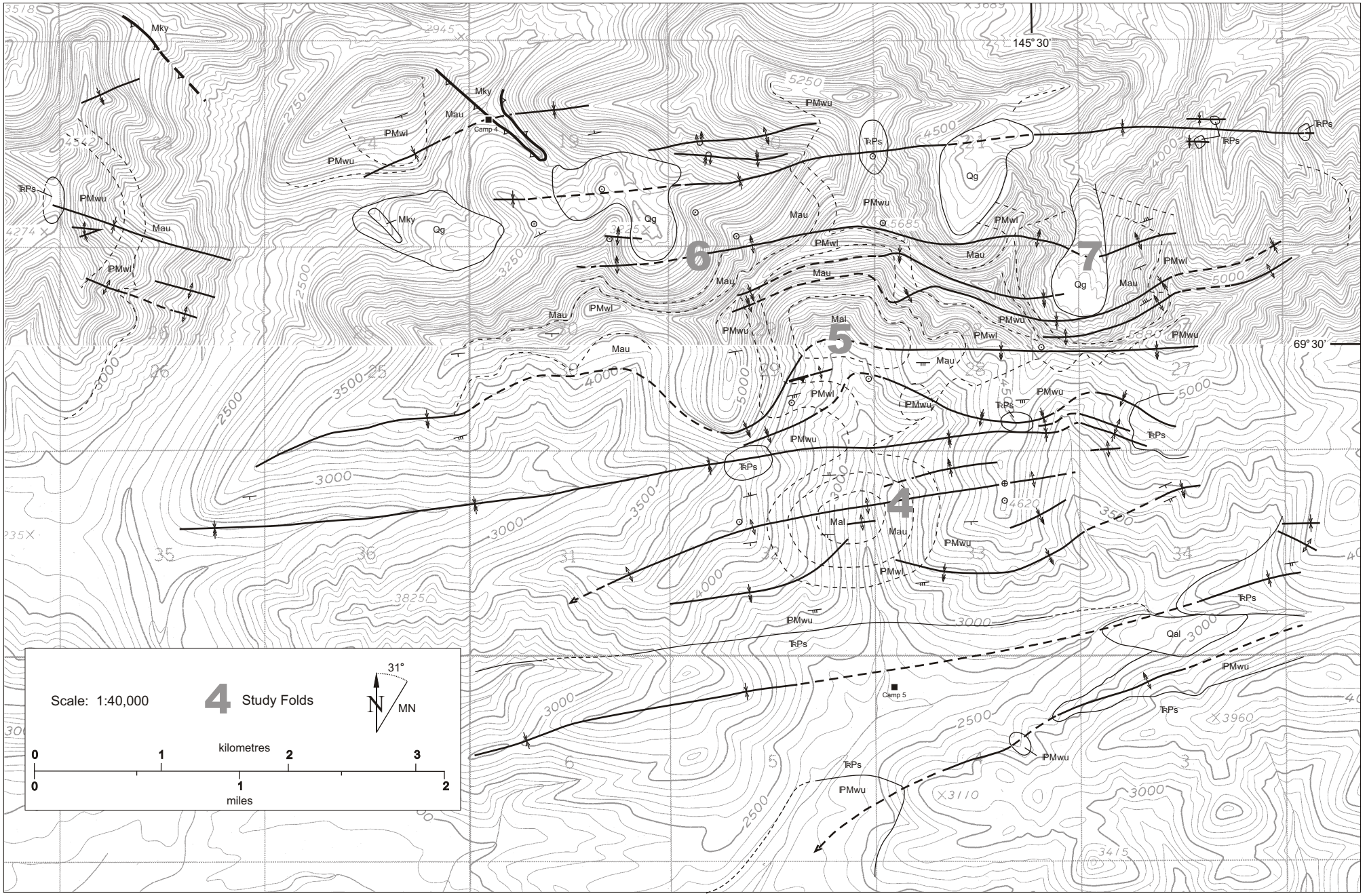

Figure 5: Preliminary bedrock geologic map of the central Shublik Mountains, Arctic National Wildlife Refuge, Alaska. See Figure 6 for explanation of symbols used.

Quaternary deposits

Qal alluvium
Qg glacial deposit
Qu undifferentiated Quaternary

Sadlerochit Group

TRPs undifferentiated Sadlerochit

Lisburne Group

IPMwu upper Wahoo Formation
IPMwl lower Wahoo Formation
Mau upper Alapah Formation
Mal lower Alapah Formation
IPMl undifferentiated Lisburne

Endicott Group

Mky Kayak Shale

Pre-Mississippian Rocks

pMu undifferentiated pre-Mississippian

Figure 6: Explanation of geologic symbols and rock type abbreviations used in Figures 4 and 5.

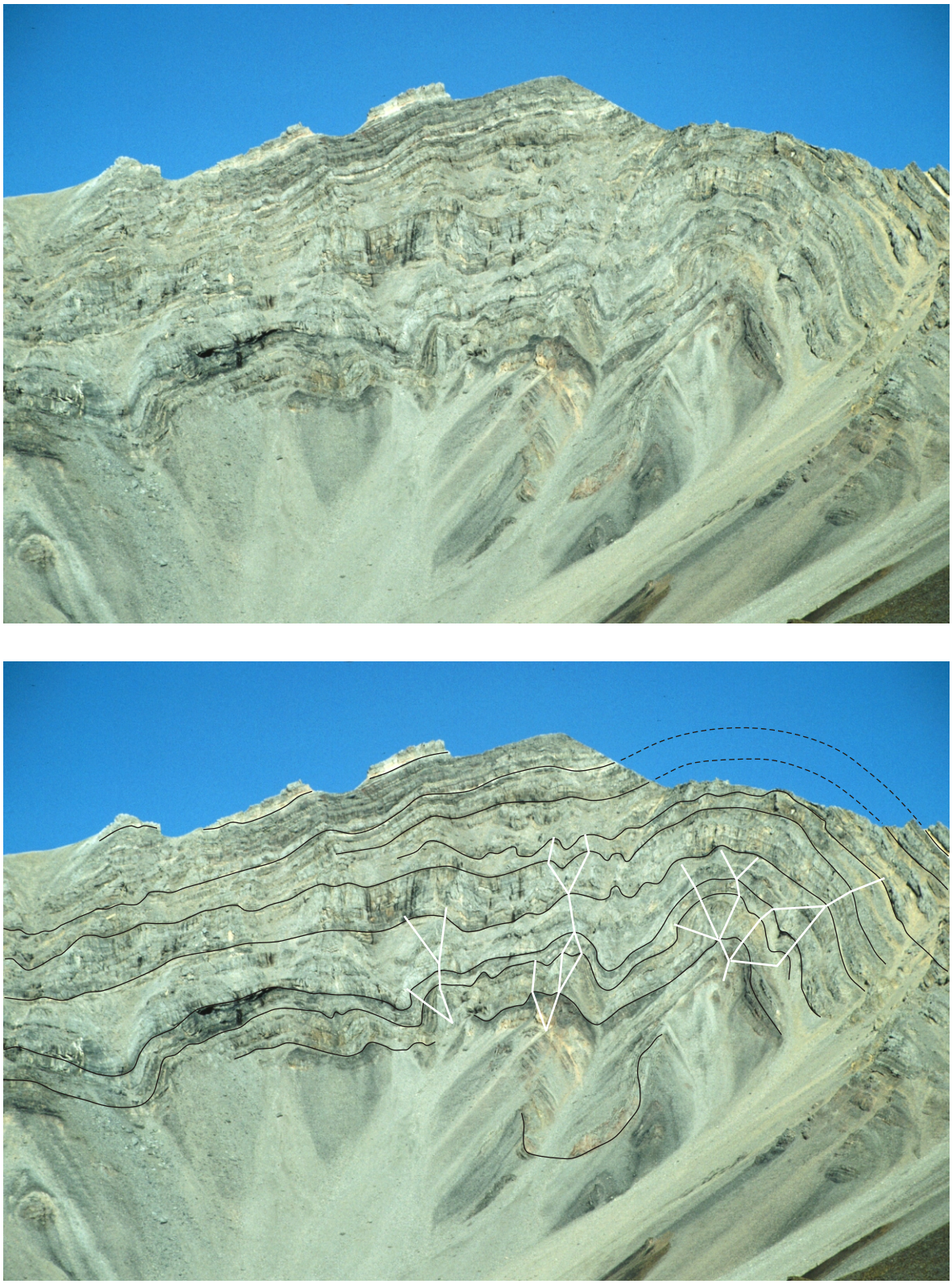

Figure 7: Photograph of Fold 3, a broad, open fold on the east side of Straight Creek in the Fourth Range, showing thickening in the core due to higher-order, disharmonic folding and homogeneous strain. Black lines on lower photo trace bedding; white lines show some of the major hinges, emphasizing their branching and disharmonic nature.

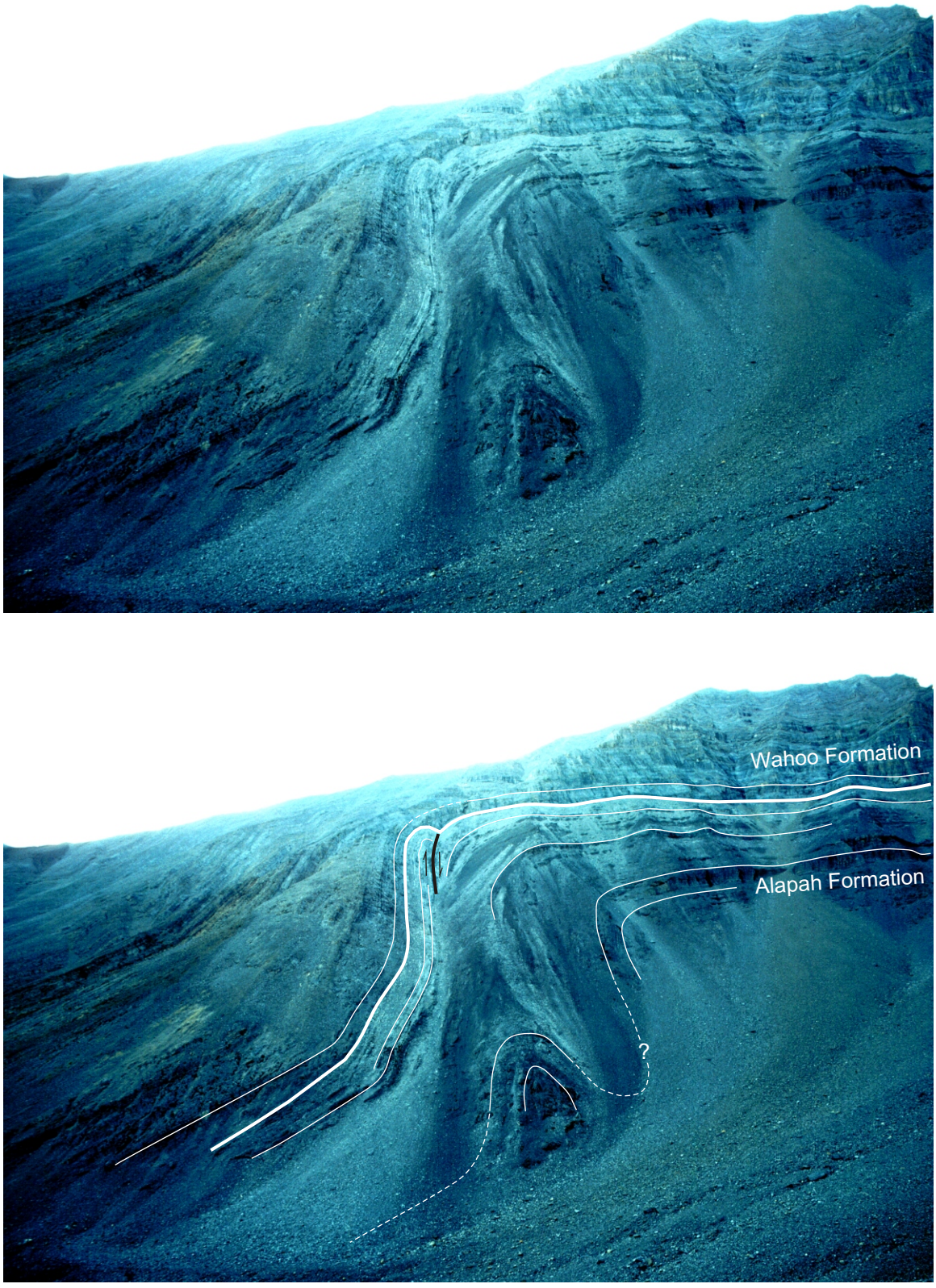

Figure 8: Photograph of Fold 5 on south side of Shublik Mountains, showing thickening in the core due to second-order folding and small-scale compressional faulting (”rabbit ear” thrust). White lines on lower photo trace bedding; heavy white line denotes contact between Wahoo and Alapah Formations. Black line traces fault.

Figure 9: Photograph of Fold 1, a tight, upright fold on the west side of Straight Creek in the Fourth Range, showing thickening in the hinge and thinning on the limbs due to penetrative homogeneous strain. Lines on right photo trace bedding. IPMI = Lisburne Limestone; TRPs = Sadlerochit Group.

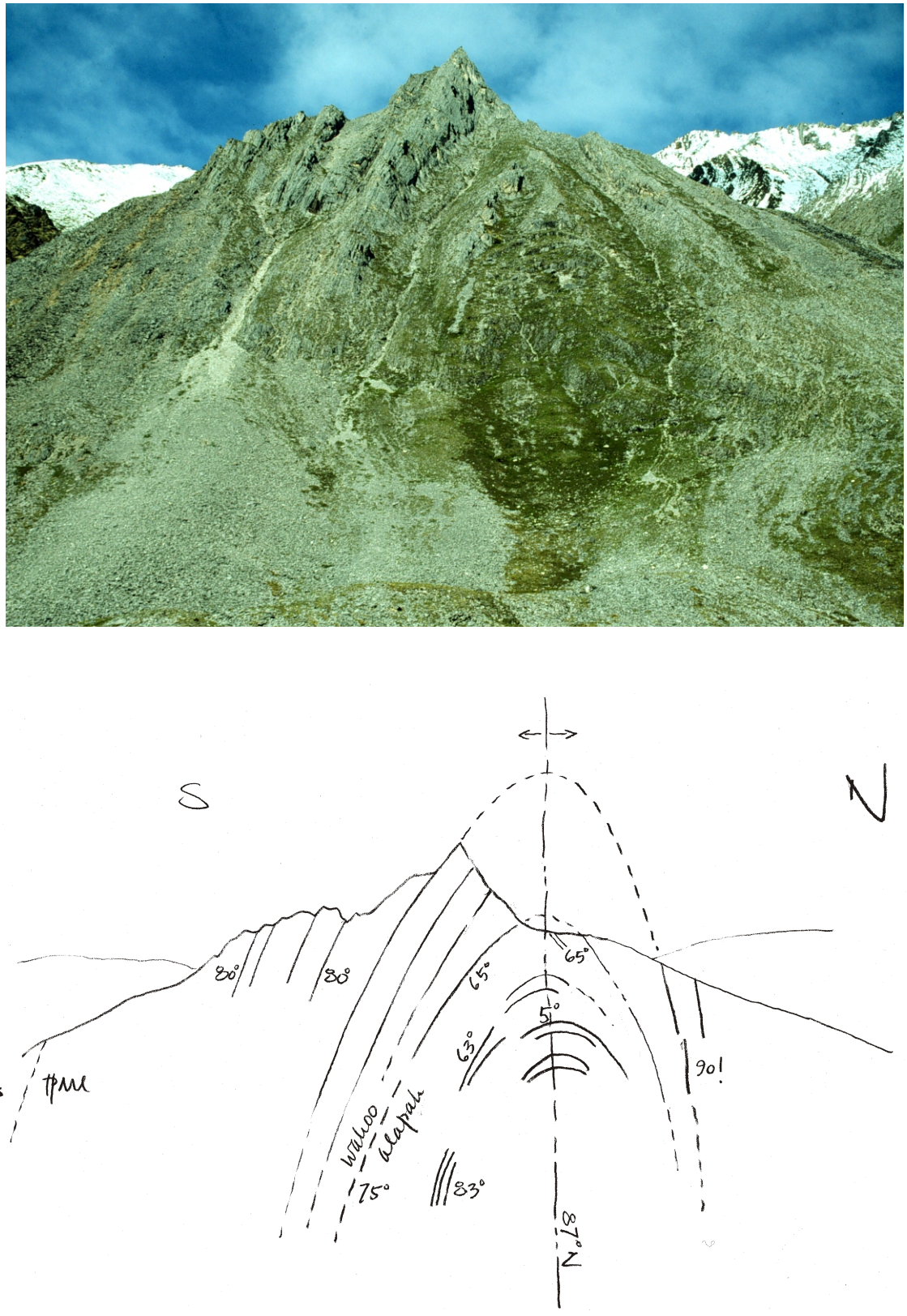

Figure 10: General shape of Fold 1, west side of Straight Creek, Fourth Range.

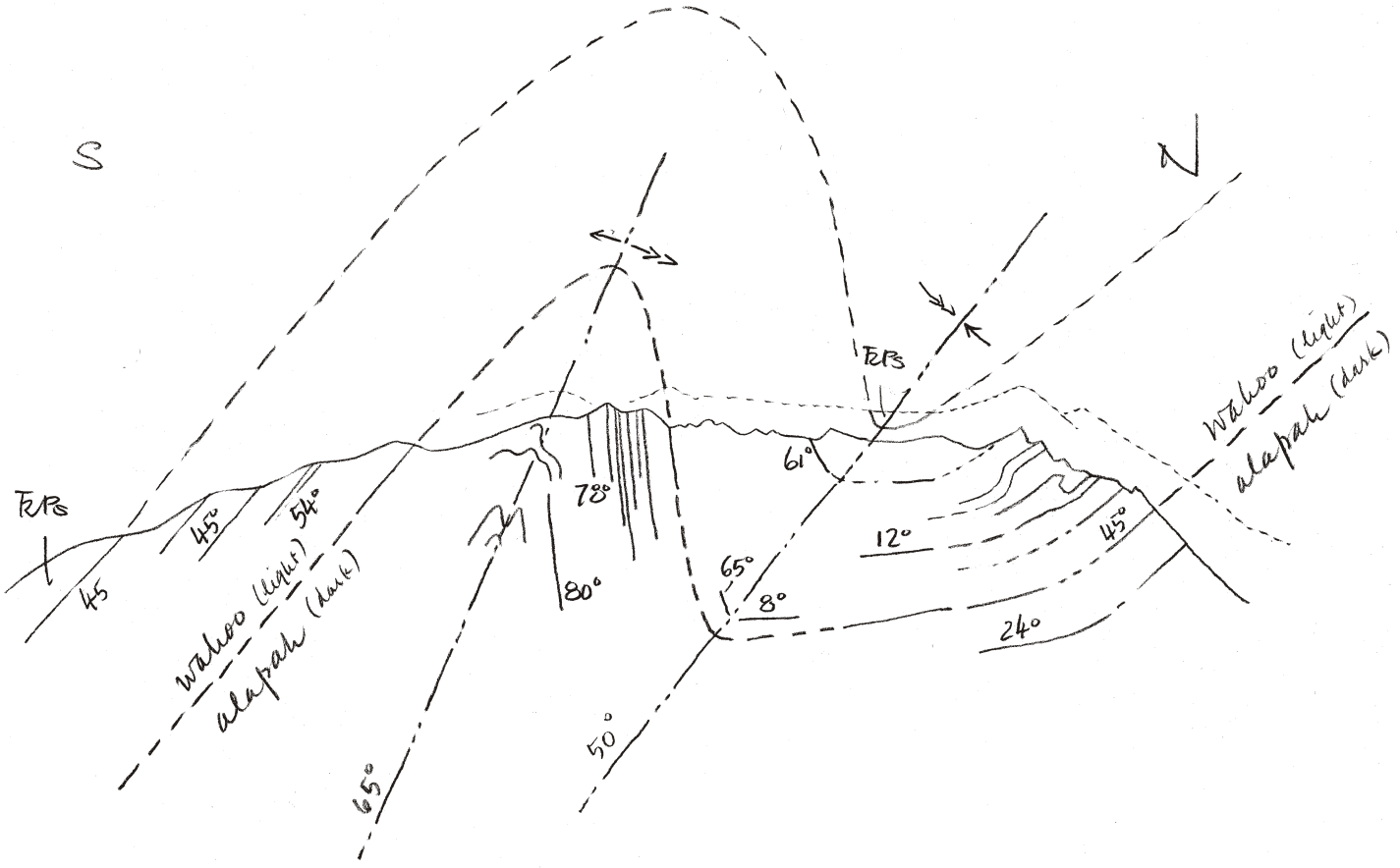

Figure 11: General shape of Fold 2, west side of Straight Creek, Fourth Range. Note: Because this was sketched and photographed from different locations, the two views don't match precisely, and dips appear very different.

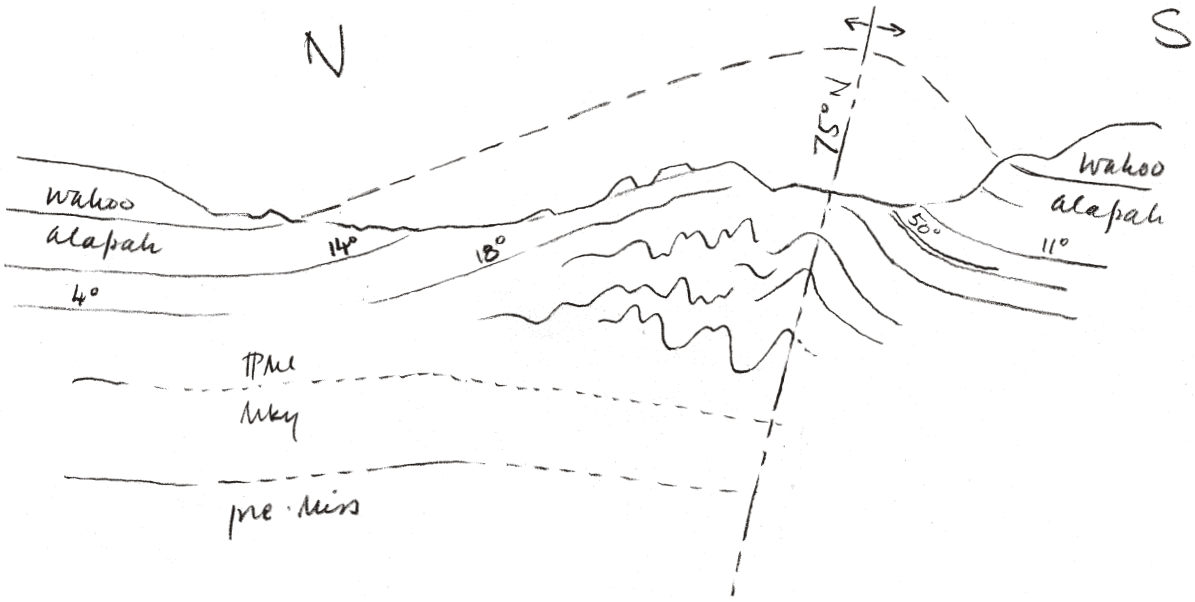

Figure 12: General shape of Fold 3, east side of Straight Creek, Fourth Range. Parasitic folds shown on sketch are schematic only; see Figure 7 for detail.

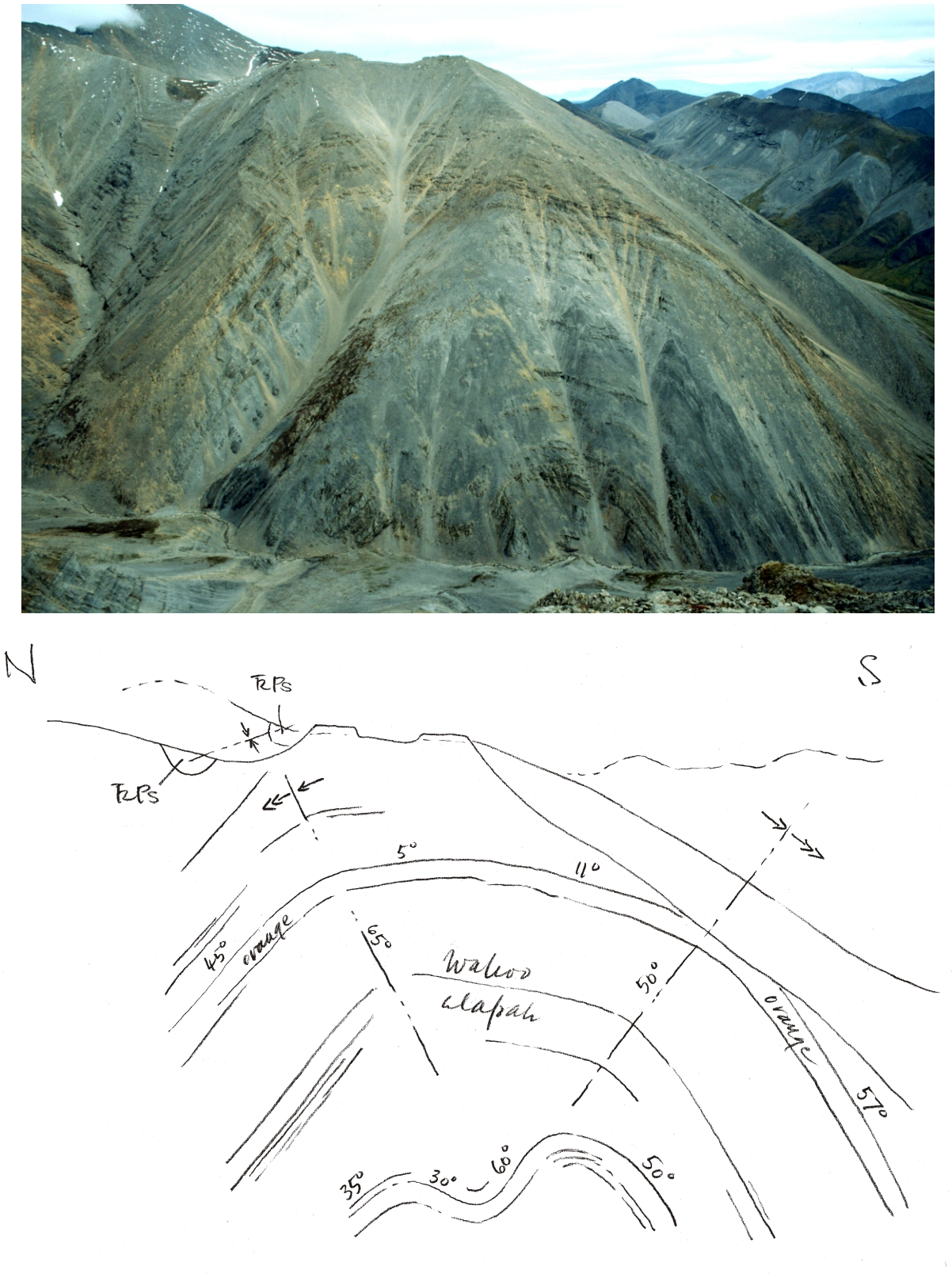

Figure 13: General shape of Fold 4, south Shublik Mountains. Orange beds in Wahoo Formation serve as markers.

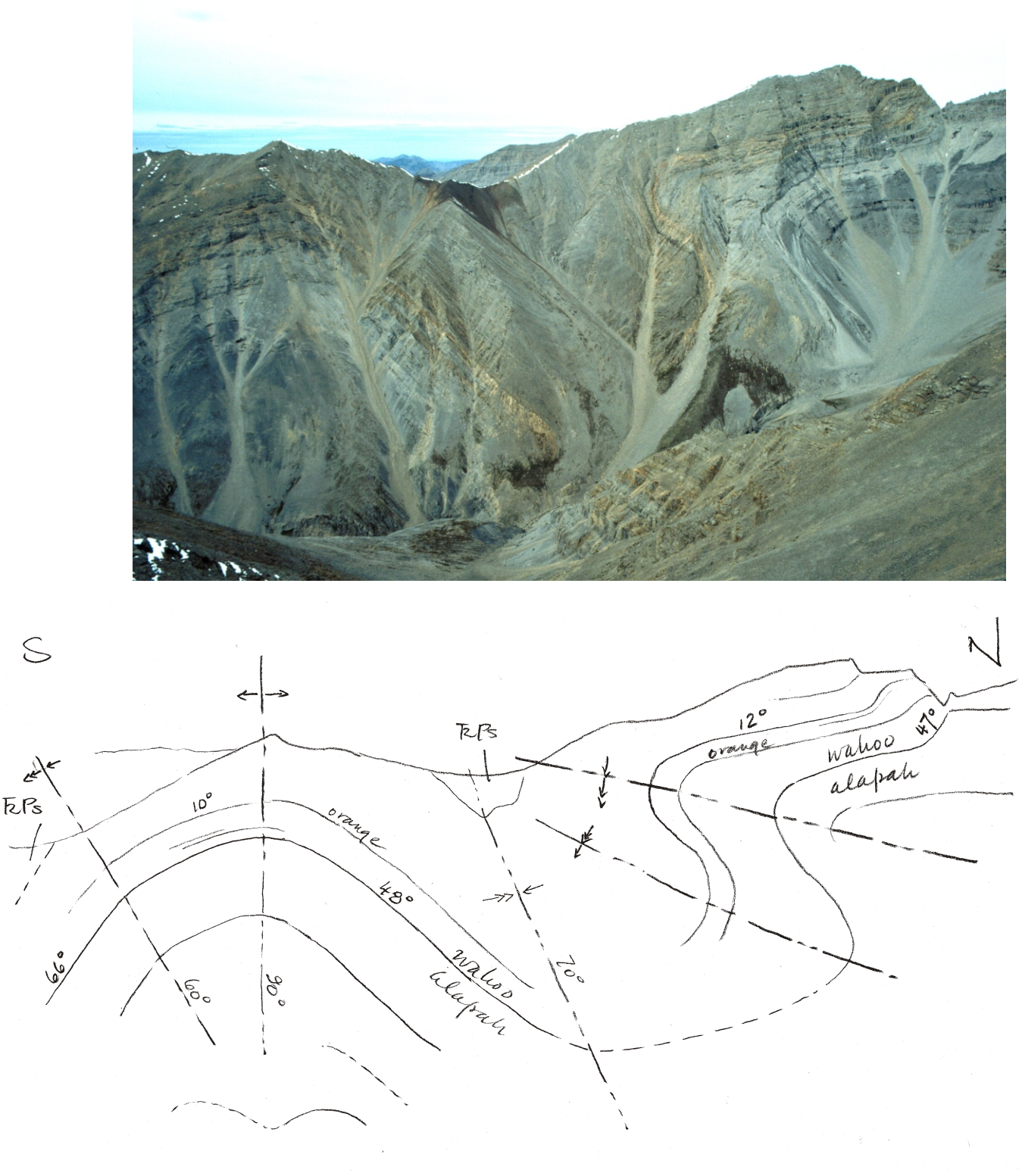

Figure 14: General shape of Folds 4 and 5, south Shublik Mountains. Shape of Fold 5 is distorted since it wraps around inside a bowl. Orange beds in Wahoo Formation serve as markers.

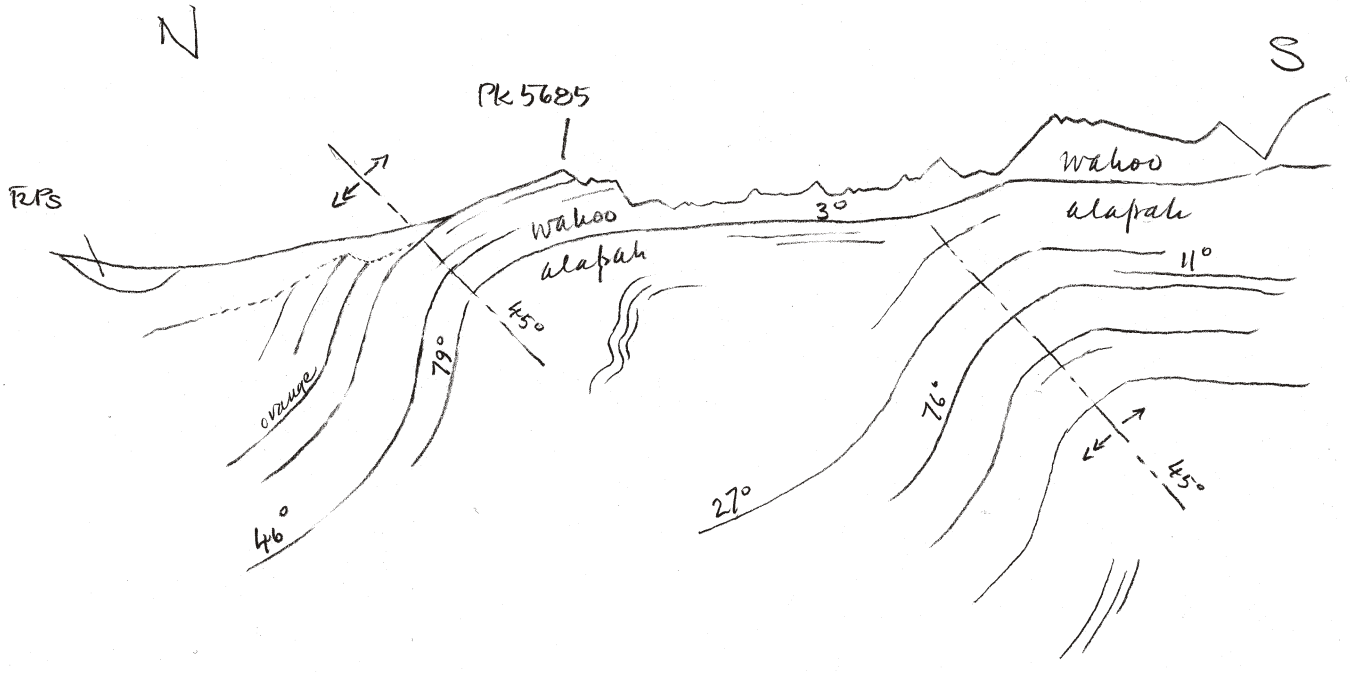

Figure 15: General shape of Fold 6, north Shublik Mountains. Orange bed in Wahoo Formation serves as marker.

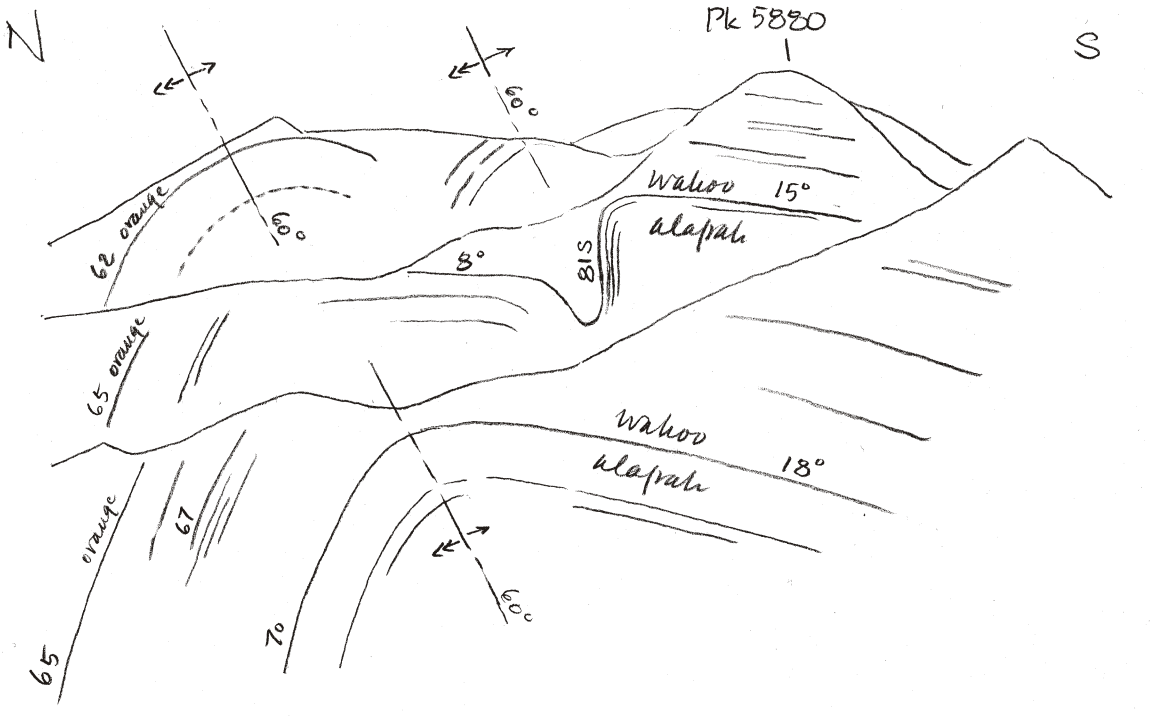

Figure 16: General shape and stratigraphy of Fold 7 (and eastward continuation of Fold 6), north Shublik Mountains. Orange beds in Wahoo Formation serve as markers.

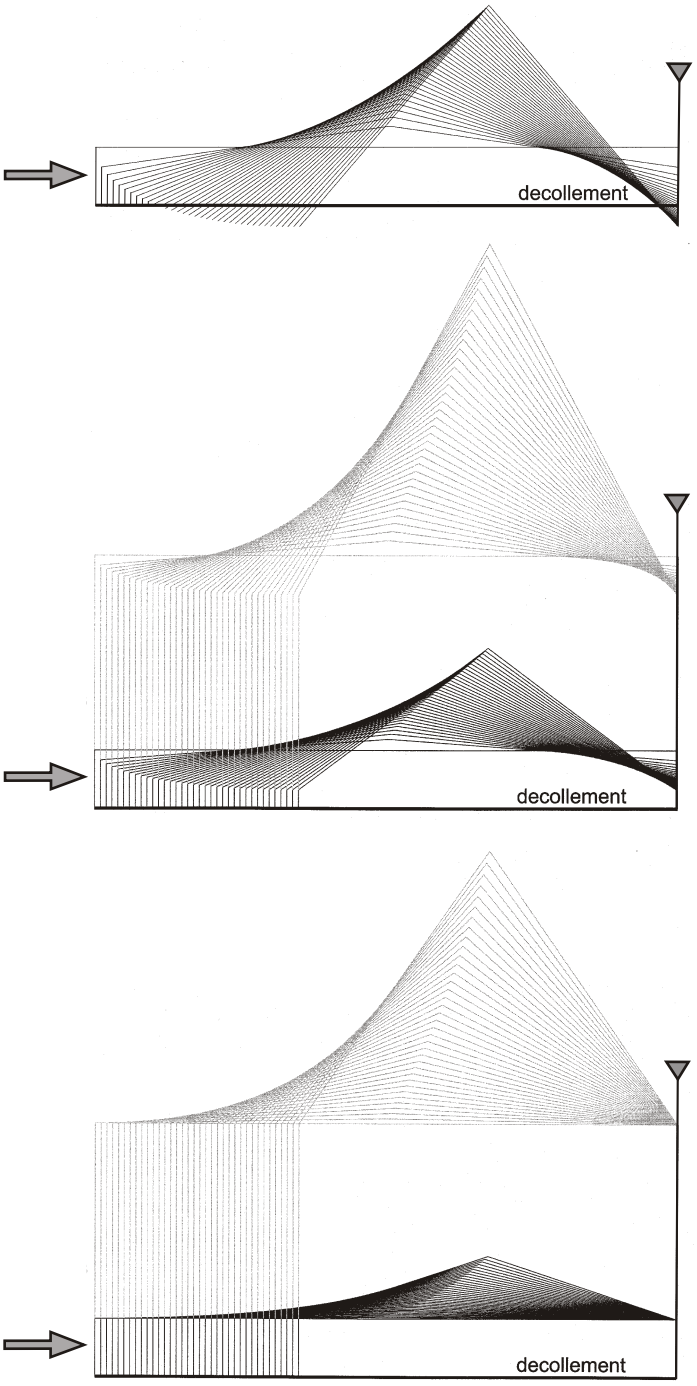

(a) Homza and Wallace Model

Bed Length: 1500 m
Vertical Displacement: 204 m
Interlimb Angle: 81.1°

(b) Hybrid Model

Bed Length: 1219 m
Vertical Displacement: 102 m
Interlimb Angle: 106.2°

(c) Epard and Groshong Model

Bed Length: 1028 m
Vertical Displacement: 0 m
Interlimb Angle: 143.3°

Figure 17: Area-balanced models for the evolution of detachment folds in the study area. For all three models, original bed length is 1500 m; original thicknesses of upper unit (Lisburne Limestone) and lower unit (Kayak Shale) are 500 m and 150 m, respectively. (For clarity, upper unit is not shown in Homza and Wallace model.) Progressive deformation is shown in 15 m increments, up to a total horizontal displacement of 525 m; statistics shown for each model reflect the fold's geometry after 525 m of horizontal displacement. In the Homza and Wallace model, the fold would lock after 150 m of horizontal displacement (assuming no additional incompetent material is introduced into the fold from outside the plane of section). In the Hybrid Model, far less thinning would occur beneath the synclines and the fold could continue to grow. The Epard and Groshong model assumes that both the upper and lower units would show equal amounts of layer-parallel shortening, which is unlikely considering their very different lithologies and competencies. Note that the Hybrid Model fold shown is only one of an infinite number possible, since the model defines a whole continuum between the Homza & Wallace and Epard & Groshong end-member models.

Fracturing in the Lisburne Group as a function of lithology and position in detachment folds

by C. L. Hanks (co-principal investigator), J. Brinton (M.S. student), Geophysical Institute and Department of Geology and Geophysics, University of Alaska, Fairbanks, Alaska 99775-5780, and J. Lorenz (visiting scientist), Sandia National Laboratories

Lisburne Group carbonates form an important naturally fractured hydrocarbon reservoir in the North Slope of Alaska. Lisburne Group carbonates are relatively undeformed in the Lisburne field, but future exploration plays in the Lisburne may be closer to the mountain front, where the Lisburne is both detachment folded and thrust faulted. Detachment folds in the Lisburne Group are widely exposed in the northeastern Brooks Range, making it an ideal natural laboratory for study of the character and distribution of fractures as a function of mechanical stratigraphy and position within a detachment fold.

Results of the 1999 field season

The focus of the 1999 field season was on fracture character and distribution in Lisburne Group rocks that are involved in detachment folds of various sizes and degrees of tightness. Localities visited are shown on figure 1 and include: the eastern Sadlerochit Mountains (location A), the Fourth Range (location D), and Shublik Mountains (locations B and C). A fifth location in Porcupine Lake Valley (location E) was also visited in preparation for the 2000 field season.

The Lisburne Group in the eastern Sadlerochit Mountains (location A, figure 1) is exposed in both the hanging wall and footwall of the rangefront fault, and provides an example of relatively little deformed Lisburne Group. This location will be used as a basis for developing a 'background' fracture character and distribution. The fracture character and distribution with respect to carbonate lithology in the eastern Sadlerochit Mountains has been well-documented by Hanks and others (1997). This location was visited primarily to familiarize researchers with Lisburne stratigraphy and the methodology of studying fractures.

Folded Lisburne Group carbonates in the Fourth Range and Shublik Mountains (locations B, C and D in figure 1) were the focus of this year's detailed study of fracture distribution and character. At each location, a map and cross section of the local structure were constructed at 1:20,000 scale (e.g., figure 2), so that detailed fracture observations could be accurately placed in their structural context. At several locations across each fold, the following observations were

made: carbonate lithology, bed thickness, and number, orientation, general character and relative age of fracture sets. A measuring tape was then placed perpendicular to each fracture set, and the following attributes were measured: spacing between each fracture encountered along the tape, orientation of each fracture, the vertical and horizontal extent of each fracture with respect to bedding, the aperture width and fill of each fracture, and the nature of the termination of each fracture. An oriented sample was then collected for petrographic, porosity and permeability analysis. The character and distribution of fractures at that location were then documented photographically.

An example of the type and character of the data collected is shown in Table 1. This information is currently being compiled for each location visited during the 1999 field season.

Preliminary observations based on the 1999 field season include:

<u>In relatively undeformed or mildly deformed Lisburne (e.g., eastern Sadlerochit Mts.):</u>

•Two distinctive fracture sets are present: an early NNW-oriented set of extension fractures and a later EW-oriented set of extension and shear fractures.

•The fracture character and distribution in both sets are clearly linked to carbonate lithology, with fine-grained lithologies having higher fracture densities than coarser-grained lithologies.

•Within each set, the fracture orientation is very consistent.

<u>In detachment folded Lisburne Group (e.g., Shublik Mts., Third Range and Fourth Range, interlimb angles of 55° to 152°):</u>

•The general relationship between lithology and fracture density remains unchanged. However, compared to fold limbs, the fracture densities in fold hinges are higher in all lithologies, and show greater vertical extent.

•In general, there are still two major fracture sets. However, fractures within each set are more variable in orientation and character. This is especially true in fold hinges, where conjugate fracture sets and shear fractures are abundant.

•The relative timing of the two fracture sets becomes more ambiguous in folded Lisburne, with

NNW-oriented fractures not everywhere clearly predating E-W-oriented fractures.

•There is strong evidence of semi-ductile deformation in the hinge zones of these folds, including strained crinoid stems and sheared stylolites.

•Other structures that would potentially destroy permeability, such as dissolution cleavage, also are present in hinge zones.

The preferential increase in fracture density, semi-ductile deformation, and dissolution cleavage in the fold hinges strongly suggest that fold hinges have remained relatively fixed during the development of the detachment fold. These observations also suggest that structural position in the detachment fold will play a major role in determining the potential reservoir character of the Lisburne Group.

Other research activity

Two co-prinicipal Investigators, C. Hanks and J. Jensen, attended an American Association of Petroleum Geologists short course on fractured reservoir characterization in Austin, Texas during early November. The purpose in attending the short course was to acquaint Jensen, a reservoir engineer, with description of fractures in the field and core; familiarize Hanks, a geologist, with reservoir modeling; and develop a joint working vocabulary on fractures, reservoir characterization, and modeling. The course also gave the scientists the opportunity to meet other researchers and professional geologists working in fractured carbonate reservoirs and learn more about the techniques others are using to describe fracture distribution.

Some of the ideas on fracture scaling presented at the course will be incorporated into this study in order to add value to the field data and to develop a better model of the distribution of fractures in various parts of a detachment fold.

Work planned for the next six months

The work during the next six months will include two tasks:

1) Compilation of the detailed field data on the distribution and character of fractures in the various detachment folds visited during the 1999 field season into an Alaska Division of Geological and Geophysical Surveys (ADGGS) Public Data File (PDF). The PDF will include:

•A detailed map and cross section of each location (e.g., figure 2)
•Compilation of the fracture data for each location (e.g., table 1)
•A preliminary interpretation of field results

The PDF should be available early in 2000.

2) More detailed analysis of the field data. This will include:

•Thin section analysis of specific lithologies to evaluate the distribution of microfractures and other structures. This information will be used to refine our models for the fracture size and spacing in various carbonate lithologies in different parts of the fold.

•Statistical analysis of fracture spacing and distribution.

<u>These analyses will be aimed at answering the following questions:</u>

•Can the increase in fracture density from the fold limbs to the fold hinges be quantified?

•Is there any relationship of carbonate lithology and bed thickness to the increase in fracture density in the fold hinges?

•To what degree are fractures evenly distributed vs. clustered (i.e., 'swarming' behavior)?

•Not all hinge areas show signs of dissolution cleavage and semi-ductile strain. Why or why not?

•Do synclinal hinges exhibit the same structures and changes in fracture density as do the anticlinal hinges?

This information will be used to further refine the field-based model of fracture distribution and character in detachment-folded Lisburne that will then be used by the reservoir engineer, Jerry Jensen, and his graduate student for their reservoir characterization and flow studies.

References

Hanks, C.L., Lorenz, J., Teufel, L, and Krumhardt, A.P., 1997, Lithologic and structural controls on natural fracture distribution and behavior within the Lisburne Group, northeastern Brooks Range and North Slope subsurface, Alaska: American Association of Petroleum Geologists Bulletin, v. 81, no. 10, p. 1700-1720.

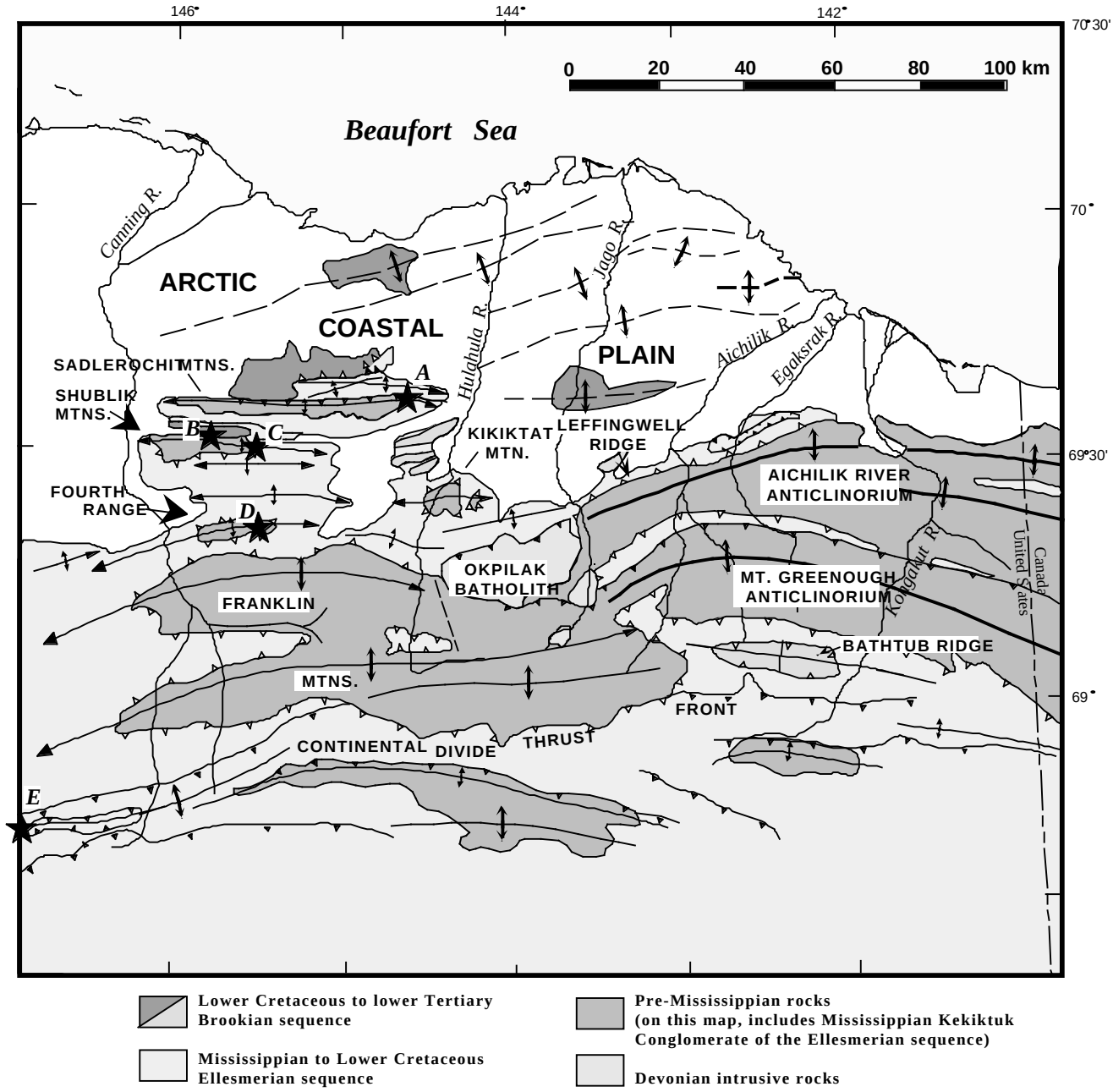

Figure 1. Geologic map of northeastern Brooks Range showing major stratigraphic units and structures. Locations of detachment folded Lisburne Group visited for detailed fracture analysis are shown with ★: **A.** eastern Sadlerochit Mts.; **B**. northern Shublik Mts.; **C**. southern Shublik Mts.; **D**. eastern Straight Creek; **E**. western Porcupine Lake valley.

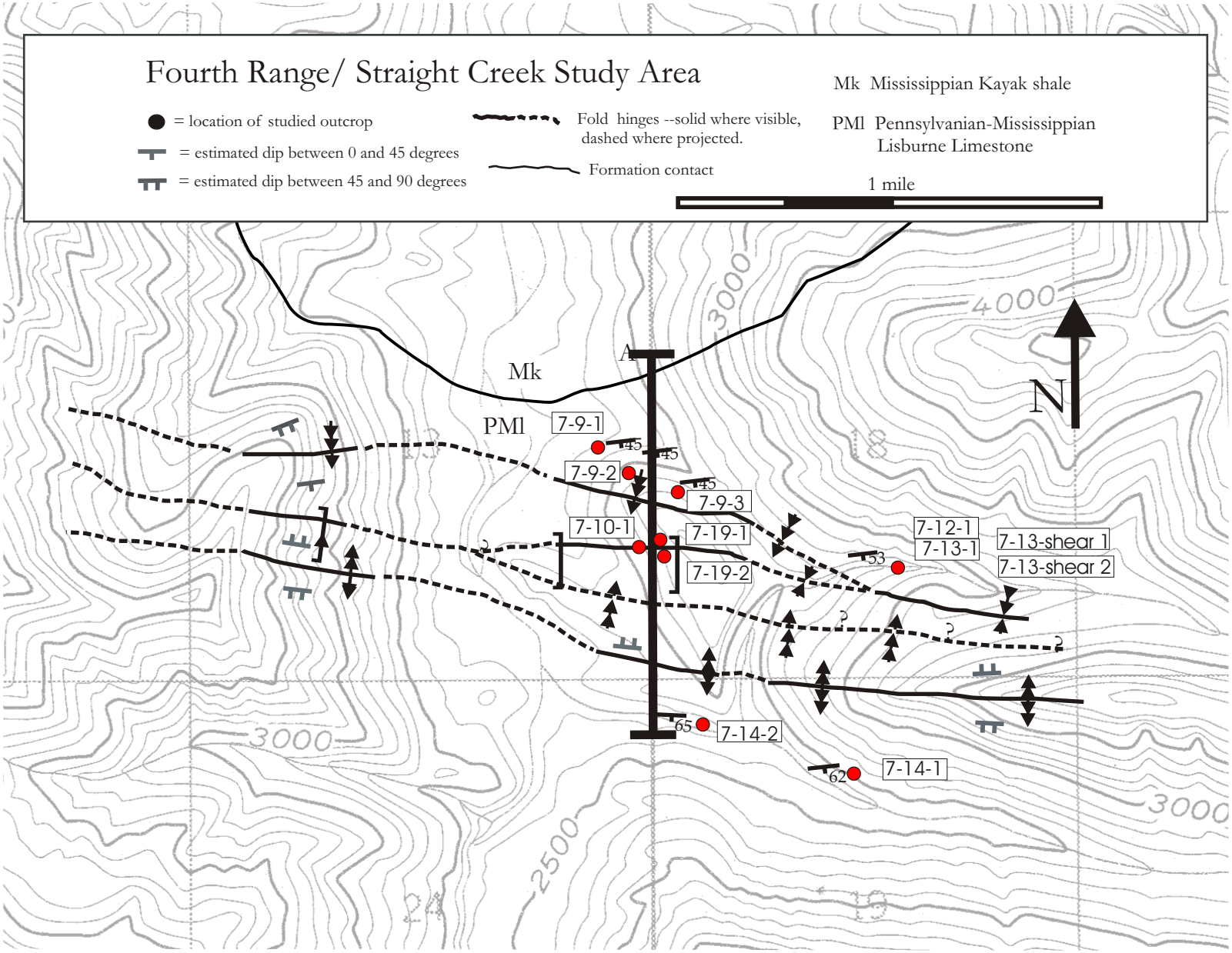

Figure 2A. Map of Straight Creek area showing local structure and locations where detailed fracture data were collected.

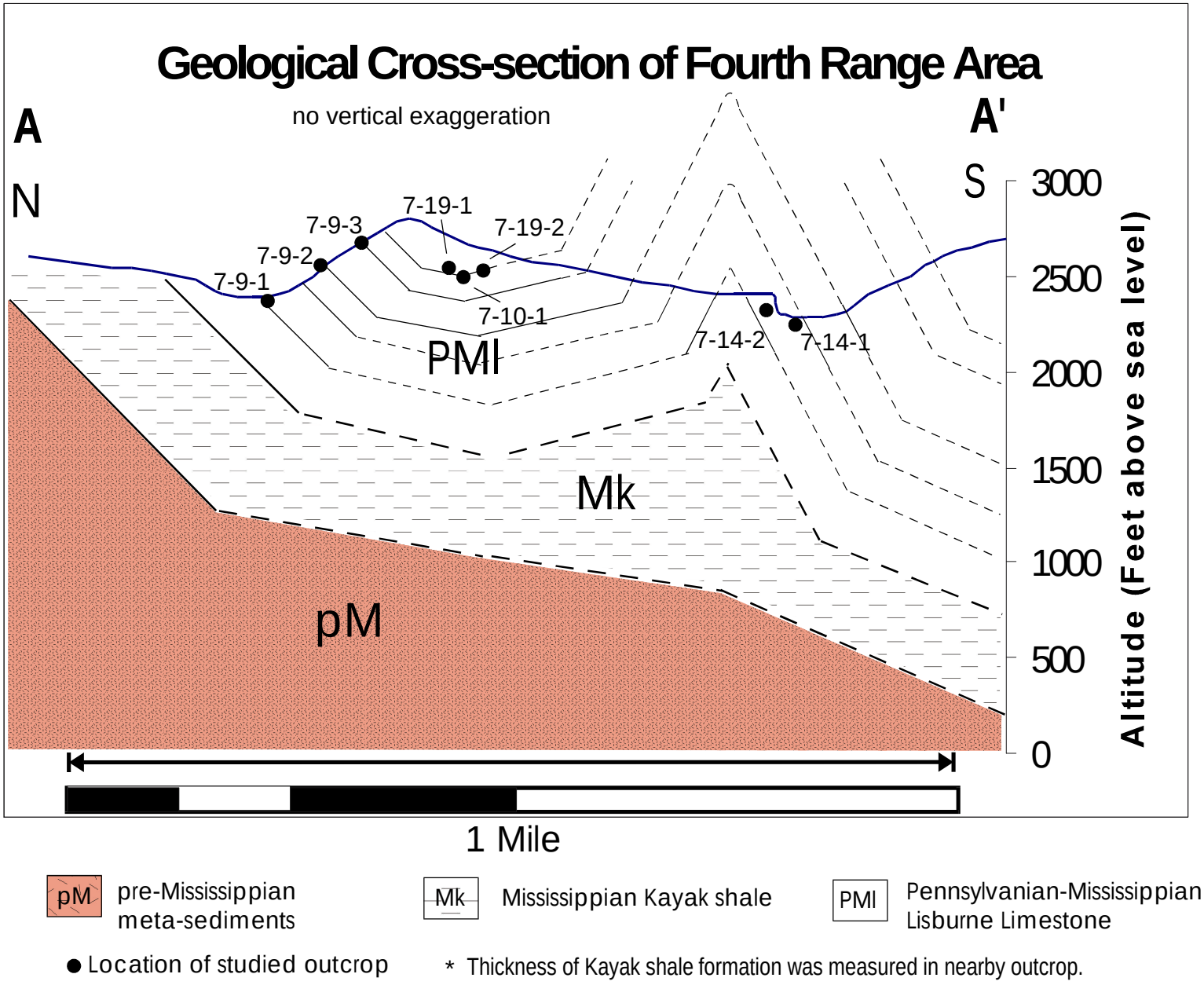

Figure 2B. Cross section of Straight Creek area showing local structure and locations where detailed fracture data were collected.

Table 1

An example of the fracture distribution, orientation and character data collected at the Straight Creek locality (location D, figure 1, and figure 2 A & B).

KEY

Spacing= Position of fracture on the measuring tape.

Distance= Distance from adjacent fracture.

Ap=aperture width

U= unable to determine aperature width

Fill indicates type and amount of fracture fill

N= no fill

Pc= partially filled with calcite

Pq= partially filled with quartz

C= totally filled with calcite

Q= totally filled with quartz

Length = Measured linear extent of fracture parallel to bedding plane.

Length descriptor indicates location of measurement

B= length was measured on the bedding plane

F= length was measured on an exposed face

U= unable to determine length

*** Due to limited fracture exposure all length and height measurements represent minimum values.

Height= Measured linear extent of fractures perpendicular to bedding

Height descriptor indicates type of fracture termination.

Term listed first indicates bottom of bed; last indicates bottom of bed; middle term (C) indicates that the fracture crosses a bedding plane.

B= terminates at bedding plane

C= crosses bedding plane

I= terminates within bedding unit

T= terminates against another fracture

M= merges with another fracture

U= unable to determine type of termination

Outcrop description **FR-7-9-1**

Bedding Plane Orient:	**Bed Thickness:**	**Formation:**	**Lithology:**	**Fossils:**	**Sample orient:**	**Photos:**	**Evidence of shear:**	**Relative Age Relations**
115 35S	**~3m**	**Alapah**	**packstone**	**crinoids(sparse)**	**255 50N**	**2-2,2-3**	**NONE**	E-W predate N-S ?

FR-7-9-1 NORTH-SOUTH

No	Spacing (meters)	Distance	Strike	Dip	Dip Direction	Length (meters)	Length descriptor	Height (meters)	Height descriptor	Ap (cm)	Fill
1	0		160	85	E	0.8	F	1.4	UI	U	indeterminable
2	0.4	0.4	175	80	E	U	U	1.9	TM	0.5	N
3	0.88	0.48	165	75	E	0.4	F	3	UU	9	N
4	1.2	0.32	155	83	E	0.15	F	2	TB	3	N
5	1.25	0.05	150	85	E	0.2	F	1.5	UB	0.1	N
6	1.4	0.15	158	80	E	0.2	F	1	MM	0.1	N
7	1.66	0.26	160	90	E	1	F	3	UU	U	N

FR 7-9-1 EAST-WEST CONJUGATES

No	Spacing (meters)	Distance	Strike	Dip	Dip Direction	Length (meters)	Length descriptor	Height (meters)	Height descriptor	Ap (cm)	Fill
0	0		70	50	N	0.8	F	0.68	BB	0.2	Pc
1	0.02	0.02	80	52	N	0.31	B	0.68	BB	0.2	Pc
2	0.06	0.04	82	50	N	0.1	B	0.12	BI	0.2	Pc
3	0.09	0.03	74	43	N	U	U	0.34	BI	0.2	Pc
4	0.12	0.03	70	65	N	U	U	0.2	BI	0.2	Pc
5	0.18	0.06	80	38	N	0.08	B	0.45	BB	0.2	Pc
6	0.3	0.12	75	53	N	U	U	1.2	BM	0.2	Pc
7	0.42	0.12	70	45	N	U	U	1.1	BI	0.2	Pc
8	0.48	0.06	80	40	N	0.15	F	2	BCB	0.2	Pc
9	0.68	0.2	U	U	U	U	U	1.5	UU	0.2	Pc
10	1	0.32	U	U	U	U	U	U	UU	0.2	Pc

FR 7-9-1	CONJUGATE FRACTURES											
No	Spacing (meters)	Distance	Strike	Dip	Dip Direction	Length (meters)	Length descriptor	Height (meters)	Height descriptor	Ap (cm)	Fill	
0	0		25	35	NW	0.15	B	0.55	BM	hairline	U	
1	0.35	0.35	338	40	NW	0.18	F	0.2	MM	hairline	U	
2	1	0.65	355	49	W	U	U	0.4	MM	hairline	U	
3	1.44	0.44	0	49	W	0.1	F	0.15	MM	hairline	U	
FR 7-9-1	MACRO N-S											
No	Spacing (meters)	Distance	Strike	Dip	Dip Direction	Length (meters)	Length descriptor	Height (meters)	Height descriptor	Ap (cm)	Fill	
1	0.7		355	75	E	6	U	8 of visible	UU	10	N	
2	1.6	0.9	342	80	E	6	U	outcrop	UU	10	N	
8	2	0.4	345	90	V	6	U	8	UU	10	N	
4	3	1	327	90	V	6	U	8	UU	10	N	
5	5.2	2.2	347	82	W	6	U	8	UU	10	N	
6	7.6	2.4	350	80	E	6	U	8	UU	10	N	
7	9.5	1.9	350	80	E	6	U	8	UU	10	N	
Outcrop description						**FR 7-9-2**						
	Bedding Plane Orient:	**Bed Thickness:**	**Formation:**		**Lithology:**	**Fossils:**	**Sample orient:**	**Photos:**	**Evidence of shear:**		**Relative Age Relations**	
	85 45S	**~3m**	**Alapah (top)**		**grain/pack**	**crinoids(sparse)**	**337 90**	**2-6,2-7,2-8,2-9**	**NONE**		N-S predate E-W	
FR 7-9-2	E-W set											
No	Spacing (meters)	Distance	Strike	Dip	Dip Direction	Length (meters)	Length descriptor	Height (meters)	Height descriptor	Ap (cm)	Fill	
1	0.1		253	63	N	0.15	B	0.25	II	0.2	N	
2	0.2	0.1	252	50	N	0.08	B	0.13	II	0	N	
3	0.29	0.09	255	42	N	0.25	B	1	BB	1	N	
4	0.33	0.04	242	65	N	U	U	0.2	II	0.5	N	
5	0.39	0.06	246	55	N	U	U	0.2	II	0.5	N	
6	0.42	0.03	256	50	N	U	U	0.1	IM	0.5	N	
7	0.45	0.03	255	45	N	0.3	B	0.3	IB	0.8	N	
8	0.5	0.05	265	42	N	0.18	B	0.6	UB	0.2	N	
9	0.66	0.16	270	50	N	0.05	B	0.35	BU	0.2	N	
10	0.75	0.09	245	55	N	0.1	B	0.35	BU	0.25	N	
11	0.85	0.1	260	43	N	0.4	B	0.31	UB	0.2	N	
12	0.9	0.05	245	36	N	0.4	B	0.31	UB	0.2	N	
13	1.05	0.15	250	42	N	0.4	B	0.3	BU	0.2	N	
FR 7-9-2	N-S											
No	Spacing (meters)	Distance	Strike	Dip	Dip Direction	Length (meters)	Length descriptor	Height (meters)	Height descriptor	Ap (cm)	Fill	
1	0.35		350	90	V	1	F	3	BU	>1	N	
2	1	0.65	352	75	E	0.3	F	3	BU	3	N	
3	1.9	0.9	340	73	E	0.6	F	7	BU	2	N	
4	3	1.1	321	70	E	0.5	F	2	BU	3	N	
5	4.6	1.6	350	90	V	1	F	7	BU	2	N	

Table 1

Outcrop description						**FR 7-9-3**						
	Bedding Plane Orient:	**Bed Thickness:**	**Formation:**		**Lithology:**	**Fossils:**	**Sample orient:**	**Photos:**	**Evidence of shear:**	**Outcrop thickness:**	**Relative Age Relations**	
	105 45S	**1m**	**upper Alapah?**		**grain/pack**	**crinoids(sparse)**	**260 68N**	**2-10,211**	**NONE**	**4m**	E-W predate N-S	
FR 7-9-3	E-W											
No	Spacing (meters)	Distance	Strike	Dip	Dip Direction	Length (meters)	Length descriptor	Height (meters)	Height descriptor	Ap (cm)	Fill	
1	0.38		250	45	N	0.3	F	2	BB	1	Pc	
2	0.55	0.17	250	75	N	0.4	F	1.7	BB	0.5	Pc	
3	0.76	0.21	245	57	N	0.1	F	1.4	BB	0.5	N	
4	0.89	0.13	215	72	NW	0.1	F	1	BI	0.2	Pc	
5	1.07	0.18	250	65	N	0.2	F	1	BI	0.2	N	
6	1.22	0.15	250	68	N	0.2	F	1	BI	0.2	Pc	
7	1.57	0.35	232	62	NW	0.3	F	2	BCI	0.5	Pc	
8	1.8	0.23	252	55	N	0.3	F	1	BCI	0.2	Pc	
9	2.1	0.3	245	60	NW	0.1	F	2.5	BCB	0.2	Pc	
10	2.4	0.3	254	50	NW	0.3	F	1.5	BCM	0.2	N	
FR 7-9-3	N-S											
No	Spacing (meters)	Distance	Strike	Dip	Dip Direction	Length (meters)	Length descriptor	Height (meters)	Height descriptor	Ap (cm)	Fill	
1	0.28		342	50	E	0.1	B	0.5	BI	0.5	N	
2	0.4	0.12	345	54	E	0.1	B	0.6	BB	1	N	
3	0.55	0.15	U	U	N/A	0.4	B	0.35	II	0	N/A	
4	0.63	0.08	350	77	E	0.4	B	0.5	BB	2	N	
5	0.77	0.14	326	55	E	0.4	B	0.15	BB	1	N	
6	1	0.23	340	76	E	0.05	B	0.25	BB	1	N	
7	1.11	0.11	345	77	E	0.15	B	0.45	BB	hairline	U	
8	1.23	0.12	350	77	E	0.3	B	0.6	BB	hairline	U	
Outcrop description						**FR 7-10-1**						
	Bedding Plane Orient:	**Bed Thickness:**	**Formation:**		**Lithology:**	**Fossils:**	**Sample orient:**	**Photos:**	**Evidence of shear:**	**Other:**	**Relative Age Relations**	
	20 8E	**1-2m**	**Alapah**		**grain/pack**	**brach, crinoids brya**	**172 68W**	**2-6,2-7,2-8,2-9**	**none**	**stylolites**	indeterminable	
										(bed indicators)		
FR 7-10-1	E-W											
No	Spacing (meters)	Distance	Strike	Dip	Dip Direction	Length (meters)	Length descriptor	Height (meters)	Height descriptor	Ap (cm)	Fill	
1	0		115	82	S	0.15	F	0.45	UB	U	U	
2	0.1	0.1	115	80	S	0.2	F	1.5	MM	0.2	N	
3	0.3	0.2	100	85	S	0.15	F	1	BI	0.2	Pc	
4	0.4	0.1	105	90	V	0.1	F	0.65	BB	0.4	N	
5	0.48	0.08	120	80	S	0.17	F	0.3	MM	1	N	
6	0.55	0.07	110	70	S	0.15	F	0.45	MM	1	Pc	
7	0.6	0.05	120	77	S	0.08	F	0.45	BM	0.2	N	
8	0.82	0.22	120	77	S	0.05	F	0.1	BI	0.2	N	
9	1.03	0.21	108	73	S	0.01	F	0.35	MM	0.2	Pc	
10	2.53	1.5	113	80	S	0.15	F	0.3	MM	4	N	
11	3.1	0.57	95	82	S	0.6	F	0.85	UU	U	U	

Table 1

FR 7-10-1	E-W "LOW ANGLE" CONJUGATE FRACTURES (SOUTH DIPPING SET)											
No	Spacing (meters)	Distance	Strike	Dip	Dip Direction	Length (meters)	Length descriptor	Height (meters)	Height descriptor	Ap (cm)	Fill	
1	0		80	15	S	0.08	F	0.6	MM	U		
2	0.1	0.1	70	35	S	U		0.3	MM	0.01	Fc	
3	0.28	0.18	65	28	S	0.15	F	0.6	MM	0.5	N	
4	0.4	0.12	65	40	S	0.03	F	0.12	MM	0.01	N	
5	0.45	0.05	85	35	S	0.05	F	0.25	MM	0.02	Pc	
6	0.72	0.27	80	45	S	0.1	F	0.15	MM	1	Pc	
7	0.86	0.14	80	53	S	0.1	F	0.05	MM	0.02	Pc	
FR 7-10-1	E-W "LOW ANGLE" CONJUGATE FRACTURES (NORTH DIPPING SET)											
No	Spacing (meters)	Distance	Strike	Dip	Dip Direction	Length (meters)	Length descriptor	Height (meters)	Height descriptor	Ap (cm)	Fill	
1	0.07		282	26	N	0		0.05	II	0	Fc	
2	0.15	0.08	280	24	N	0.01	F	0.4	FF	0.02	Pc	
3	0.2	0.05	290	20	N	0.02	F	0.6	FF	0.02	Pc	
4	0.25	0.05	298	30	N	0.02	F	0.15	FF	0.02	N	
5	0.55	0.3	298	50	N	0.15	F	0.6	UU	U	U	
6	0.72	0.17	295	26	N	0.1	F	0.52	UF	1	N	
7	1.03	0.31	305	24	N	0.11	F	0.37	UF	2	N	
8	1.3	0.27	320	32	N	0.4	F	0.4	UU	U	U	
FR 7-10-1	N-S											
No	Spacing (meters)	Distance	Strike	Dip	Dip Direction	Length (meters)	Length descriptor	Height (meters)	Height descriptor	Ap (cm)	Fill	
1	0		167	79	W	0.4	F	0.9	BB	1.5	N	
2	0.05	0.05	170	83	W	0.1	F	0.6	UF	0.5	N	
3	0.1	0.05	162	70	W	0.05	F	0.35	BF	0.5	N	
4	0.26	0.16	160	75	W	0.15	F	0.75	BB	0.2	Pc	
5	0.48	0.22	150	67	W	0.1	B	0.62	IB	0.1	Pc	
6	0.68	0.2	175	72	W	20	F	0.9	UU	U	U	
Outcrop description						**FR 7-12-1**						
	Bedding Plane Orient:	**Bed Thickness:**	**Formation:**		**Lithology:**	**Fossils:**	**Sample orient:**	**Photos:**	**Evidence of shear:**		**Relative Age Relations**	
	128 52S	**1.7 M**	**Wahoo**		**mudstone**	**brach, crinoids brya**	**15 72E**	**2-28,-29,-30,-31**	**Top north, en echelon fractures**		only 1 frax set	
FR 7-12-1	N-S											
No	Spacing (meters)	Distance	Strike	Dip	Dip Direction	Length (meters)	Length descriptor	Height (meters)	Height descriptor	Ap (cm)	Fill	
1	0.04		15	70	E	0.1	F	2	UU	0.02	N	
2	0.1	0.06	3	82	E	0.05	F	0.7	UU	1	Fc	
3	0.15	0.05	10	75	E	0.1	F	0.25	UU	0.01	Fc	
4	0.2	0.05	20	72	E	0.1	F	1	UU	1	Pc	
5	0.3	0.1	20	65	E	0.15	F	0.5	UU	0.5	Pc	
6	0.37	0.07	15	72	E	0.05	F	0.5	UU	1	Pc	
7	0.44	0.07	15	90	E	0.12	F	0.9	UU	0.5	Pc	
8	0.52	0.08	25	90	E	0.1	F	0.5	UU	1	Pc	
9	0.56	0.04	20	74	E	0.1	F	0.8	UU	0.8	Pc	
10	0.6	0.04	13	72	E	0.1	F	1	UU	0.5	Pc	
11	0.68	0.08	12	72	E	0.08	F	1	UU	U	U	

Table 1

Outcrop description						**FR 7-13-1A Waterfall**						
	Bedding Plane Orient:	**Bed Thickness:**	**Formation:**		**Lithology:**	**Fossils:**	**Sample orient:**	**Photos:**	**Evidence of shear:**		**Relative Age Relations**	
	124 53 S	**2.4 M**	**Wahoo?**		**mudstone**	**none**	**82 35S**	**3-1**	**extensive, right lateral, shear zones**		E-W predate N-S	
FR 7-13-1A N-S												
No	Spacing (meters)	Distance	Strike	Dip	Dip Direction	Length (meters)	Length descriptor	Height (meters)	Height descriptor	Ap (cm)	Fill	
1	0.1		5	90	V	0.2	F	1	BB	0.2	Pc	
2	0.2	0.1	u	u		0.2	F	1	BB	0.1	N	
3	0.26	0.06	5	80	E	0.1	F	2	BB	0.4	N	
4	0.31	0.05	2	83	E	0.2	F	0.3	BB	0.2	N	
5	0.36	0.05	7	72	E	0.15	F	0.7	BI	1	Pc	
6	0.48	0.12	11	90	V	0.1	F	0.4	BI	0.2	Pc	
7	0.57	0.09	15	75	E	0.15	F	2	BB	0.4	Pc	
8	0.63	0.06	0	75	E	0.05	F	1	BB	0.1	Fc	
9	0.7	0.07	u	u		0.1	F	0.4	IB	0.2	Fc	
10	0.75	0.05	0	76	E	0.05	F	1	BB	0.1	Pc	
FR 7-13-1B E-W												
No	Spacing (meters)	Distance	Strike	Dip	Dip Direction	Length (meters)	Length descriptor	Height (meters)	Height descriptor	Ap (cm)	Fill	
1	0		210	30	W	0.5	F	1	BB	1	N	
2	0.52	0.52	210	32	W	0.1	F	1	BB	1	N	
3	0.82	0.3	220	31	W	0.2	F	1	BB	2	N	
4	1.2	0.38	220	36	W	0.05	F	0.7	BB	2	N	
5	1.4	0.2	215	48	W	0.15	F	0.3	BB	1	N	
6	1.5	0.1	325	40	W	0.1	F	0.4	BB	0.5	N	
7	1.55	0.05	235	30	W	0.1	F	0.4	BB	1	N	
Outcrop description						**FR 7-13-1 Shear Zone**						
	Bedding Plane Orient:	**Bed Thickness:**	**Formation:**		**Lithology:**	**Fossils:**	**Sample orient:**	**Photos:**	**Evidence of shear:**		**Relative Age Relations**	
	124 53 S	**2.4 M**	**Wahoo?**		**mudstone**	**none**	**none**	**3-2,3-3,3-4**	**extensive, right lateral, shear zones**		shear frax predate	
FR 7-13-1 Shear Zone											N-S and E-W frax	
No	Spacing (meters)	Distance	Strike	Dip	Dip Direction	Length (meters)	Length descriptor	Height (meters)	Height descriptor	Ap (cm)	Fill	
1	0		28	70	E	U	U	0.3	II	1	Fc	
2	0.1	0.1	10	55	E	U	U	0.3	II	1	Fc	
3	0.3	0.2	30	65	E	U	U	0.3	II	1	Fc	
4	0.4	0.1	30	67	E	U	U	0.3	II	1	Fc	
5	0.5	0.1	28	42	E	U	U	0.3	II	1	Fc	

Table 1

Outcrop description						**FR 7-13-2 Shear Zone**						
	Bedding Plane Orient:	**Bed Thickness:**	**Formation:**		**Lithology:**	**Fossils:**	**Sample orient:**	**Photos:**	**Evidence of shear:**			
	124 53 S	**2.4 M**	**Wahoo?**		**mudstone**	**none**	**none**	**3-5, 3-6**	**extensive, right lateral, shear zones**			
FR 7-13-2												
No	Spacing (meters)	Distance	Strike	Dip	Dip Direction	Length (meters)	Length descriptor	Height	Height descriptor	Ap (cm)	Fill	
1	0		287	85	N	0.2	U	0.2	II	0.1	Fc	
2	0.01	0.01	290	80	N	0.2	U	0.2	II	0.1	Fc	
3	0.02	0.01	278	78	N	0.2	U	0.2	II	0.1	Fc	
4	0.03	0.01	290	85	N	0.2	U	0.2	II	0.1	Fc	
5	0.04	0.01	285	85	N	0.2	U	0.2	II	0.1	Fc	
6	0.05	0.01	288	80	N	0.2	U	0.2	II	0.1	Fc	
7	0.06	0.01	286	70	N	0.2	U	0.2	II	0.1	Fc	
8	0.07	0.01	280	80	N	0.2	U	0.2	II	0.1	Fc	
9	0.08	0.01	280	75	N	0.2	U	0.2	II	0.1	Fc	
10	0.09	0.01	290	82	N	0.2	U	0.2	II	0.1	Fc	
Outcrop description						**FR 7-14-1**						
	Bedding Plane Orient:	**Bed Thickness:**	**Formation:**		**Lithology:**	**Fossils:**	**Sample orient:**	**Photos:**	**Evidence of shear:**	**Other:**	**Relative Age Relations**	
	92 62S	**1.5 meter**	**Wahoo upper?**		**muddy/**	**crinoids**	**100 62S**	**3-7 to 3-9**	**none**	**no slicks**	N-S predate both E-W sets	
FR 7-14-1	N-S				**wackestone**							
No	Spacing (meters)	Distance	Strike	Dip	Dip Direction	Length (meters)	Length descriptor	Height (meters)	Height descriptor	Ap (cm)	Fill	
1	0		25	75	E	2	B	0.1	BB	1	Pc	
2	0.14	0.14	0	83	E	1.5	B	0.1	BI	2	Pc	
3	0.23	0.09	5	82	E	1.5	B	0.2	BI	0.1	Pc	
4	0.4	0.17	2	85	E	1	B	0.05	BI	0.2	Pc	
5	0.64	0.24	15	80	E	1	B	0.05	BI	0.2	Pc	
6	0.72	0.08	0	80	E	0.2	B	0.05	BI	0.2	Pc	
7	0.9	0.18	16	84	E	1	B	0.05	BI	1	Pc	
8	1.05	0.15	340	85	E	0.7	B	0.1	BB	U	U	
FR 7-14-1	E-W											
No	Spacing (meters)	Distance	Strike	Dip	Dip Direction	Length (meters)	Length descriptor	Height (meters)	Height descriptor	Ap (cm)	Fill	
1	0.13		323	45	NE	0.15	B	0.25	BB	0.1	Pc	
2	0.21	0.08	327	52	NE	0.05	B	0.27	BB	0.5	Pc	
3	0.52	0.31	337	50	NE	0.05	B	0.4	BB	0.5	Pc	
4	0.6	0.08	335	60	NE	0.08	B	0.5	BB	0.5	Pc	
5	0.85	0.25	330	75	NE	0.05	B	0.6	BB	0.2	Pc	
6	1	0.15	342	74	NE	0.1	B	0.6	BB	1	Pc	
7	1.35	0.35	342	66	NE	0.1	B	1	BB	0.2	Pc	
FR 7-14-1	Micro E-W											
No	Spacing (meters)	Distance	Strike	Dip	Dip Direction	Length (meters)	Length descriptor	Height (meters)	Height descriptor	Ap (cm)	Fill	
1	0.02		U	U	NE	0.1	B	0.2	BB	0.1	Fc	
2	0.03	0.01	322	34	NE	0.1	B	0.2	BB	0.1	Fc	
3	0.05	0.02	310	35	NE	0.1	B	0.2	BB	0.1	Fc	
4	0.06	0.01	318	40	NE	0.1	B	0.2	BB	0.1	Fc	
5	0.07	0.01	312	45	NE	0.1	B	0.2	BB	0.1	Fc	
6	0.1	0.03	308	42	NE	0.11	B	0.2	BB	0.1	Fc	
7	0.13	0.03	314	41	NE	0.1	B	0.2	BB	0.1	Fc	

Table 1

Outcrop description					**FR 7-14-2**							
	Bedding Plane Orient:	**Bed Thickness:**	**Formation:**		**Lithology:**	**Fossils:**	**Sample orient:**	**Photos:**	**Evidence of shear:**	**Other:**	**Relative Age Relations**	
	264 75S	**1-2m**	**Upper Wahoo**		**wackestone**	**crinoids, brach, bryz**	**115 90S**	**3-10 to 3-14**	**none**	**BP small stylolites**	N-S predate E-W	
FR 7-14-2	MACRO SET N-S				**(muddy)**							
No	Spacing (meters)	Distance	Strike	Dip	Dip Direction	Length (meters)	Length descriptor	Height (meters)	Height descriptor	Ap (cm)	Fill	
1	0.48		2	58	E	3	B	0.1	IU	0.5	Pc	
2	0.92	0.44	0	65	E	3	B	0.05	II	0.5	Pc	
3	1.4	0.48	358	62	E	1.5	B	0.05	BI	0.1	Pc	
4	1.95	0.55	0	70	E	2	B	0.05	BB	1	Pc	
5	2.45	0.5	15	50	E	2	B	0.05	II	1	Pc	
6	3.24	0.79	3	65	E	4	B	0.05	BU	0.5	Pc	
7	3.8	0.56	355	56	E	0.5	B	0.02	BB	0.5	Pc	
FR 7-14-2	MICROSET (N-S)											
No	Spacing (meters)	Distance	Strike	Dip	Dip Direction	Length (meters)	Length descriptor	Height (meters)	Height descriptor	Ap (cm)	Fill	
1	0.05		352	60	E	0.5	B	0.01	BB	0.1	Pc	
2	0.06	0.01	350	58	E	0.5	B	0.01	BB	0.1	Pc	
3	0.17	0.11	345	57	E	0.7	B	0.01	BB	0.1	Pc	
4	0.15	-0.02	355	58	E	0.5	B	0.01	BB	0.1	Pc	
5	0.17	0.02	354	62	E	1	B	0.01	BB	0.1	Pc	
6	0.2	0.03	352	68	E	0.5	B	0.01	BB	0.1	Pc	
FR 7-14-2	MEZZO SET (NE-SW)											
No	Spacing (meters)	Distance	Strike	Dip	Dip Direction	Length (meters)	Length descriptor	Height (meters)	Height descriptor	Ap (cm)	Fill	
1	0		192	43	W	0.57	B	0.02	BB	1	Pc	
2	0.3	0.3	195	40	W	0.15	B	0.01	BI	0.1	Fc	
3	0.5	0.2	204	40	W	0.07	B	0.02	BB	2	Pc	
4	0.63	0.13	205	37	W	0.12	B	0.03	BB	0.1	Pc	
5	0.83	0.2	219	52	W	0.5	B	0.01	BB	1	Pc	
6	1	0.17	206	42	W	0.5	B	0.05	BB	0.5	Pc	
7	1.27	0.27	230	41	W	0.1	B	0.01	BI	0	N	
8	1.5	0.23	215	41	W	0.2	B	0.02	BB	0.1	Pc	
9	1.83	0.33	208	35	W	0.4	B	0.05	BB	1	N	
10	2.1	0.27	308	37	W	0.3	F	0.05	BU	0.5	Pc	
Outcrop description						**FR7-19-1**						
	Bedding Plane Orient:	**Bed Thickness:**	**Formation:**		**Lithology:**	**Fossils:**	**Sample orient:**	**Photos:**	**Other:**	**no evidence of shear**	**Relative Age Relations**	
	115 26 S	**1-2m**	**Upper Wahoo**		**grainstone**	**bryz, crinoids,**	**7191a:295 74N**	**3/19**	**dissolution cleavage orientation: 295 75N**		indeterminable	
						stromatalites	**7191b: 262 84N**		**chert nodules (Boudin Style)**			
							7191c: 340 75E					
FR7-19-1	BED A (E-W)						**7191d: 340 72E**					
No	Spacing (meters)	Distance	Strike	Dip	Dip Direction	Length (meters)	Length descriptor	Height (meters)	Height descriptor	Ap (cm)	Fill	
1	0.17		265	78	N	0.02	B	0.5	BU	1	Pc	
2	0.24	0.07	272	78	N	0.05	F	0.15	BU	1	Pc	
3	0.4	0.16	280	80	N	0.1	F	0.35	MM	0.1	Pc	
4	0.48	0.08	252	84	N	0.1	F	0.35	MM	0.1	Pc	
5	0.52	0.04	290	90	V	0.3	F	0.7	BU	0.1	Pc	
6	0.68	0.16	246	73	N	0.12	F	0.22	FU	0.1	Pc	
7	0.75	0.07	300	80	N	0.05	B	0.6	BU	0.1	Pc	
8	0.97	0.22	295	80	N	0.1	B	0.25	BM	0.5	Pc	
9	1	0.03	287	80	N	0.1	F	0.2	BM	0.5	Pc	
10	1.28	0.28	289	90	V	0.15	F	0.45	BU	U	U	
FR7-19-1	BED D (N-S)											
No	Spacing (meters)	Distance	Strike	Dip	Dip Direction	Length (meters)	Length descriptor	Height (meters)	Height descriptor	Ap (cm)	Fill	
1	0.35		213	24	NE	0.2	B	0.6	BU	0.4	N	
2	0.52	0.17	255	44	N	0.05	B	0.75	BU	0.2	Pc	
3	0.95	0.43	248	31	N	0.4	B	1	BU	1	N	
4	1.07	0.12	254	36	N	1	B	0.93	FB	0.3	N	

Table 1

Outcrop description						**FR 7-19-2**						
	Bedding Plane Orient:	**Bed Thickness:**	**Formation:**		**Lithology:**	**Fossils:**	**Sample orient:**	**Evidence of shear:**		**Photos:**	**Relative Age Relations**	
	278 39N	**2.5 meters**	**Alapah**		**grainstone**	**crinoids**	**7192:138 47S**	**None**		**3-20 to 3-24**	N-S predate E-W	
FR 7-19-2	N-S											
No	Spacing (meters)	Distance	Strike	Dip	Dip Direction	Length (meters)	Length descriptor	Height (meters)	Height descriptor	Ap (cm)	Fill	
1	0		357	71	E	0.6	F	2	UU	2	N	
2	0.65	0.65	4	82	W	1	F	2.5	UU	2	Pc	
3	1.05	0.4	7	71	W	0.5	F	2	UBU	3	Pc	
4	1.5	0.45	0	71	W	0.4	F	1.5	UB	1	Pc	
5	2	0.5	6	76	W	1	F	1.5	UB	3	Pc	
FR 7-19-2	E-W											
1	0.26		100	84	N	0.5	B	1	BU	3	N	
2	0.45	0.19	95	80	N	0.5	B	0.6	BU	3	N	
3	0.58	0.13	100	80	N	0.2	B	0.2	BU	0.5	Pc	
4	0.65	0.07	97	85	N	0.5	B	0.7	BU	U	U	

Table 1